Architect-Engineering Services for Environmental Engineering Services at Various Navy and Marine Corps Activities, Pacific Basin and Indian Ocean Areas
Contract No. N62742-05-D-1873
Amendment 11
Task Order No. 0009

Ocean Current Study
Ocean Dredged Material Disposal Site
Apra Harbor, Guam
Final Report

Prepared For:

Department of the Navy
Naval Facilities Engineering Command Pacific
258 Makalapa Drive, Suite 100
Pearl Harbor, Hawaii 96860-3134

August 2007

Ocean Current Study
Ocean Dredged Material Disposal Site
Apra Harbor, Guam

Final Report

Prepared For:

Department of the Navy
Naval Facilities Engineering Command Pacific
258 Makalapa Drive, Suite 100
Pearl Harbor, Hawaii 96860-3134

Prepared By:

Weston Solutions, Inc.
2433 Impala Drive
Carlsbad, California 92008

Under Contract To:
Belt Collins Hawaii Ltd.
2153 North King Street, Suite 200
Honolulu, Hawaii 96819

August 2007

TABLE OF CONTENTS

LIST OF TABLES

LIST OF FIGURES

ACRONYMS AND ABBREVIATIONS

ADDAMS	Automated Dredging and Disposal Alternatives Management System
CTD	Conductivity/Temperature/Depth
E	East
EIS	Environmental Impact Statement
ENSO	El Niño/Southern Oscillation
GEPA	Guam Environmental Protection Agency
GIS	Geographic Information System
GovGuam	Government of Guam
ITM	Inland Testing Manual
LCPW	Lower Circumpolar Water
MEI	Multivariate ENSO Index
MLLW	Mean Lower Low Water
MODAS	Modular Ocean Data Assimilation System
N	North
NAVFAC/PAC	Naval Facilities Engineering Command, Pacific
NAVO	Naval Oceanographic Office
NCOM	Navy Coastal Ocean Model
NLOM	Navy Layered Ocean Model
NOAA	National Oceanographic and Atmospheric Administration
NOGAPS	Navy Operational Global Atmospheric Prediction System
NPDW	North Pacific Deep Water
NPEC	North Pacific Equatorial Current
ODMDS	Ocean Dredged Material Disposal Site
PAG	Port Authority of Guam
PEAC	Pacific ENSO Applications Center
SAIC	Science Applications International Corporation
SFDODS	San Francisco Deep Ocean Disposal Site
SRF	Ship Repair Facility
SSH	Sea Surface Height
SSS	Sea Surface Salinity
SST	Sea Surface Temperature
STFATE	Short Term FATE Model
USACE	U.S. Army Corps of Engineers
USEPA	U.S. Environmental Protection Agency
ZSF	Zone of Siting Feasibility

UNITS of MEASURE

cm/s	centimeters per second
cy	cubic yards
ft	feet
ft/s	feet per second
in	inches
km	kilometers
km^2	square kilometers
m	meters
m^3	cubic meters
mcy	million cubic meters
mm	millimeters
nm	nautical miles
sq. nm	square nautical miles
°	degrees (of latitude or longitude)

1.0 INTRODUCTION

1.1 Background

Both the Navy and the Port Authority of Guam (PAG) have plans to expand their operations in Apra Harbor, Guam. Expansion of the Apra Harbor Naval Complex and Commercial Port is necessary to accommodate increases in vessel and cargo traffic, newer classes of vessels and dockside maintenance and support operations. Expansion plans would require construction dredging activities to increase water depths for the safe navigation of military and commercial vessels.

Currently, the Navy has planned a number of construction dredging projects in both Inner and Outer Apra Harbor. Approximately 1,500,000 cy (1,146,832 m^3) of dredged material is anticipated to be generated as a result of these projects (Sato [Naval Facilities Engineering Command, Pacific (NAVFAC/PAC)] 2007). By the year 2036, up to 1,200,000 cy (917,466 m^3) of sediment will likely need to be dredged as part of maintenance dredging projects within Apra Harbor in support of Navy operations (MEC-Weston 2005). Also, construction and maintenance dredging by the PAG may be initiated in the future at Commercial Port as part of a deep draft wharf project and at Agana Boat Basin, Agat Marina and Tumon Bay (for recreational swimming purposes) generating an unknown volume of dredged material for disposal (Guam Environmental Protection Agency [GEPA], 2000).

An ocean dredged material disposal site (ODMDS) would provide the Navy and PAG with an alternative to upland disposal or beneficial use of clean dredged materials and additional capacity for the disposal of dredged materials. Currently, the Navy has three existing dewatering facilities (Orote Point, Ship Repair Facility [SRF], and Field 5 located between Marine Drive and Sumay Drive) and is considering the possible construction of an additional dewatering facility at an open field located south of the Commissary. The three existing dewatering facilities are near capacity. The open field located south of the Commissary is estimated to have a capacity of 250,000 cy (191,139 m^3). These existing and proposed dewatering facilities do not have sufficient capacity for the anticipated volume of dredged material to be generated over the next 30 years.

1.2 Purpose and Need

To initiate the designation of an ODMDS, a Zone of Siting Feasibility (ZSF) study was completed that identified two suitable alternatives for the placement of a potential ODMDS offshore of Guam (Weston 2006). The next steps in the process of a potential ODMDS designation are an assessment of the short and long-term fate and potential effects of dredged material pursuant to disposal operations. Therefore, the purpose of this study was to evaluate oceanographic current data as modeled by the Naval Oceanographic Office (NAVO) in order to understand the regional current regime and to use these data in both a U.S. Army Corps of Engineers (USACE) developed model (Short-Term FATE of dredged material disposal in open water; STFATE) and a model developed by Science Applications International Corporation (SAIC; the Hamilton model) for the U.S. Environmental Protection Agency (USEPA) to predict the transport and deposition of dredged material offshore of Guam.

1.3 Study Area

The ZSF study identified the regulatory, technical, logistical, economic and environmental issues, including social and cultural resource concerns which would constrain the placement of a potential ODMDS. Once identified, these constraints were layered within a geographic information system (GIS) to determine areas not suitable for the placement of an ODMDS. Next, an economic feasibility analysis was conducted to determine the maximum practical extent in which dredged material disposal operation could be conducted. Areas beyond the limits of any constraints, but within the limits of the economic feasibility arc, were determined to be suitable alternatives for the placement of an ODMDS.

Figure 1 illustrates all the eliminated areas, or constraints, due to navigational lanes and hazards, Government of Guam (GovGuam) jurisdictional boundaries, marine protected areas, parks, ocean outfalls, fishing areas, visual resources and continental shelf considerations. Due to the rapidly increasing project depths, many of the eliminated areas were contained within the GovGuam jurisdictional boundary. For example, the marine preserves extend to a depth of -600 ft (-183 m) MLLW, which occurs within 1.0 nm (1.9 km) of shore and within the GovGuam jurisdictional boundary. Figure 2 superimposes the economic feasible distances for maintenance and construction dredging projects onto the areas eliminated from further consideration.

The results of the ZSF study suggested there were two regions located offshore of Guam that may be suitable for placement of an ODMDS. Since both maintenance and construction dredging projects may dispose of dredged material at the ODMDS, the inner arc, that dependent on maintenance dredging projects, was chosen to set the outer limit of feasibility. The first region, northwest of the entrance to Outer Apra Harbor, is approximately 8.9 nm (16.4 km) offshore of Guam (Figure 2). This region occupies an area approximately 45 sq. nm (152 km^2). The second region, north of the entrance to Outer Apra Harbor, is approximately 12.4 nm (23.0 km) away. This northern region occupies an area approximately 17 sq. nm (58 km^2).

The present study assesses oceanographic currents in a 1° x 1° area (60 x 60 nm), extending beyond the boundaries of the proposed ODMDS placement areas to approximately 32 nm (59 km) to the north and 40 nm (74 km) to the west of the entrance to Outer Apra Harbor. Figure 3 illustrates the region for which current data were evaluated and superimposes the two areas determined suitable for the location of an ODMDS as identified in the ZSF. It was necessary to evaluate currents outside the immediate vicinity of the ODMDS alternative sites in order to determine consistency, or variability, of the regional current patterns and to understand the currents that dredged material may be subject to as a consequence of horizontal dispersion after the initial placement of material.

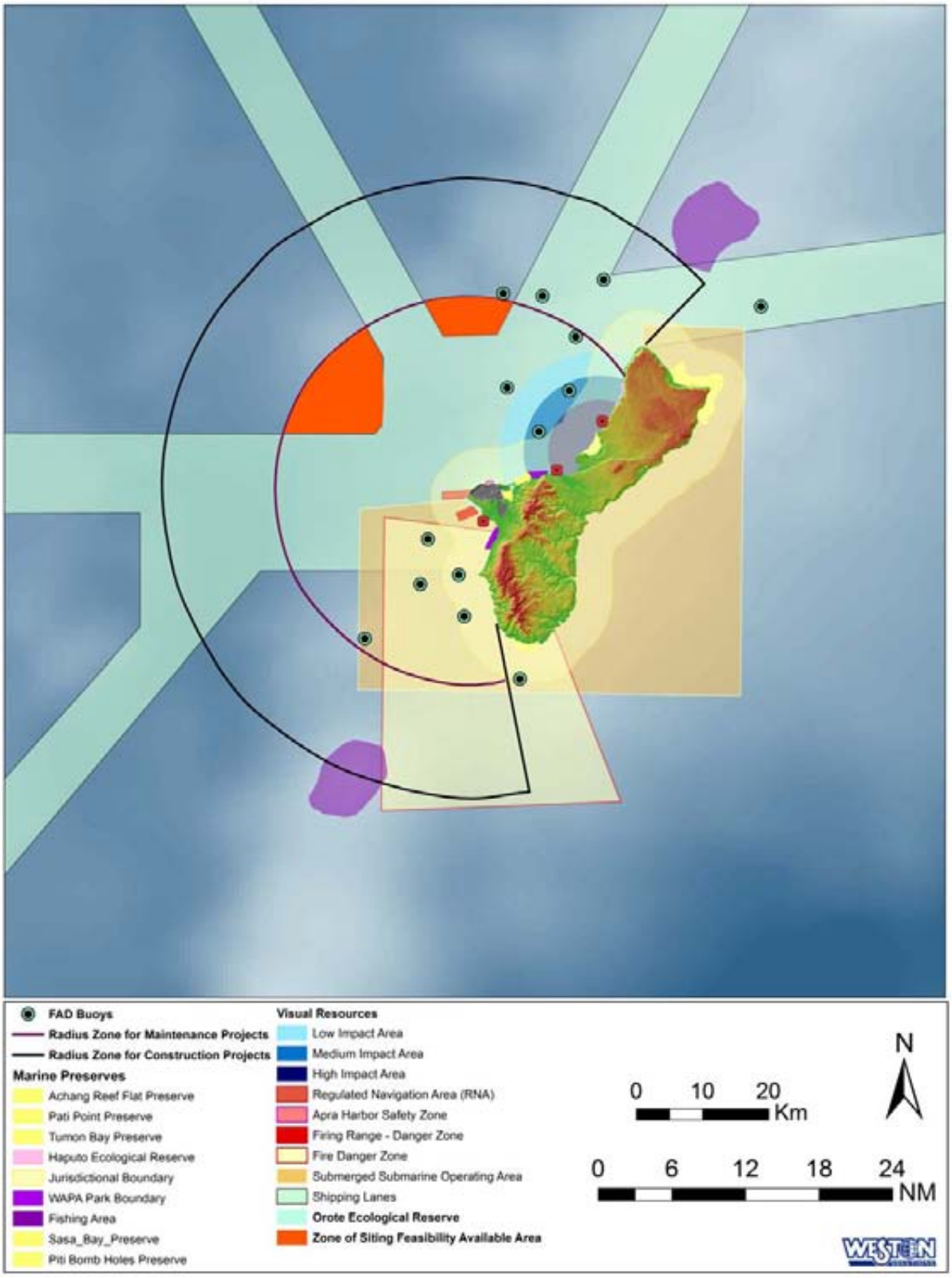

Figure 1. Combined ZSF Eliminated Areas

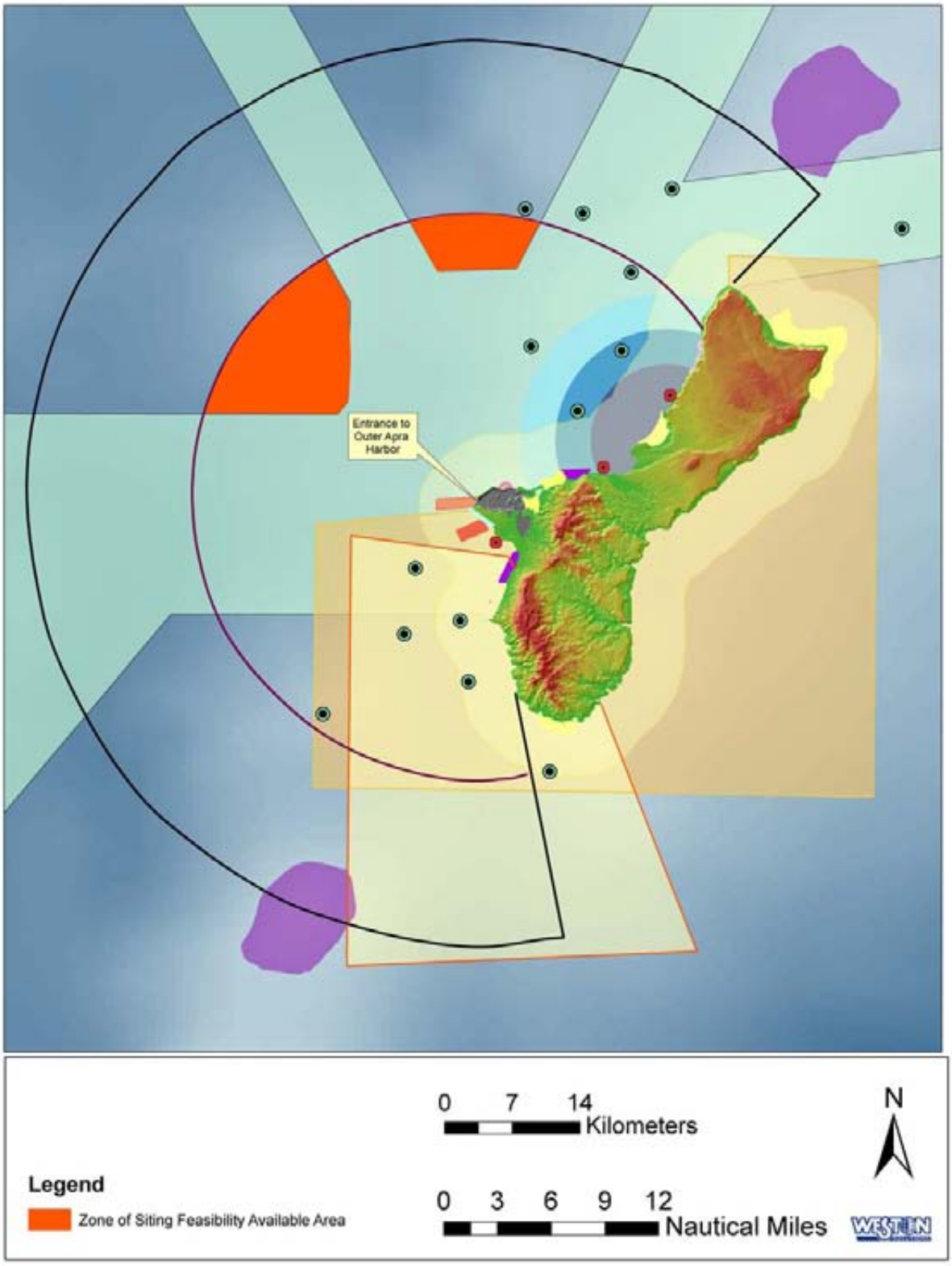

Figure 2. Zone of Siting Feasibility

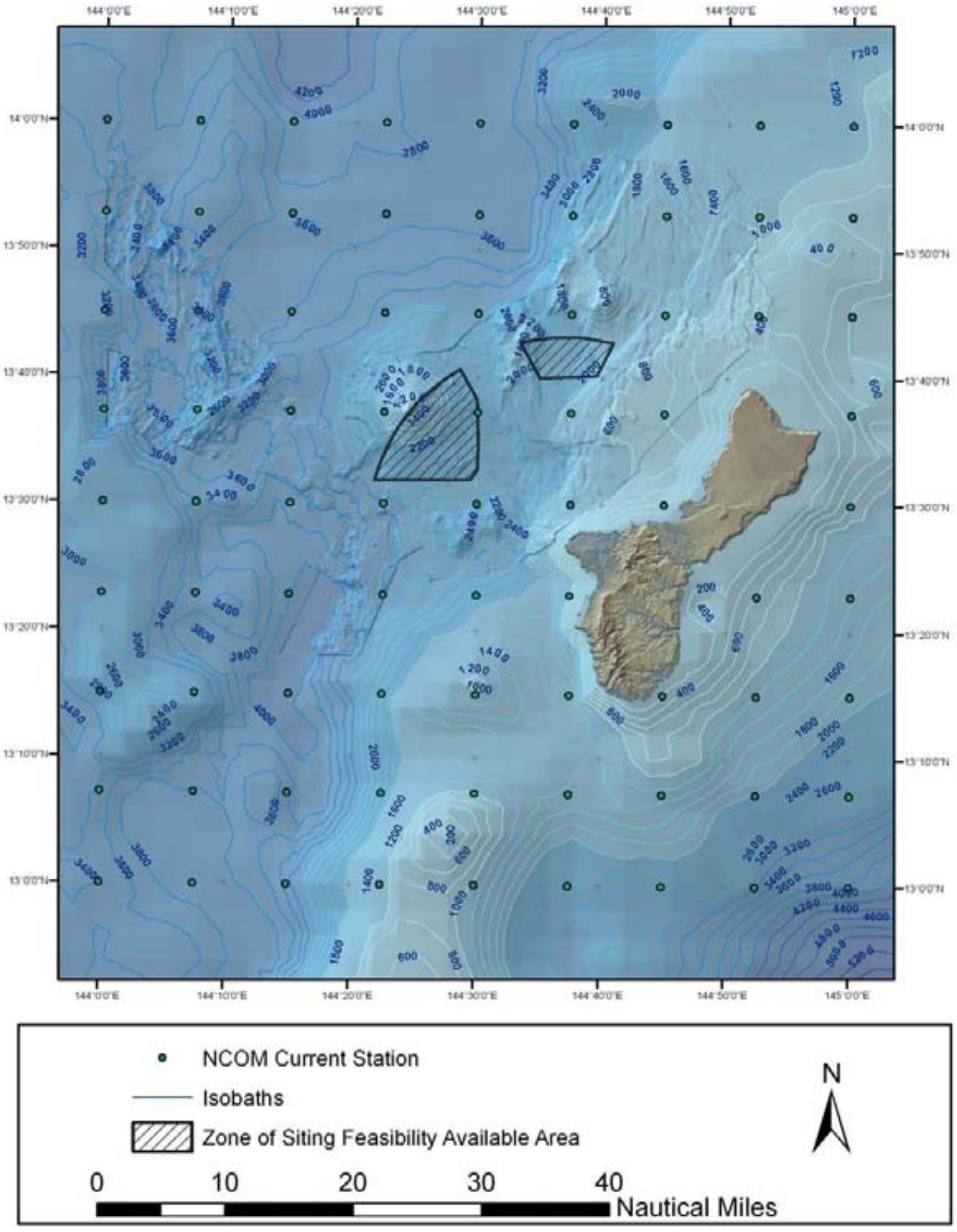

Figure 3. Regional Study Area and Bathymetry

2.0 NAVY COASTAL OCEAN MODEL (NCOM)

The global Navy Coastal Ocean Model (NCOM) is an assimilative ocean model nowcast/forecast system developed and administered by NAVO. NCOM was the source of oceanographic current data used in this study. Resolution is 1/8°, or 7.5 x 7.5 nm. Input parameters for the model are satellite-measured sea surface temperature (SST) and sea surface height (SSH; altimetry) derived from the Modular Ocean Data Assimilation System (MODAS) and Navy Layered Ocean Model (NLOM), respectively. SST and SSH measurements are then used to project a vertical profile of temperature and density, from which thermohaline currents are derived. Thermohaline currents occur at depth and are driven by differences in density rather than wind patterns, which derive surface currents. Surface currents are derived from atmospheric conditions provided by the Navy Operational Global Atmospheric Prediction System (NOGAPS) which force NCOM predictions. Ocean depth and coastline boundaries used in the NCOM are based on a global dataset of two minute (1/30°) bathymetry data. Tidal currents were not incorporated in the model results.

For the validation of NCOM, Barron et al. (2007) used both available observational data and other global ocean models for comparison. The validation of this model assesses the actual operational implementation and covers almost six years of modeling (from 1998 to early 2003). Overall, the assimilative model is an improvement over current global ocean models, specifically for the upper ocean nowcasts because it integrates multiple input parameters.

The model was validated using relevant observational data (e.g. SSH, SST, sea surface salinity [SSS], surface speed, surface kinetic energy) at several locations throughout the oceans (e.g., Bay of Bengal, the Aleutians, the Kuroshio current and other locales; Barron et al. 2007). For the most part, the model results compare well with the *in situ* data used for validation. For example, NCOM results of both the Gulf Stream and the Kuroshio were more realistic of conditions as compared to the Shallow-Water Analysis and Forecast System (SWAFS) Northworld Model in use at the NAVO. Along the coast of Japan, the assimilative model was more realistic of both surface and 100 m current speeds. In addition, the global NCOM did not produce the unrealistic gyres of the Kuroshio along the southern coast of Japan which is seen in the SWAFS model. It should be noted that there is some uncertainty along western boundary regions. The global NCOM was successful in modeling currents around the Indian Ocean, particularly the Arabian Sea. Also, as this is a global ocean model, features and ocean processes which are on a horizontal scale of 10 km or less cannot be represented. Finally, there is limited data on the continental shelf from NLOM and in MODAS, therefore there is reduced information about the SSH near NLOM boundaries, specifically at depths less than 600 m. But with the integration of these two models, NCOM provides prognostic model coverage, including the midlatitude regions, the Arctic and southern oceans, and coastal regions which have at-rest depths at a minimum of 5 m.

NCOM results are available at 40 different user-defined levels , or depths (i.e., 0 ft [0 m], 33 ft [10 m], 330 ft [100 m] depth, etc.), over 3-hour time intervals. Results are typically provided in NetCDF format, consisting of current vectors u and v for each x, y, z and time increment. At a minimum, archived data are available for the previous year and may be available for even earlier dates.

NCOM results tend to have a high degree of accuracy for regions within large scale currents, such as Guam located in the North Pacific Equatorial Current (NPEC). However, due to model resolution, model results are less accurate along nearshore areas. A preliminary assessment of the model accuracy offshore of Guam suggests a high degree of confidence in the model results between 7.5 and 15 nm (14 and 28 km) offshore of Guam. The closest inshore boundaries of the two areas identified in the ZSF study as suitable for a potential ODMDS are 9 and 10 nm (17 and 19 km) offshore of Guam.

Subsurface temperatures have been validated using *in situ* data (i.e., conductivity/temperature/ depth CTD profiles) and modeled ocean currents have been validated using drifter trajectories and acoustic Doppler current profiler data.

3.0 DATA POST-PROCESSING

Current data were provided for the entire 2005 calendar year. Data were provided for a 1° x 1° square area bounded by 14° North (N) and 13° N latitude in the north and south, respectively and 145° East (E) and 144° E longitude in the east and west, respectively (Figure 3). Thus, at the resolution of the model (1/8°), data were provided at 81 discrete locations. At each of these stations, data were provided for 17 separate depths. Currents were provided at finer (shorter) intervals near the surface with increasingly coarse (longer) intervals at deeper depths (Table 1). At each station and depth, current data were provided for each six hour increment. Current data were provided as u (east-west) and v (north-south) vectors. At each location and for each vector, a single NetCDF format electronic file was provided.

Table 1. Depth Intervals of NCOM Derived Current Data

Depth Intervals of NCOM Data	
(meters)	**(≈feet)**
0	0
10	33
20	66
30	100
40	130
50	165
75	250
100	330
200	650
300	1000
400	1,300
500	1,650
1,000	3,300
1,500	4,900
2,000	6,550
2,500	8,200
3,000	9,850

The individual vector files were combined and converted to text files using a NetCDF reader, ANDX. The text files were then read and combined into a database using SAS® (SAS 2006). During processing of the text files, the individual vector data were used to calculate speed and direction for each location and depth.

Next, a series of plots were made in Grapher (Golden Software 2005). Rose diagrams representing the frequency distribution of current directions and speed for each depth at a single location and vector plots representing daily averaged current velocities at each location by month and depth were created. These plots provided a cursory review of the spatial (both horizontal and vertical) as well as temporal patterns in the data. Once patterns were identified, more quantitative statistical analyses were conducted using SAS software to identify significant trends or differences in the currents.

Concurrently, the SAS® database files were exported to a GIS database. GIS is a useful tool for the graphical representation of complex geographic datasets. GIS was used primarily for interpolating the current velocity data between locations and overlaying the footprints of the dredged material deposits on regional bathymetry.

4.0 PHYSICAL OCEANOGRAPHY - CURRENTS

The oceanographic current patterns identified through the processing of the NCOM data were evaluated on both regional and site-specific scales. The regional current patterns were evaluated for two reasons: 1) to provide context for interpreting the site-specific current patterns and 2) for comparison to previously published information on the regional currents to assess the suitability of using NCOM data rather than conducting site-specific current studies. The site-specific current patterns from the NCOM model focused on the two areas identified in the ZSF as suitable for the placement of an ODMDS. The current regimes in these two areas were subsequently used as input parameters to the STFATE and Hamilton/SAIC models to predict the transport and deposition of dredged material through the water column and onto the seafloor.

4.1 Regional Patterns

A brief summary of the geography of Guam provides a context for understanding the regional oceanographic current patterns. Guam is the southernmost island in the Marianas Island Arc centered at approximately 13.50° N, 144.75° E. In this area, the Marianas Island Arc trends from the southwest to the northeast and consists of multiple seamounts and banks which separate the East Mariana Basin from the West Mariana Basin. The island lies directly in the trajectory of the NPEC which flows in response to the trade winds in a westerly direction typically between 10° N and 15° N.

4.1.1 Surface Currents

Figure 4 illustrates the surface currents on a regional scale. It contains 12 separate vector plots, one for each month of the year, for a near surface layer (33 ft [10 m] depth). In each monthly plot, daily averaged currents for each of the 81 stations are presented. Appendix A contains similar graphics for each of the layers evaluated. Figure 5 through Figure 8 are graphical

interpolations of these data generated from a GIS that show the mean current direction and speed for the dry and wet seasons.

During the fall and winter months (predominantly the dry season; Figure 4 through Figure 6), surface currents tend to be quite uniform, having a significant west-northwesterly component across much of the study area. As the surface current approaches and bifurcates around Guam from the east, the currents in the southern portion of the study area tend to be more westerly, while currents in the northern portion of the study area tend to be towards the west-northwest. Once past Guam and beyond the site-specific study areas, these currents converge, with the currents in the southern portion of the study area trending more northwesterly and currents in the northern portion of the study area trending more westerly. This pattern creates an area of variable current patterns directly in the lee of the island, with surface currents capable of flowing back towards Guam on occasion. This pattern is most evident in February and March when the surface currents are highly uniform, however, it is also observed in the three preceding months (October through January) and one succeeding month (April).

In the summer months (predominantly the wet season; Figure 4, Figure 7 and Figure 8), surface currents are slightly more variable on a month to month basis and the net current direction tends to flow in more southwesterly direction. During this time, the currents approaching Guam in the southern portion of the study area continue to be predominantly to the west, but having an increasingly greater southwesterly component through time such that currents approaching Guam in September are primarily trending to the southwest. The currents approaching Guam in the northern portion of the study typically trend towards the west-southwest, with directional variability being greater than those observed in the south during the same time period. In the lee of the island, the area of variable current patterns continued to persist.

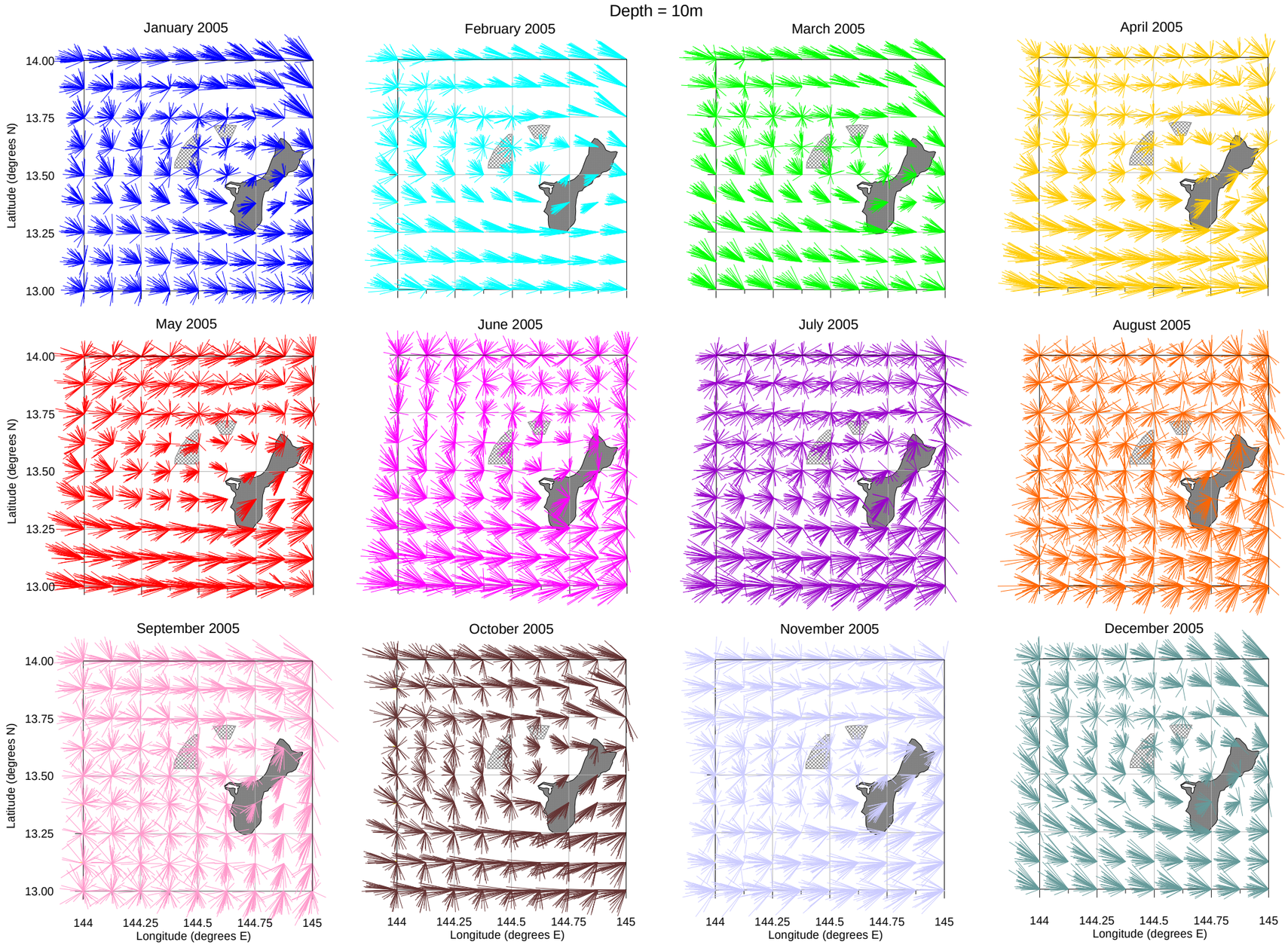

Figure 4. Vector Plots of Daily Averaged Current Velocities by Month for Each Location at 33 ft (10 m) Depth

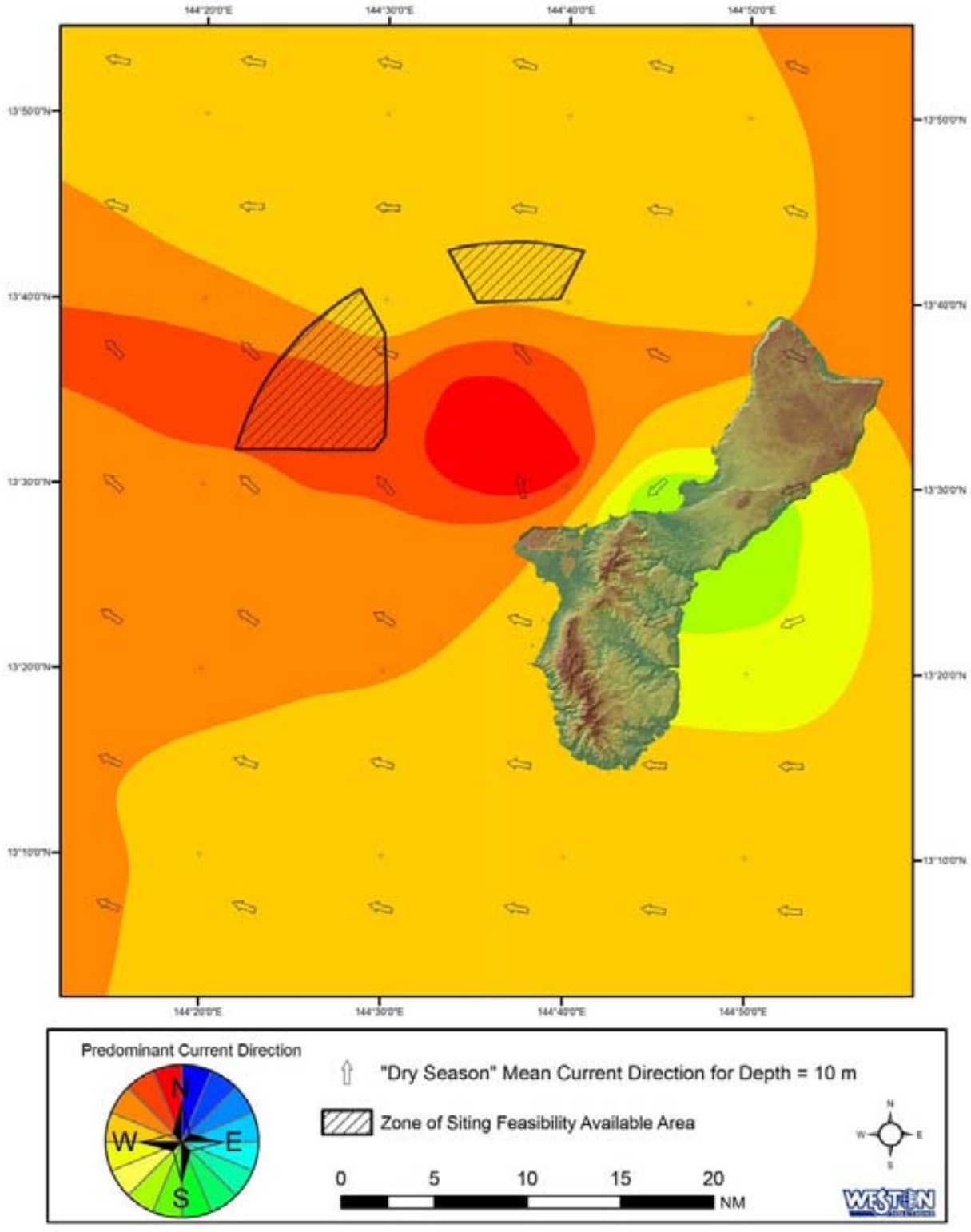

Figure 5. Interpolation of Mean Current Directions at 10 Meters Depth for the Dry Season

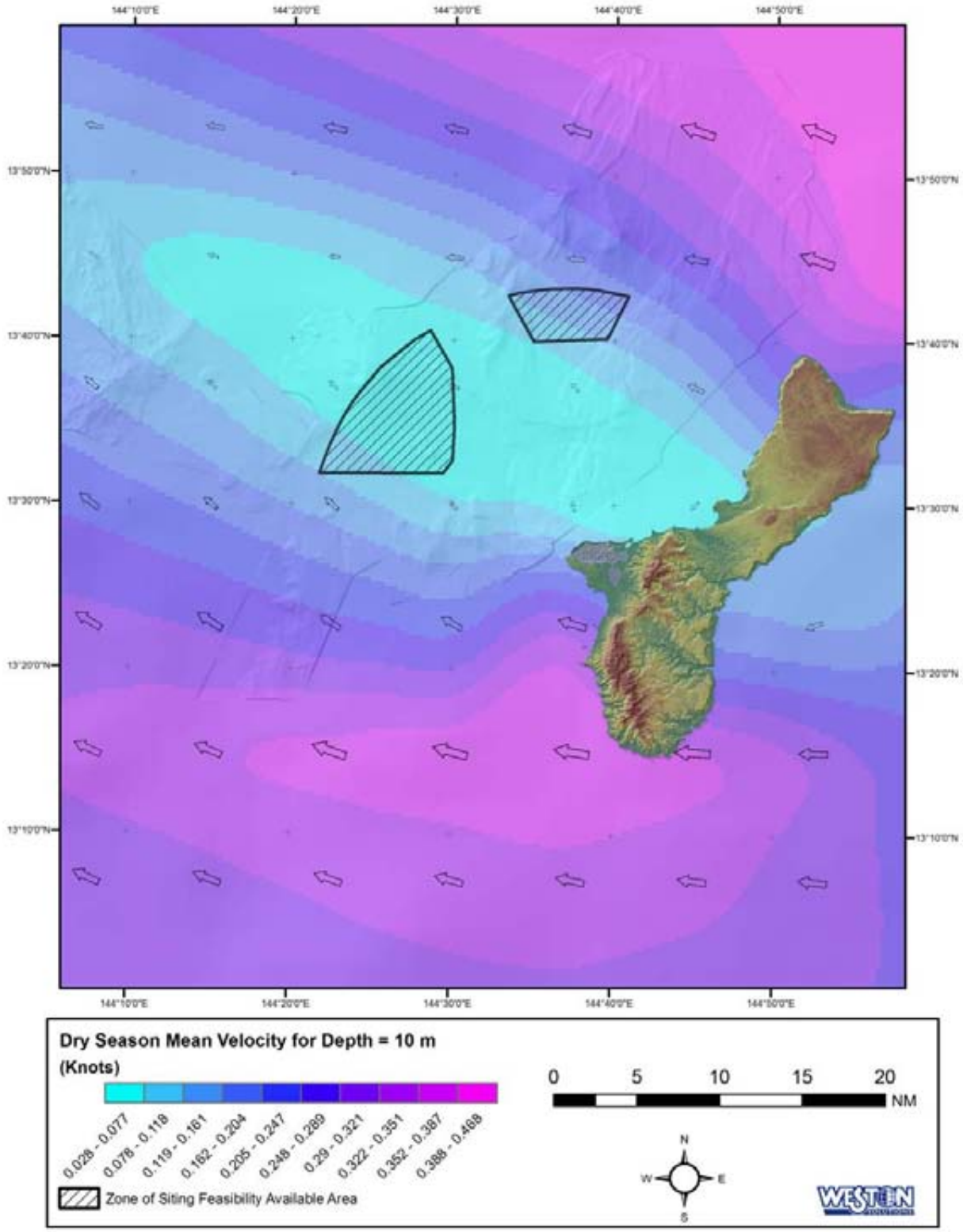

Figure 6. Interpolation of Mean Current Speeds at 10 Meters Depth for the Dry Season

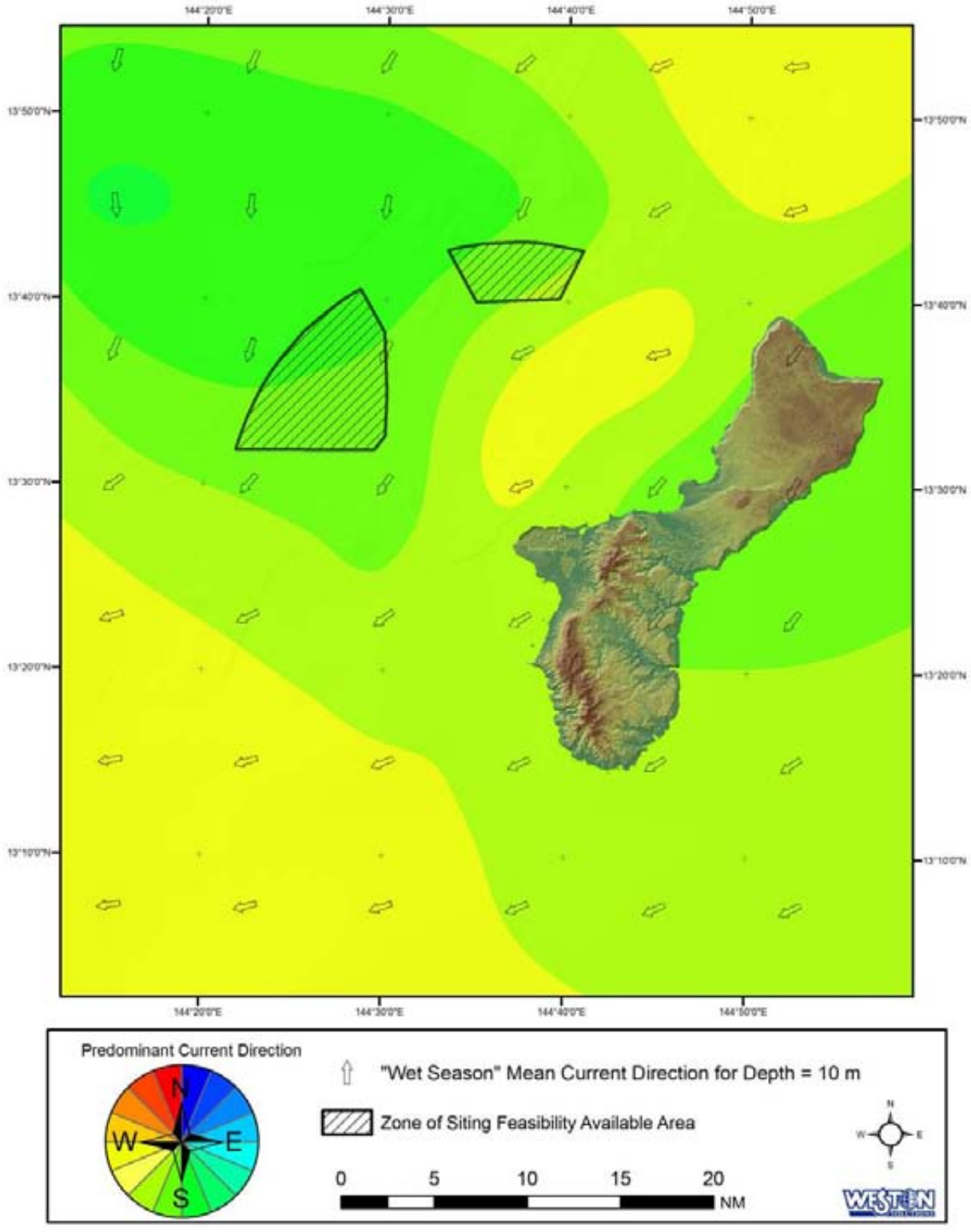

Figure 7. Interpolation of Mean Current Directions at 10 Meters Depth for the Wet Season

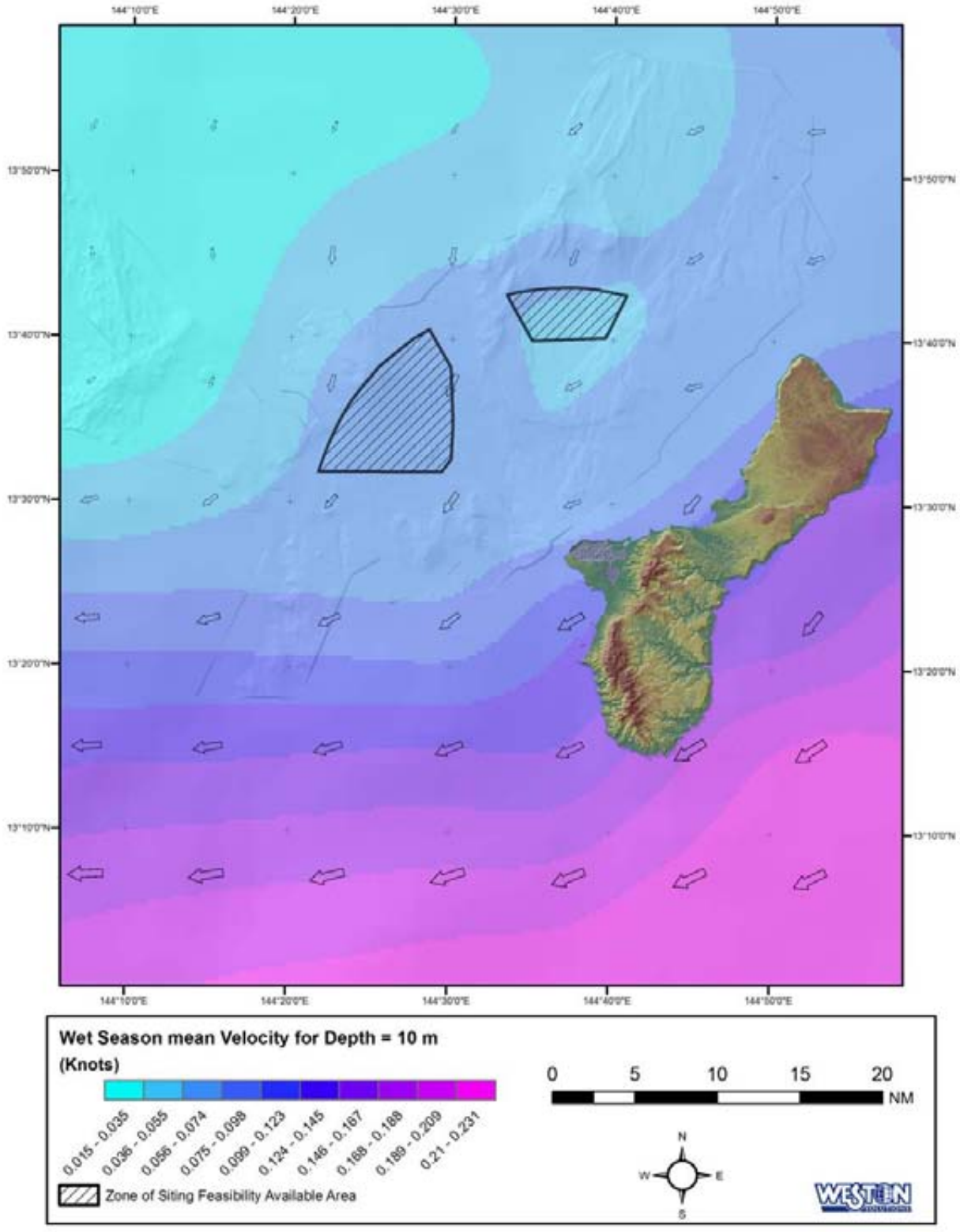

Figure 8. Interpolation of Mean Current Speeds at 10 Meters Depth for the Wet Season

Figure 9 through Figure 12 are vector plots for the four stations (southeast, northeast, southwest and northwest, respectively) that bound the regional study area and Figure 13 is a vector plot for a station near the center of the regional study area and representative of the northwest alternative potential placement site. Each vector represents a single six-hour increment; data were not daily-averaged. Similarly, Figure 14 through Figure 17 are rose diagrams for the four stations (southeast, northeast, southwest and northwest, respectively) that bound the regional study area and Figure 18 is a rose diagram for a station near the center of the regional study area and representative of the northwest alternative potential site. Each rose diagram represents daily-averaged currents for the entire year, illustrating a directional frequency distribution in 5 degree bins and current speeds. These figures are an alternative method for presenting the same information as Figure 4, however, instead of showing data from all stations at a single depth interval, they show data from a single station at all depth intervals.

These figures confirm the characteristics of the regional current patterns in the surface layer and provide information on any intermediate and bottom layer current patterns. For example, comparing the surface layers shown in the vector plot for station 14° N, 145° E, located in the northeastern corner of the regional study area (Figure 10), with the surface layers shown in the vector plot for station 13.625° N, 144.5° E, located near the center of the regional study area and in the lee of the island (Figure 13), the consistency throughout the year in current velocity in the northeast corner and the high variability in current velocity in the lee of this island is evident. The vector plots show periods of strong, uniform currents lasting two to three weeks separated by periods of inconsistent velocities.

For the most part, the current pattern observed at the surface is evident to depths of approximately 650 to 1,000 ft (200 to 300 m). Though similar directional patterns, the current speeds typically decrease from an average of 0.33-0.49 ft/s (10-15 cm/s) with a maximum of about 0.98 ft/s (30 cm/s) at the surface to an average of 0.16 ft/s (5 cm/s) with a maximum of about 0.33 ft/s (10 cm/s) at 1,000 ft (300 m) depth.

4.1.2 Intermediate Layer Currents

Similar to previous figures, Figure 19 and Figure 20 illustrate the intermediate layer currents on a regional scale and Figure 21 through Figure 28 are graphical interpolations of these data generated from a GIS that show the mean current direction and speed for the dry and wet seasons. Figure 19 shows the upper portion of this layer at 1,300 ft (400 m) depth and Figure 20 shows the lower portion of this layer at 4,900 ft (1,500 m) depth. At 1,300 ft (400 m), seasonal differences in the current pattern are apparent, but negligible. Throughout most of the year, the currents approach Guam from the east, similar to the currents at the surface. At this intermediate depth, the currents begin to show evidence of flowing along the isobaths, with the structure of the Marianas Ridge influencing current patterns. Directly east and southeast of Guam, the currents tend in a southwesterly direction, then once past the southern part of the island, the currents uniformly turn towards the northwest. Along the western boundary of the regional study area, the currents are strong and towards the north. Directly on the west side of Guam, the currents wrapping around the southern tip of the island turn further, trending northeast and eventually returning to the eastern side of the island as they cross the Rota Banks, just north of Guam. Currents approaching northeast of Guam, north of the Rota Banks, flow in a uniform westerly direction.

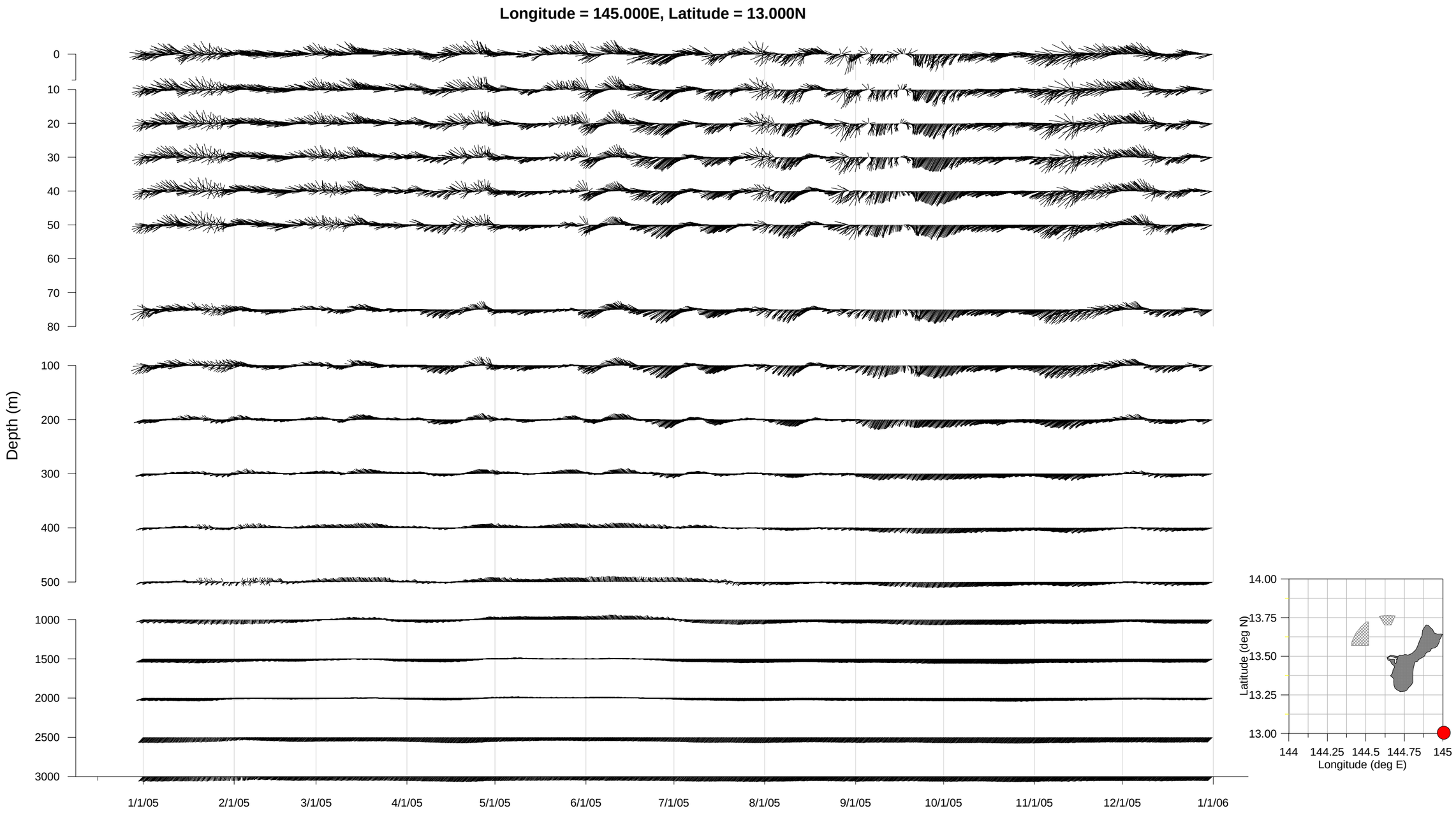

Figure 9. Vector Plots of Current Velocity by Depth for the Southeast Regional Boundary

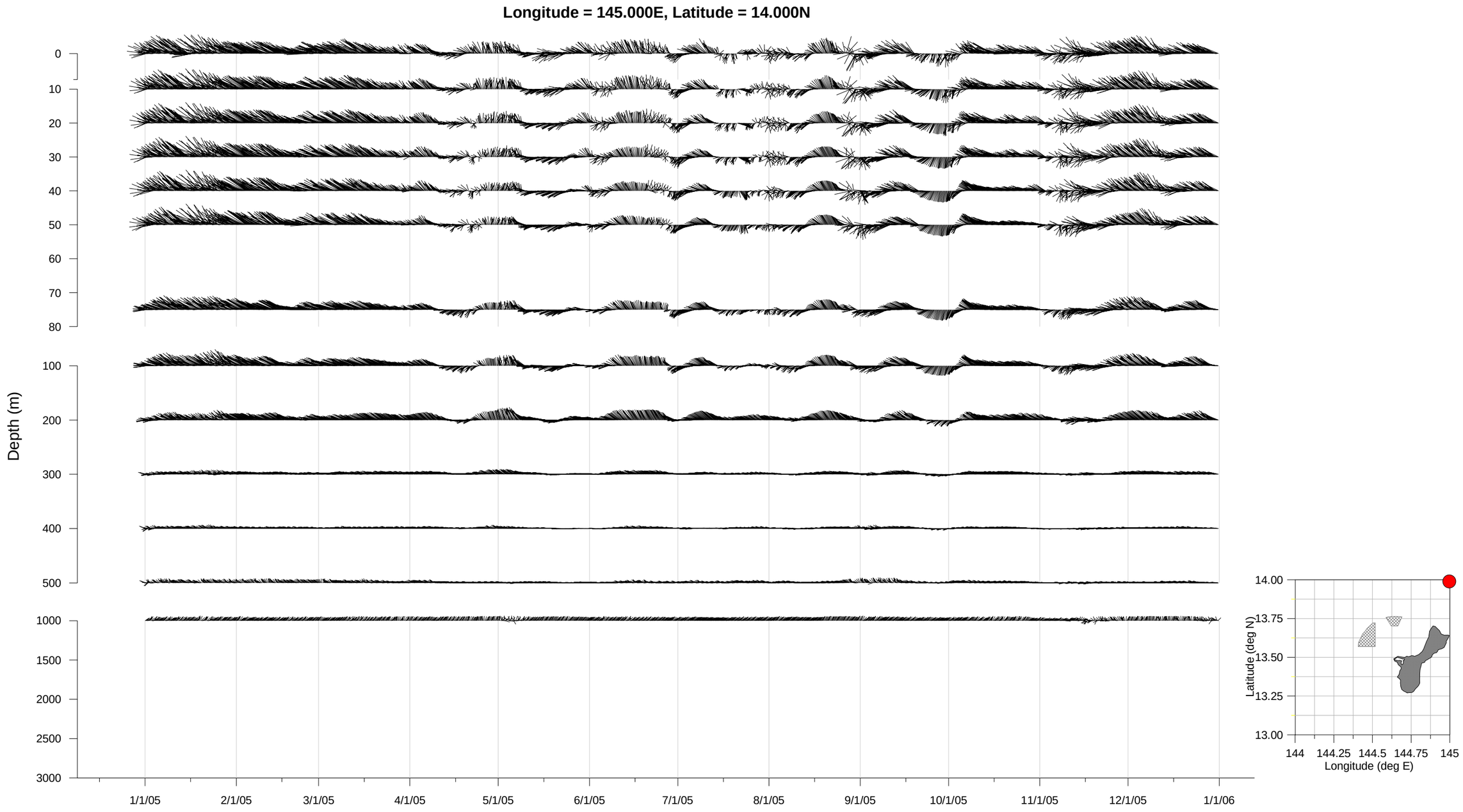

Figure 10. Vector Plots of Current Velocity by Depth for the Northeast Regional Boundary

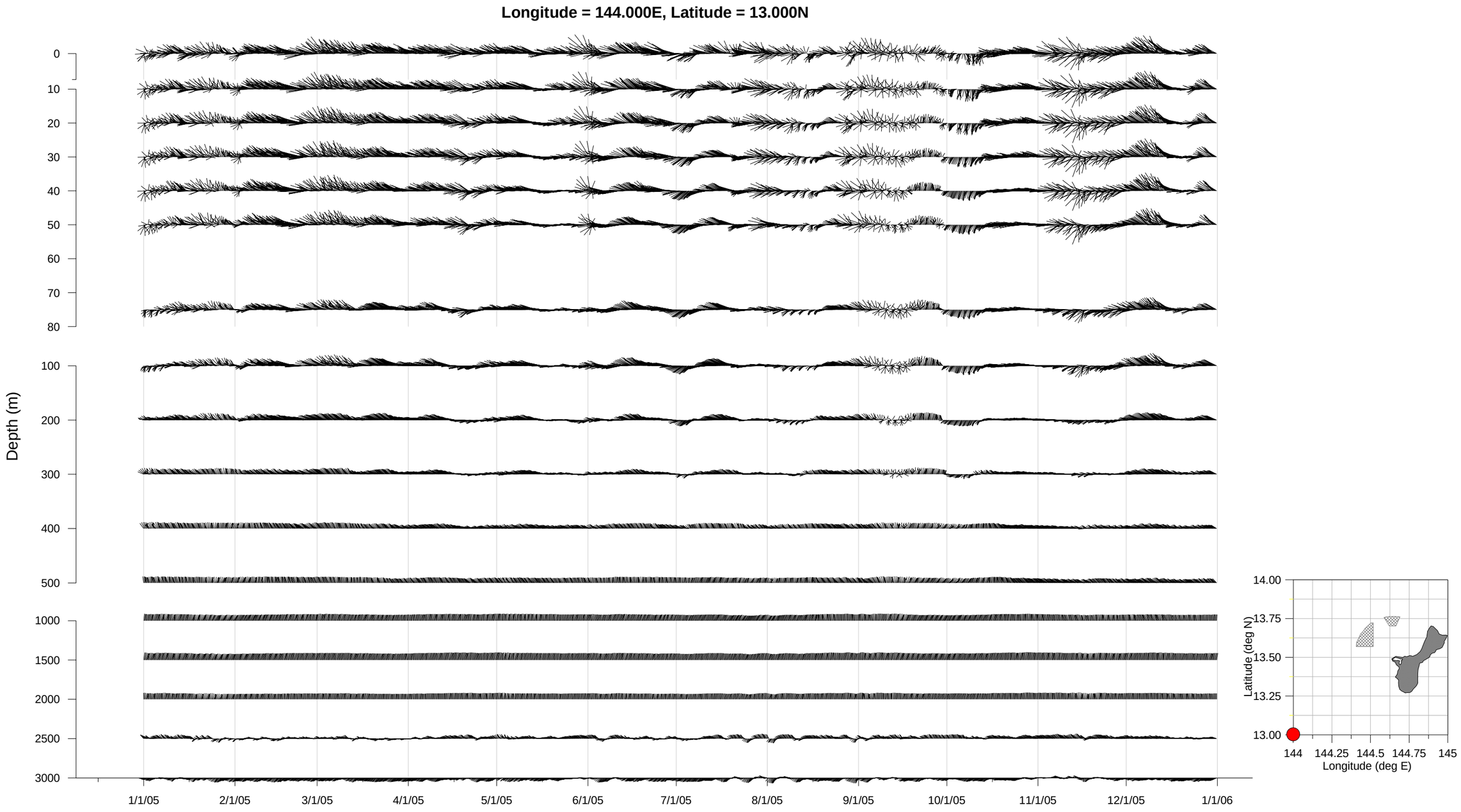

Figure 11. Vector Plots of Current Velocity by Depth for the Southwest Regional Boundary

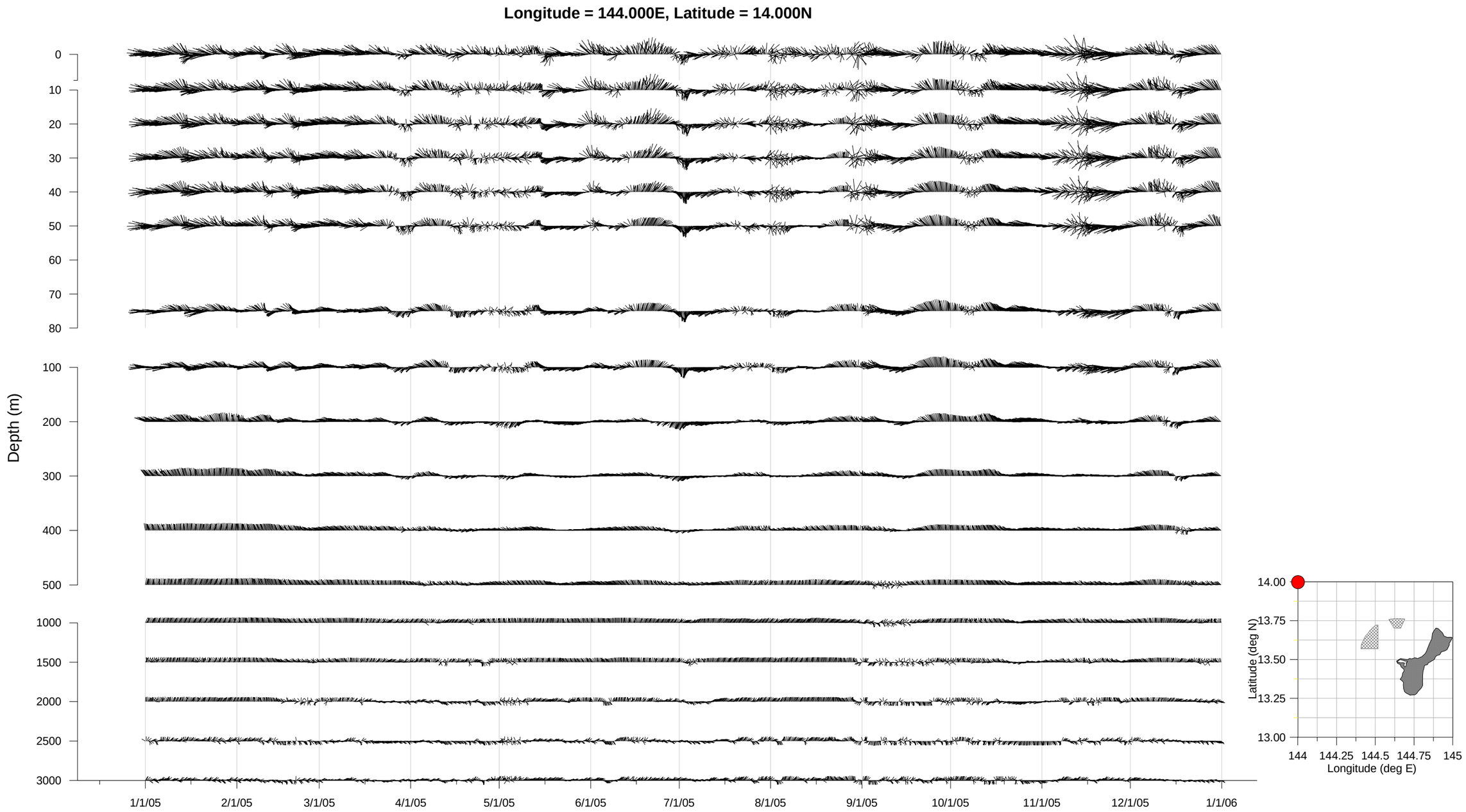

Figure 12. Vector Plots of Current Velocity by Depth for the Northwest Regional Boundary

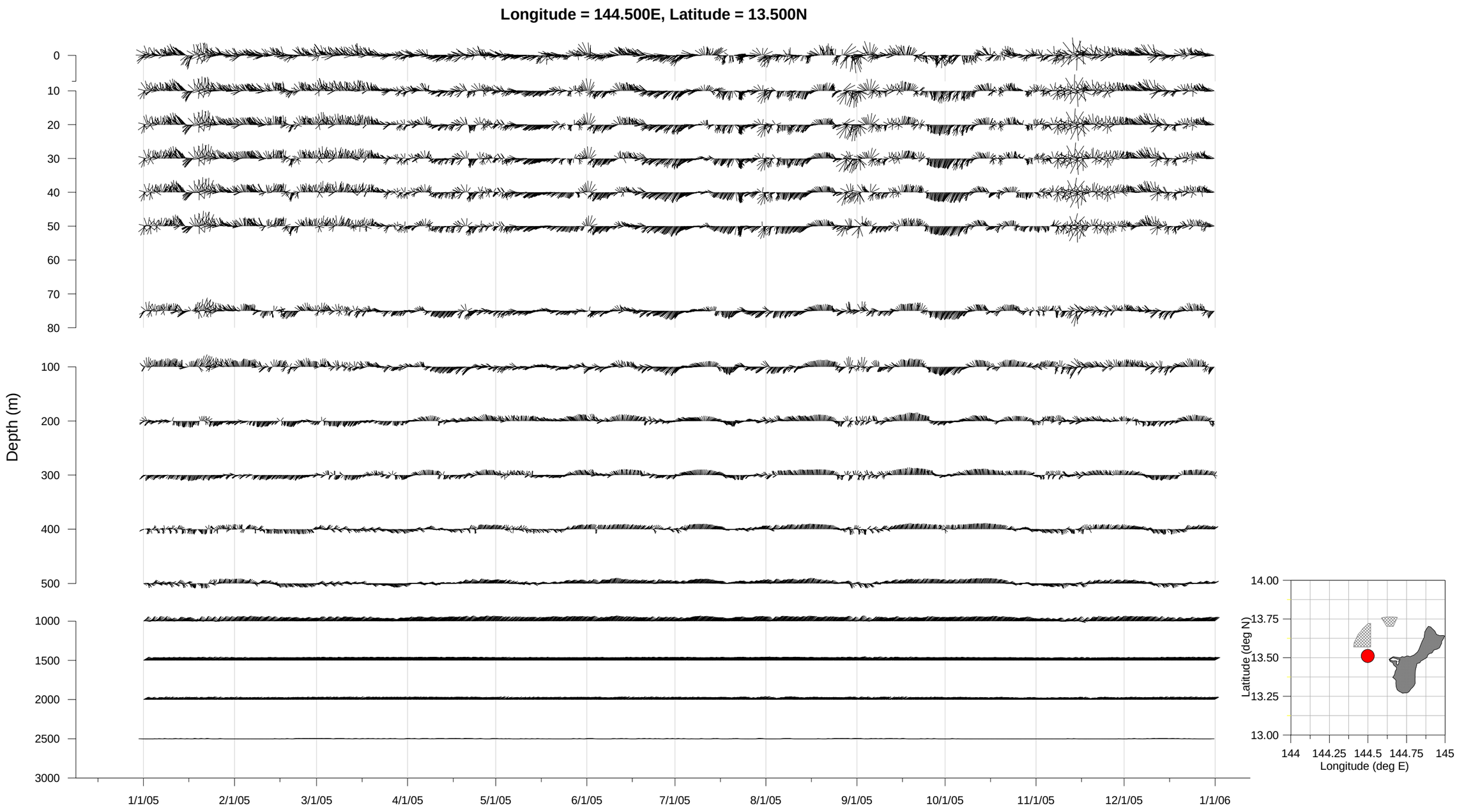

Figure 13. Vector Plots of Current Velocity by Depth for a Location Near the Northwest ODMDS Alternative Area.

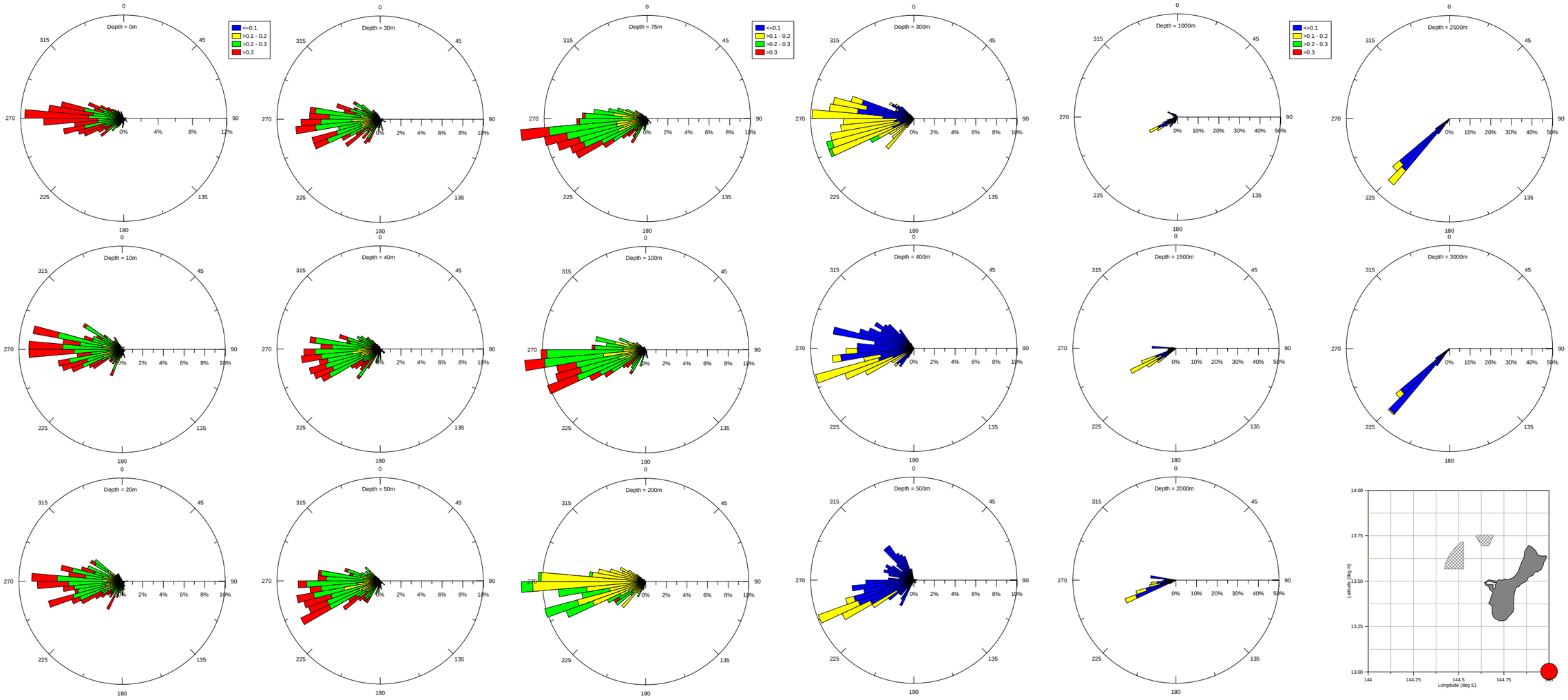

Figure 14. Rose Diagram of Current Velocities by Depth for the Southeast Regional Boundary

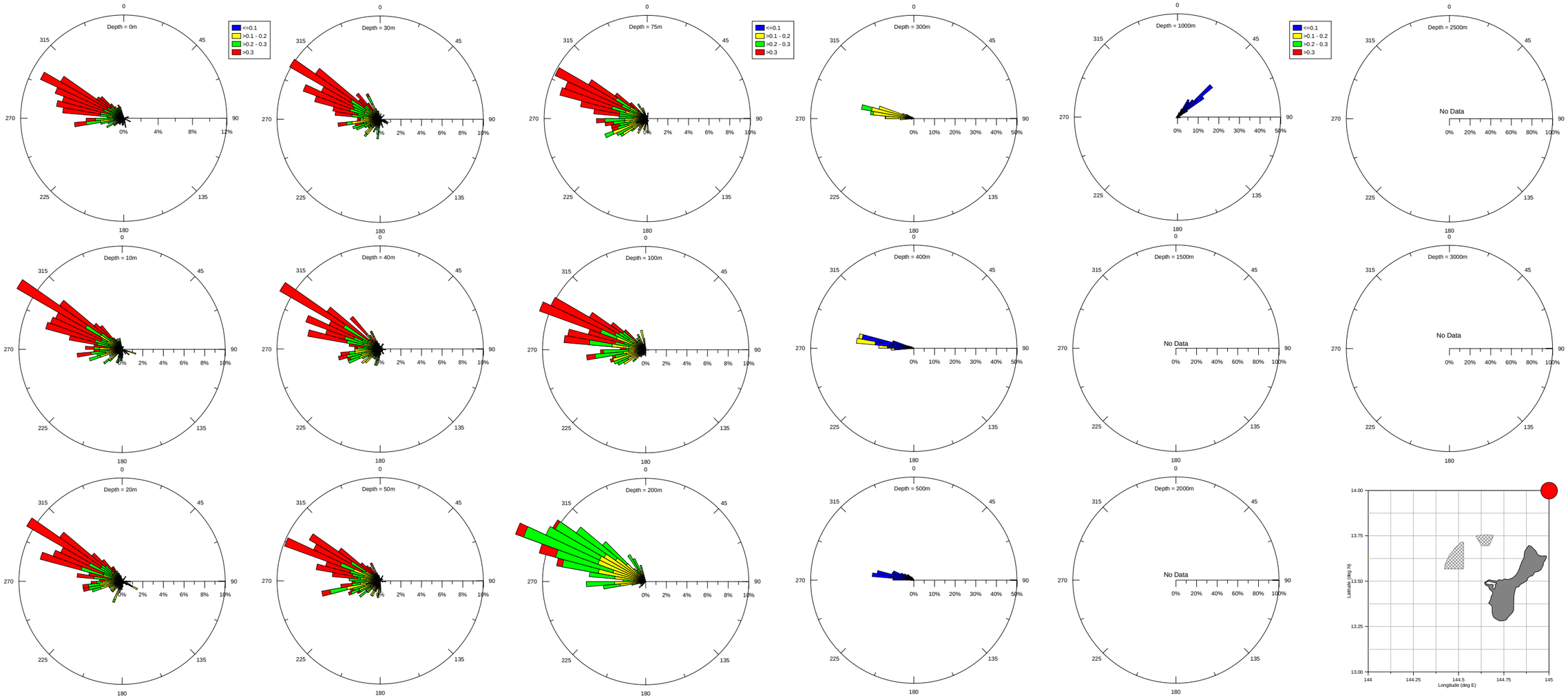

Figure 15. Rose Diagram of Current Velocities by Depth for the Northeast Regional Boundary

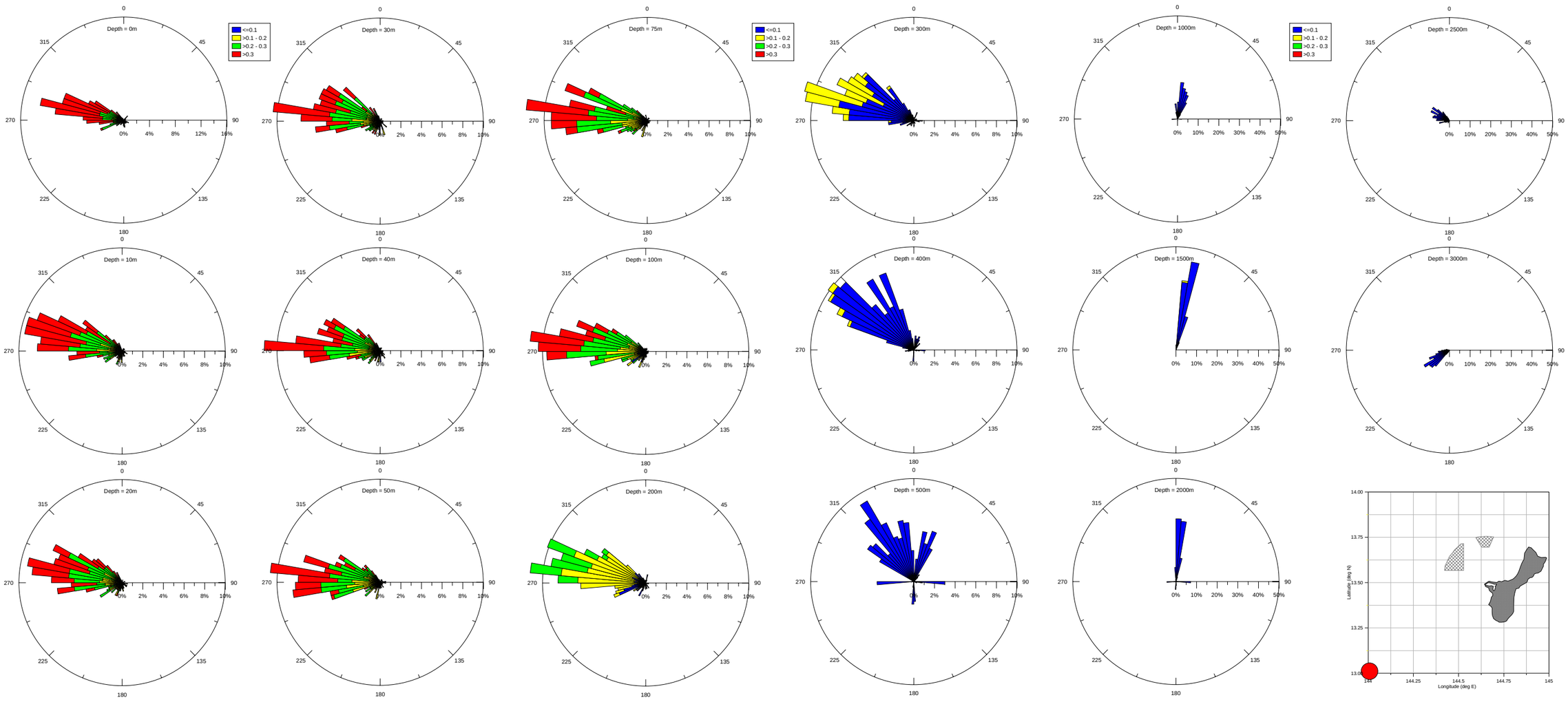

Figure 16. Rose Diagram of Current Velocities by Depth for the Southwest Regional Boundary

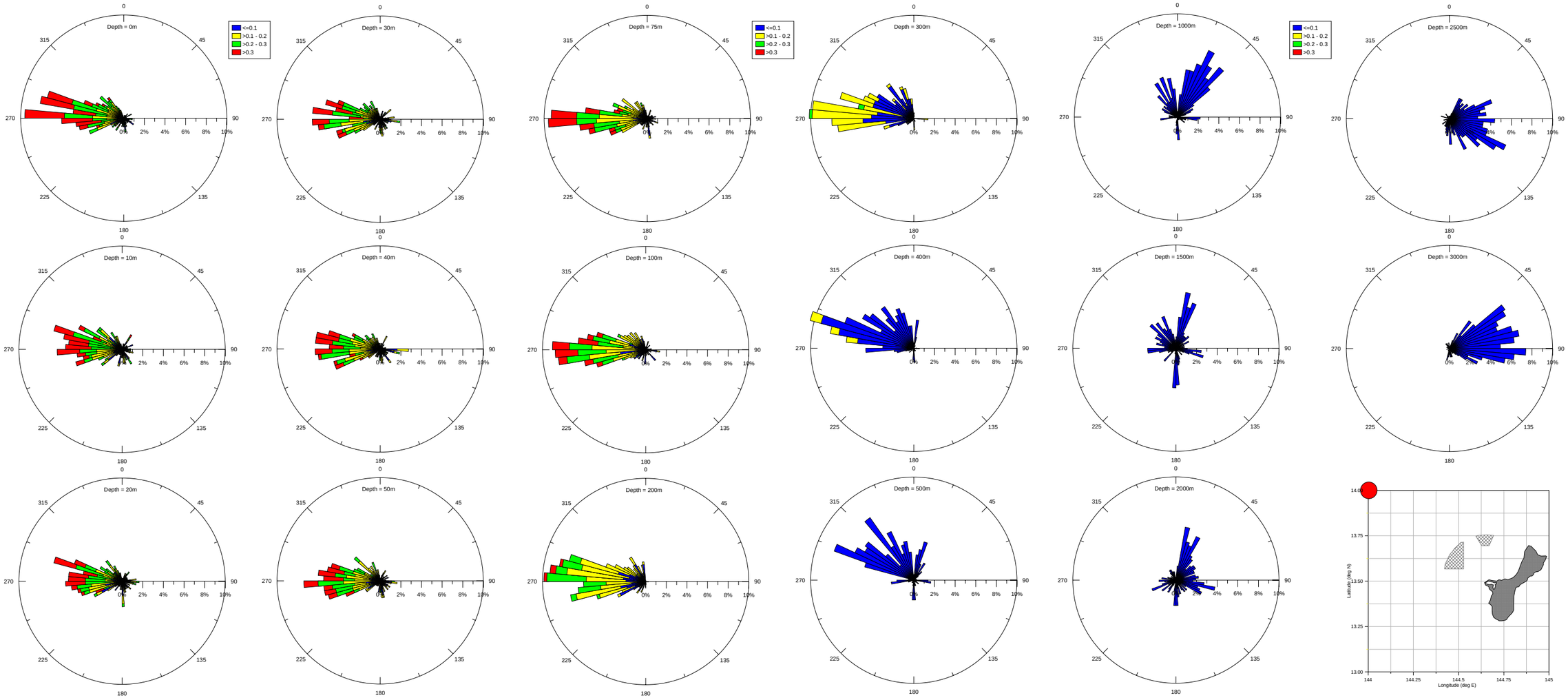

Figure 17. Rose Diagram of Current Velocities by Depth for the Northwest Regional Boundary

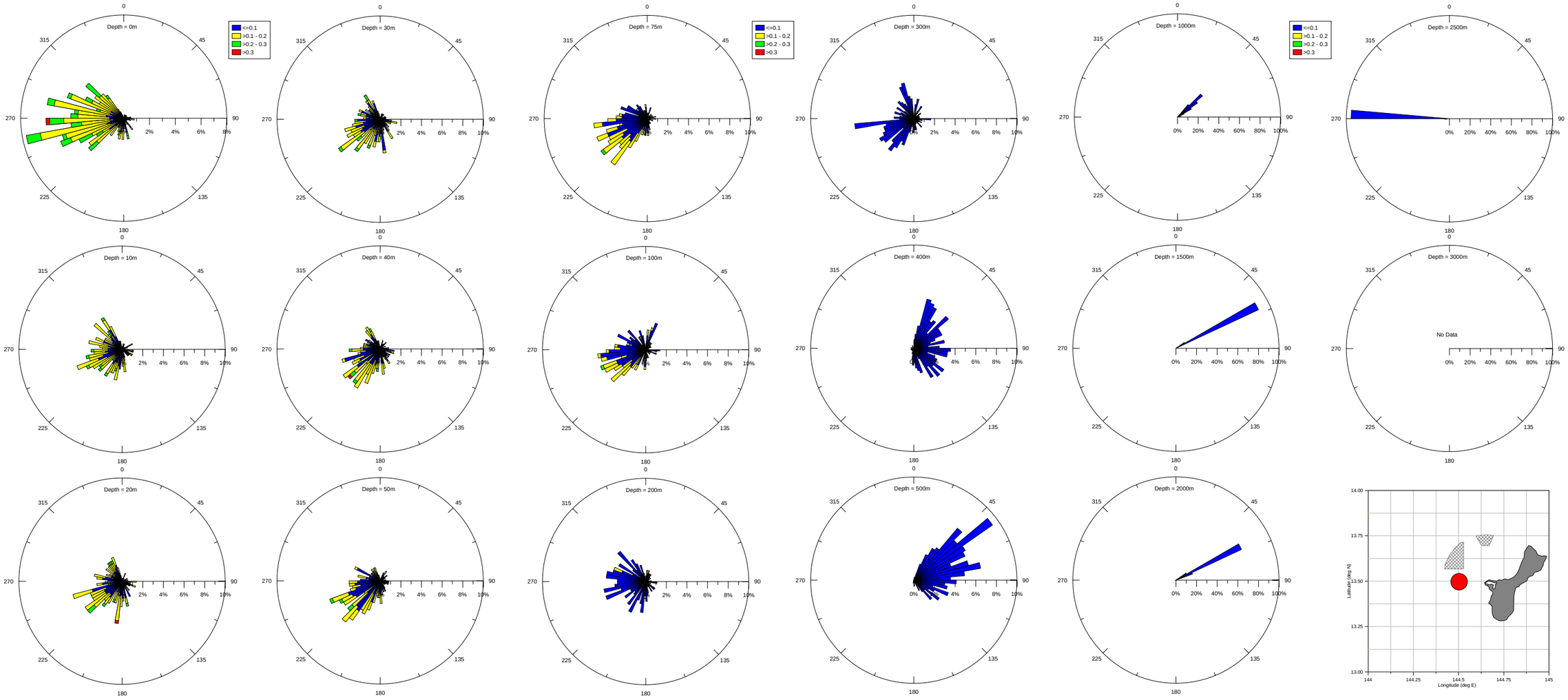

Figure 18. Rose Diagram of Current Velocities by Depth for a Location Near the Northwest ODMDS Alternative Area

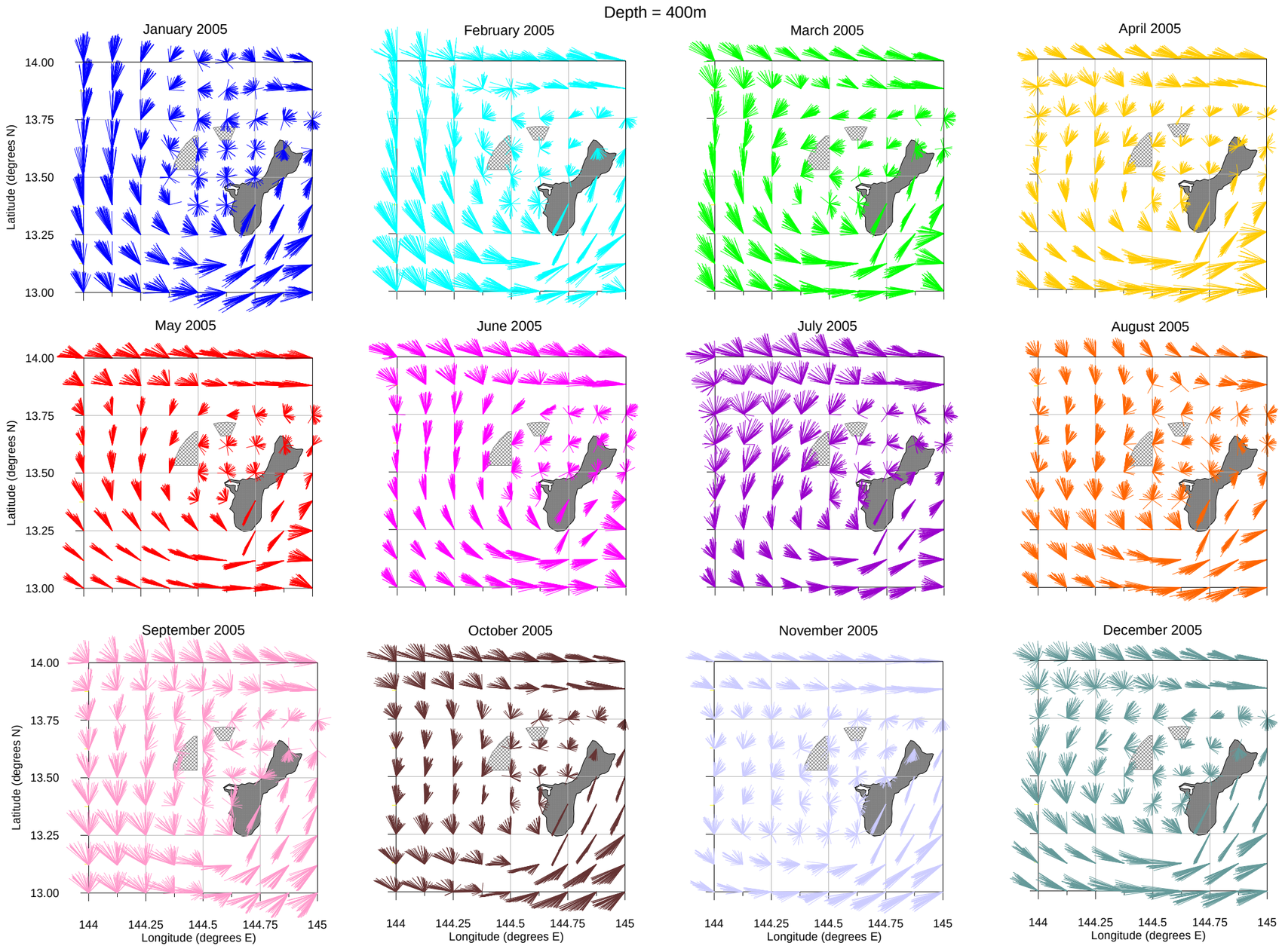

Figure 19. Vector Plots of Daily Averaged Current Velocities by Month for Each Location at 1,300 ft (400 m) Depth

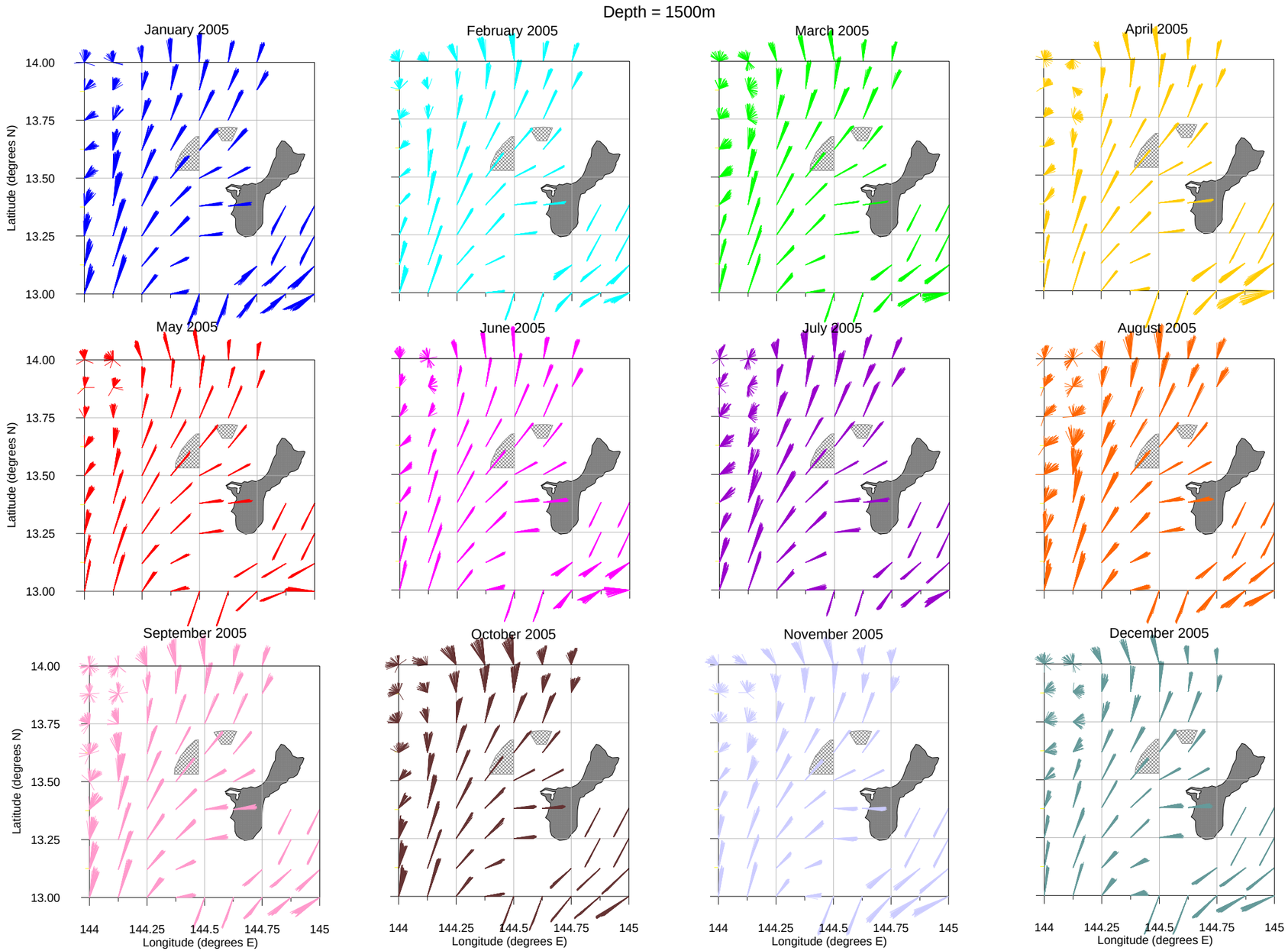

Figure 20. Vector Plots of Daily Averaged Current Velocities by Month for Each Location at 4,900 ft (1,500 m) Depth

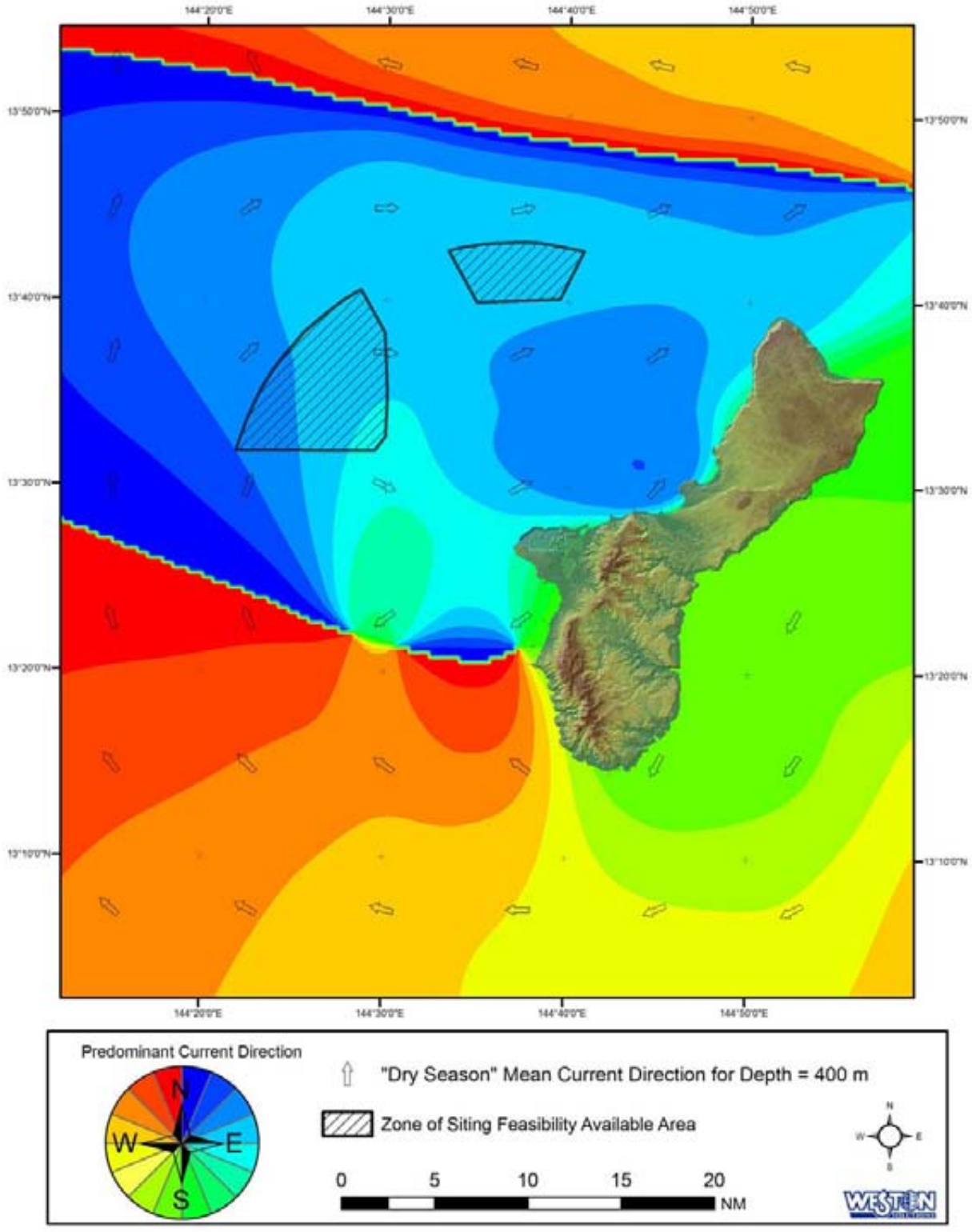

Figure 21. Interpolation of Mean Current Directions at 400 Meters Depth for the Dry Season

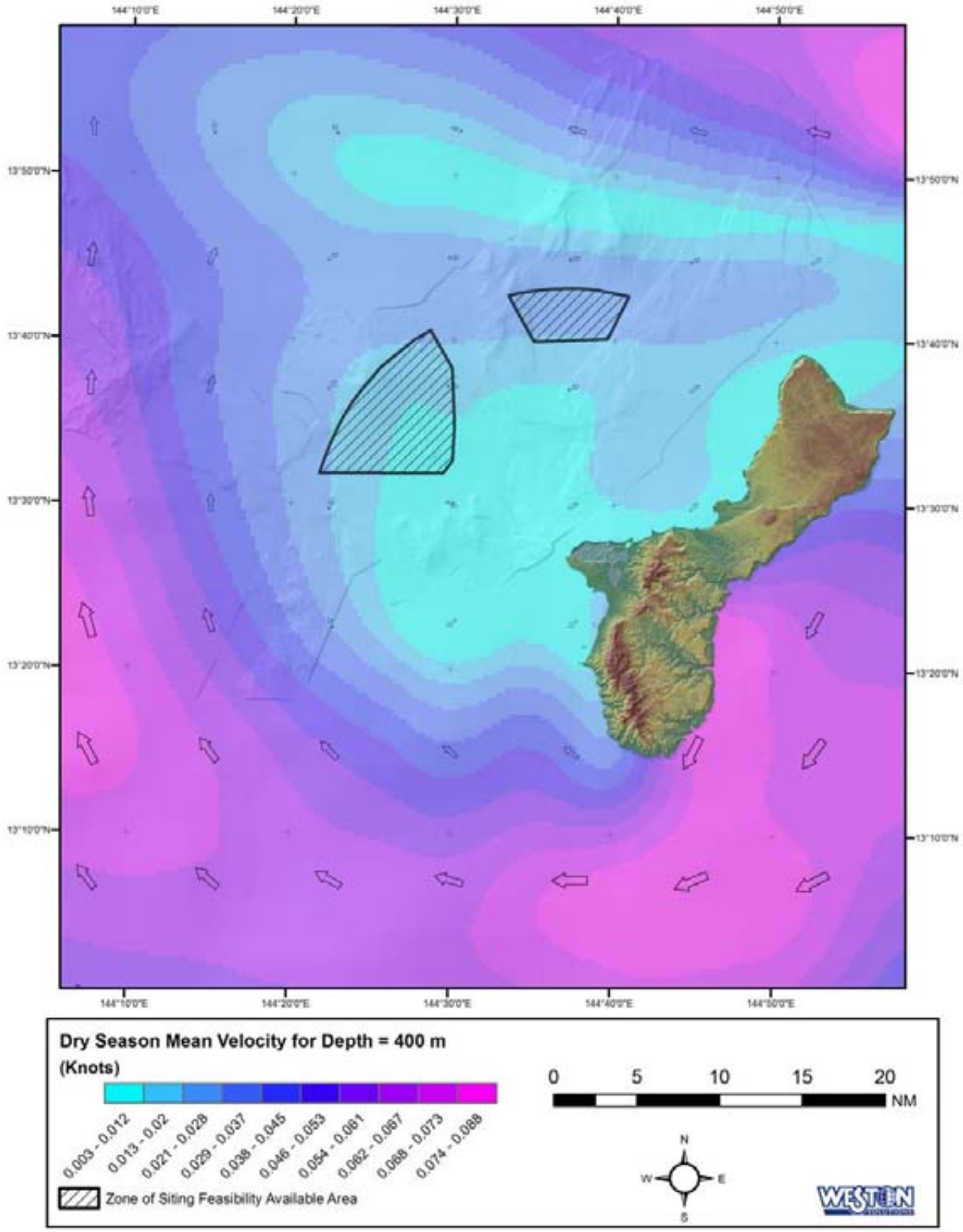

Figure 22. Interpolation of Mean Current Speeds at 400 Meters Depth for the Dry Season

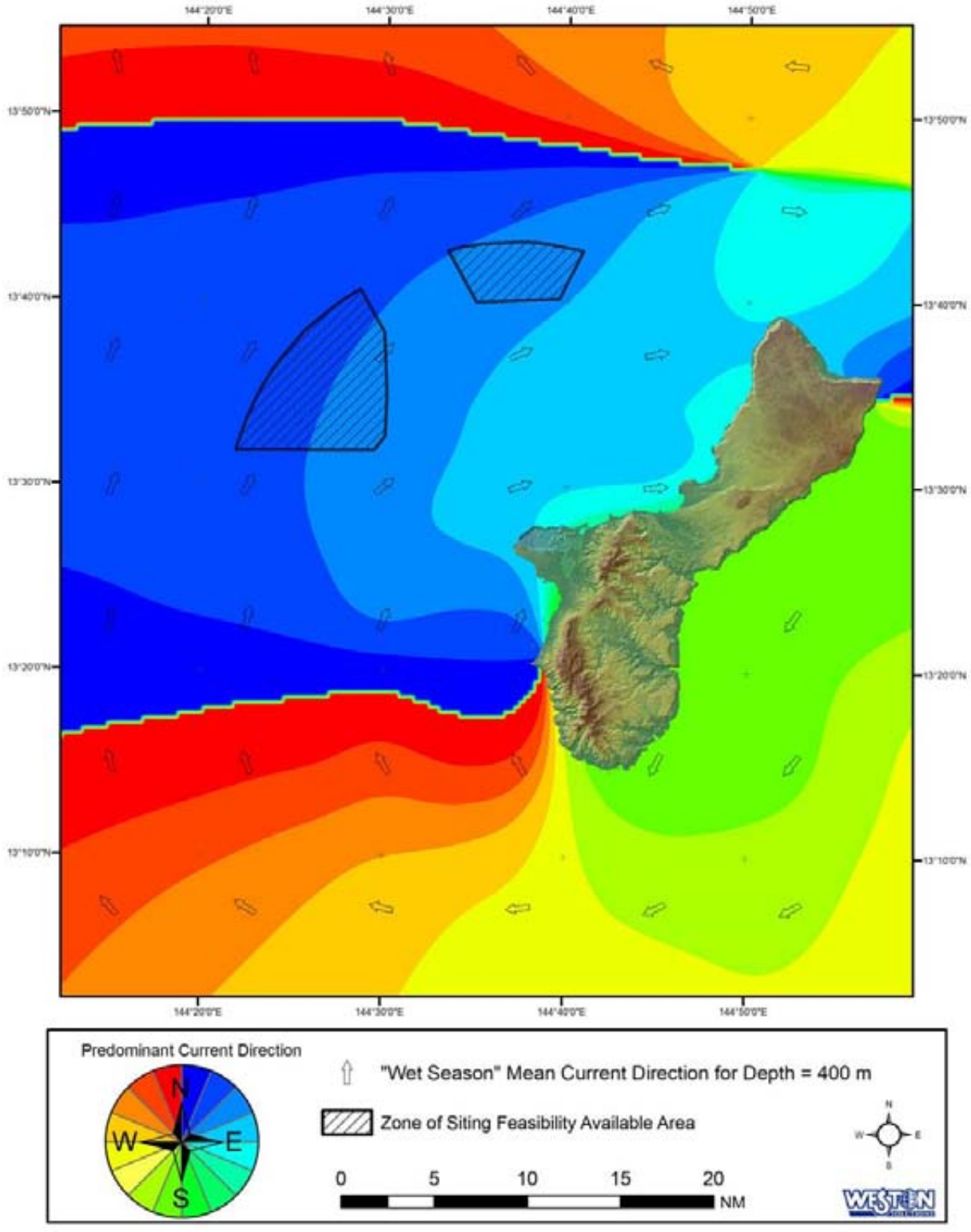

Figure 23. Interpolation of Mean Current Directions at 400 Meters Depth for the Wet Season

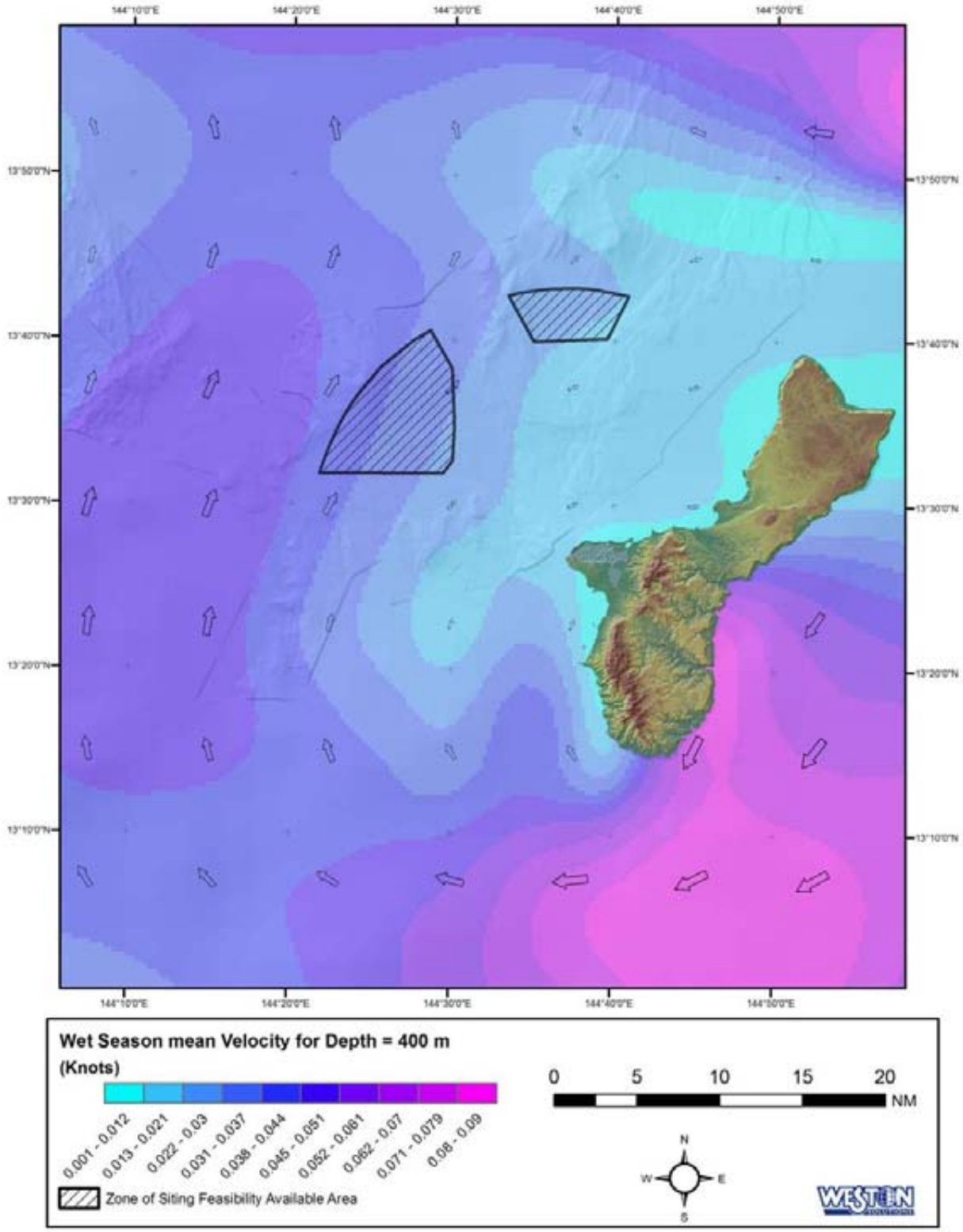

Figure 24. Interpolation of Mean Current Speeds at 400 Meters Depth for the Wet Season

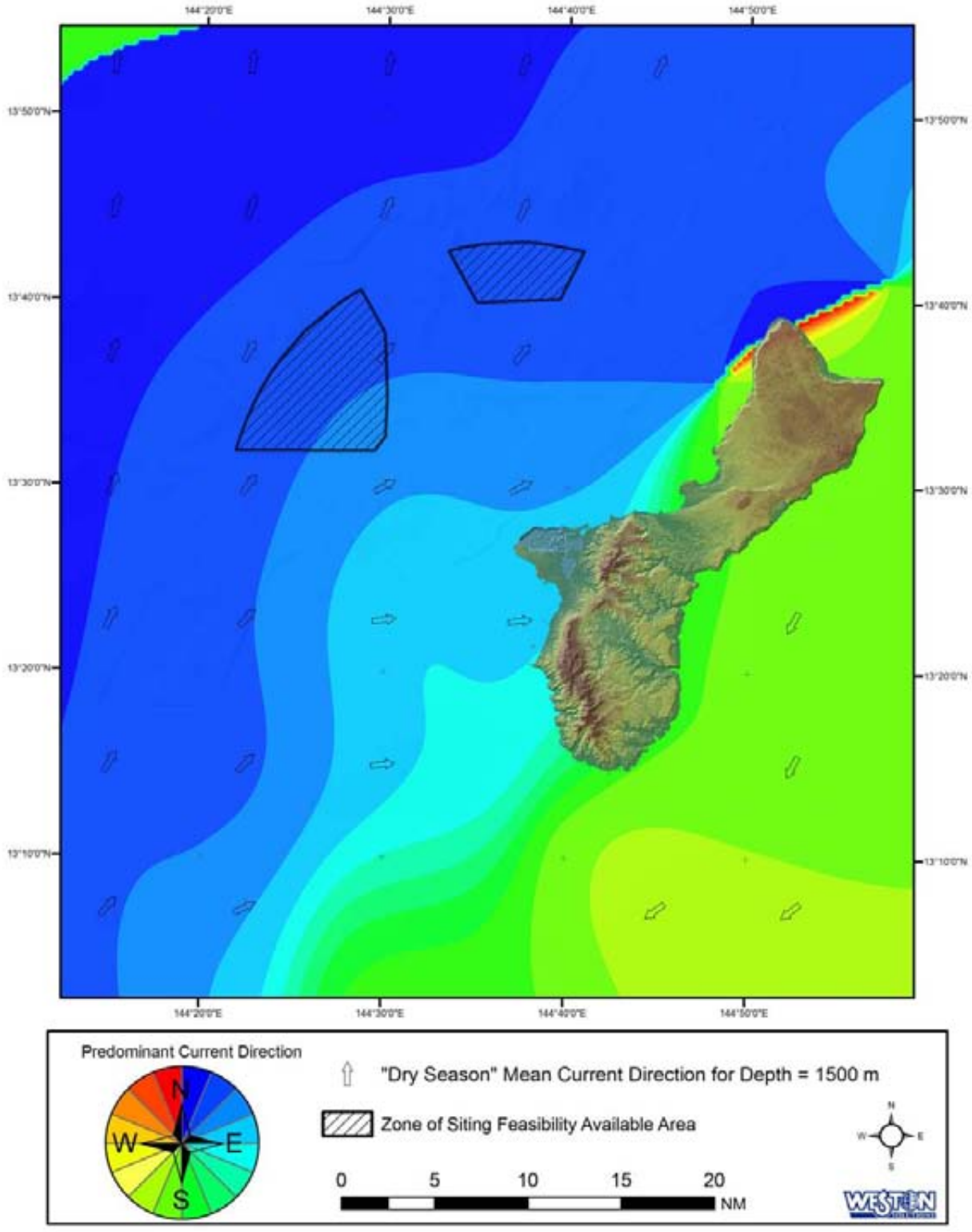

Figure 25. Interpolation of Mean Current Directions at 1500 Meters Depth for the Dry Season

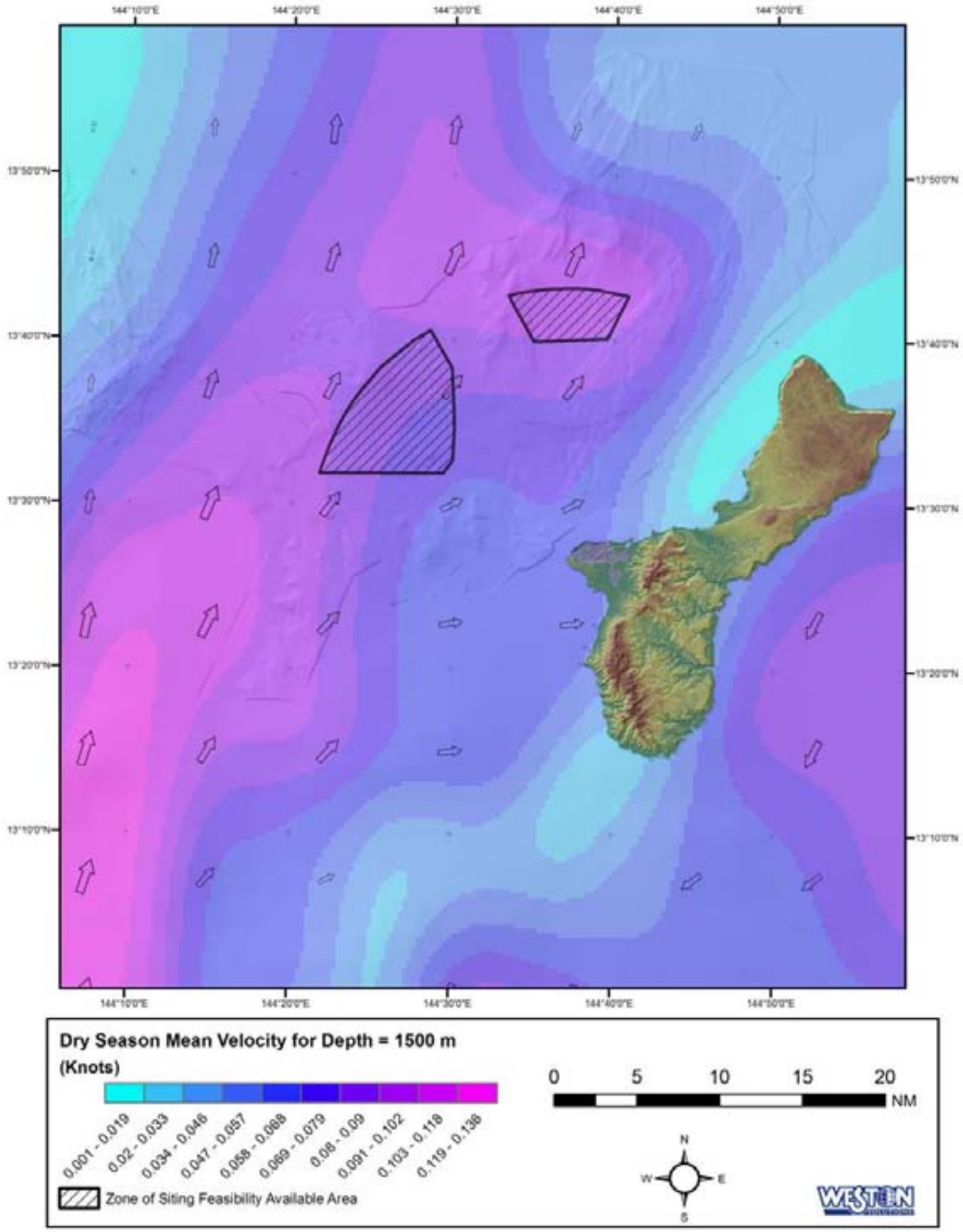

Figure 26. Interpolation of Mean Current Speeds at 1500 Meters Depth for the Dry Season

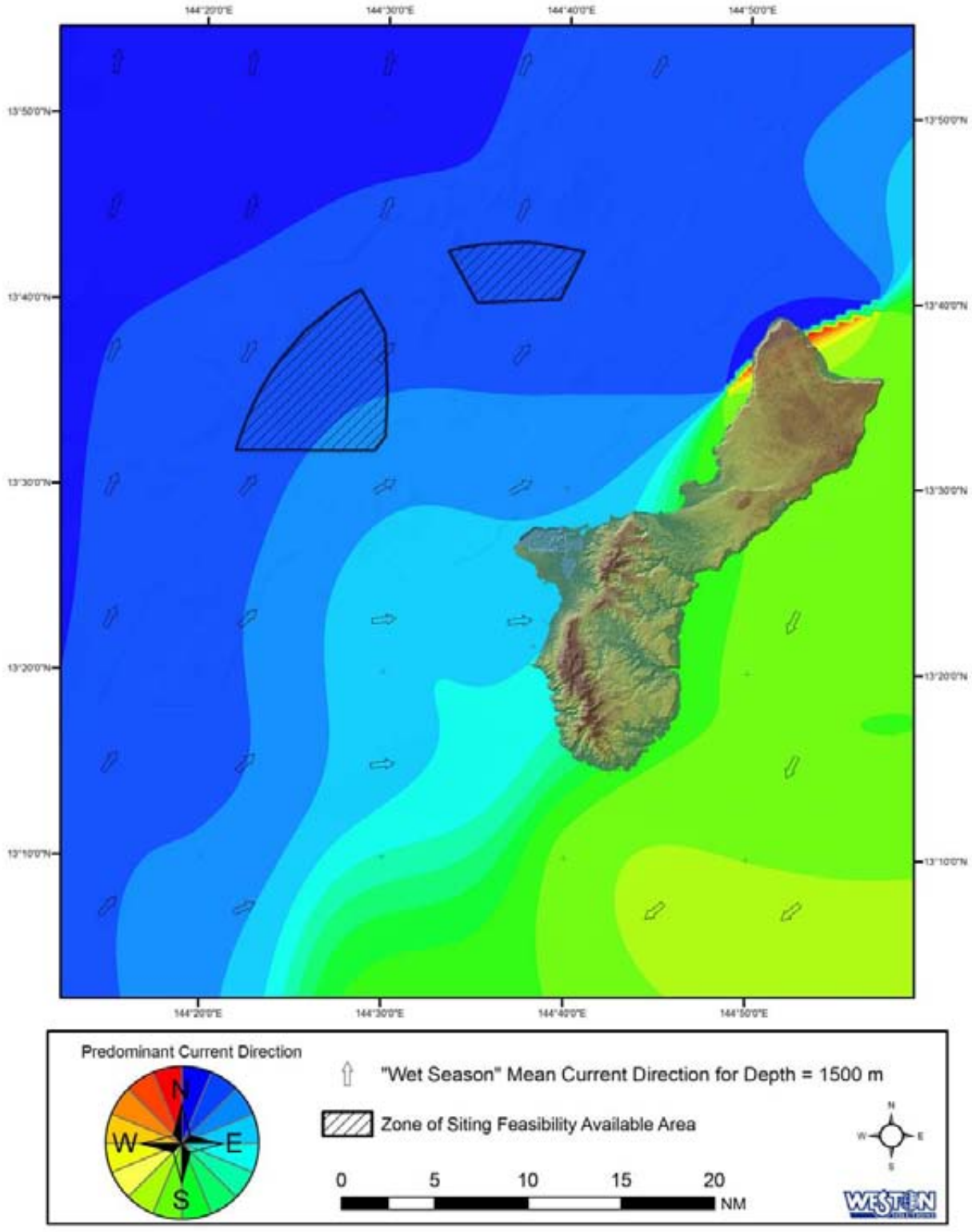

Figure 27. Interpolation of Mean Current Directions at 1500 Meters Depth for the Wet Season

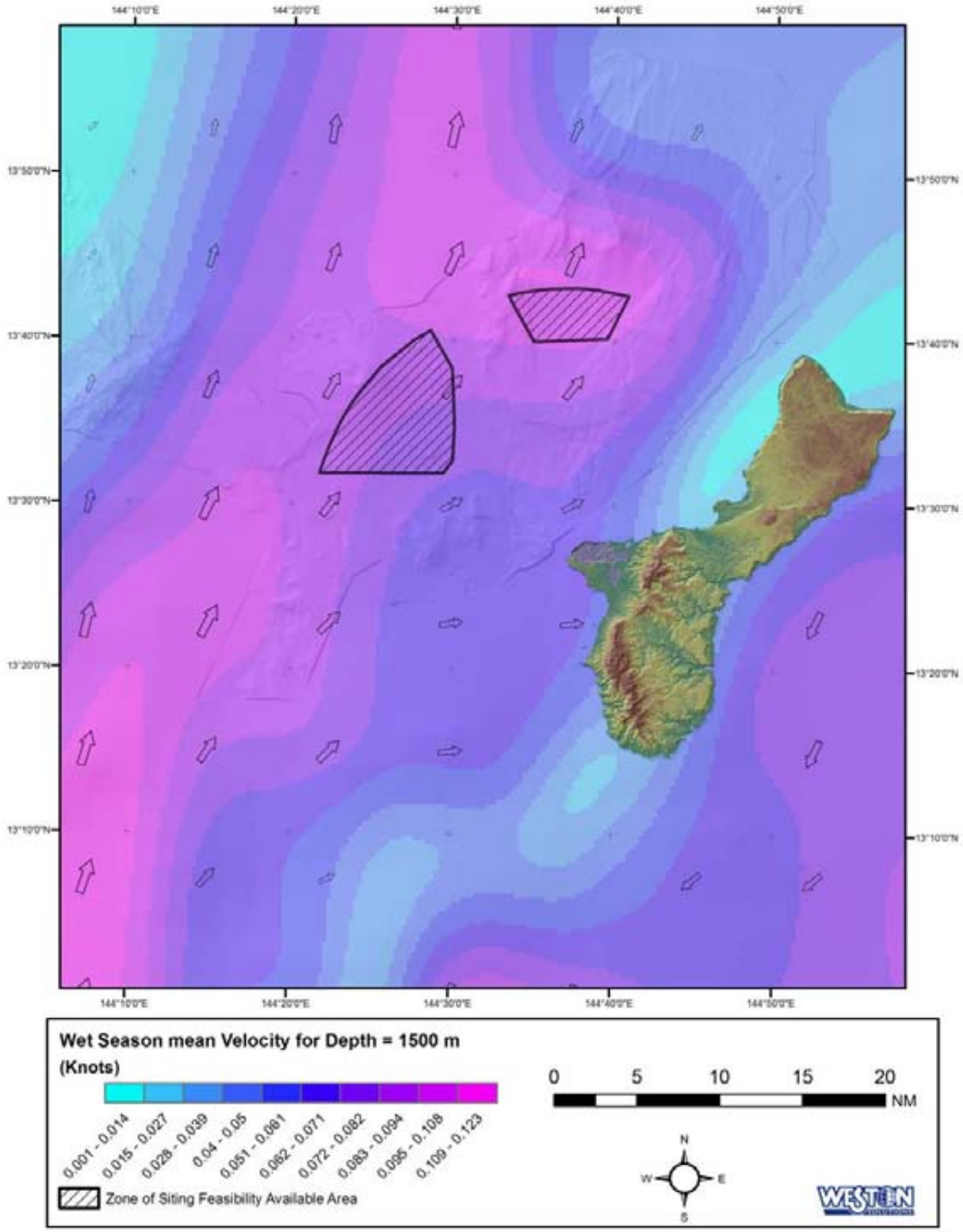

Figure 28. Interpolation of Mean Current Speeds at 1500 Meters Depth for the Wet Season

At 4,900 ft (1,500 m) depth, there is no evidence of seasonal patterns. The Marianas Ridge, which trends from the southwest of Guam and continues towards the northeast is apparent and strongly influences the current patterns. On the east side of the Marianas Ridge, currents are highly uniform, trending in a southwesterly direction along isobaths at an average speed of 0.16 ft/s (5 cm/s). It is not evident if the currents at this depth, approaching Guam from the Eastern Marianas Basin, flow through a gap in the ridge or if another water body is responsible for the currents on the west side of the Marianas Ridge, however, on the west side of Guam, currents at 4,900 ft (1,500 m) are also highly uniform, though flowing counter to the currents on the east side of the ridge, in a north-northeast direction along isobaths at an average speed of about 0.07-0.16 ft/s (2-5 cm/s).

4.1.3 Bottom Currents

Similar to previous figures, Figure 29 illustrates the bottom layer currents on a regional scale and Figure 30 through Figure 33 are graphical interpolations of these data generated from a GIS that show the mean current direction and speed for the dry and wet seasons. Two distinct bottom currents are evident, depending on the relation to the Marianas Ridge. East of the Marianas Ridge, the bottom current below 8,200 ft (2,500 m) continued to be very uniform and trends in a southwesterly direction at an average speed of about 0.10-0.13 ft/s (3-4 cm/s), flowing along isobaths, similar to the currents in the intermediate layer. West of the Marianas Ridge, there appeared to be a poorly developed countercurrent relative to the intermediate layer with eratic currents, ranging from a north-northwesterly direction to a south-southwesterly direction, though areas with a predominant easterly component occur. Current speeds averaged about 0.03-0.07 ft/s (1-2 cm/s). There were no seasonal differences in the bottom currents (Figure 34).

4.2 ODMDS Alternative Site-Specific Patterns

The two areas identified during the ZSF study as suitable locations for the placement of an ODMDS occur approximately 8.9 and 12.4 nm (16.4 and 23.0 km) northwest and north of the entrance to Outer Apra Harbor, respectively. These locations are both in the area of highly variable currents in the lee of the island, as described in the previous section (Regional Patterns, Surface Currents). With the exception of the surface currents during the winter months, the current regime for both these areas is very similar (Figure 34).

4.2.1 Surface Currents

4.2.1.1 Northwest Alternative

Surface currents are shown in the vector plots in Figure 13 and Figure 35 and the corresponding rose diagrams in Figure 18 and Figure 36. Surface currents at the northwest alternative tend to be highly variable during most of the year, with periods of strong and consistent southward flowing pulses during the wet weather season.

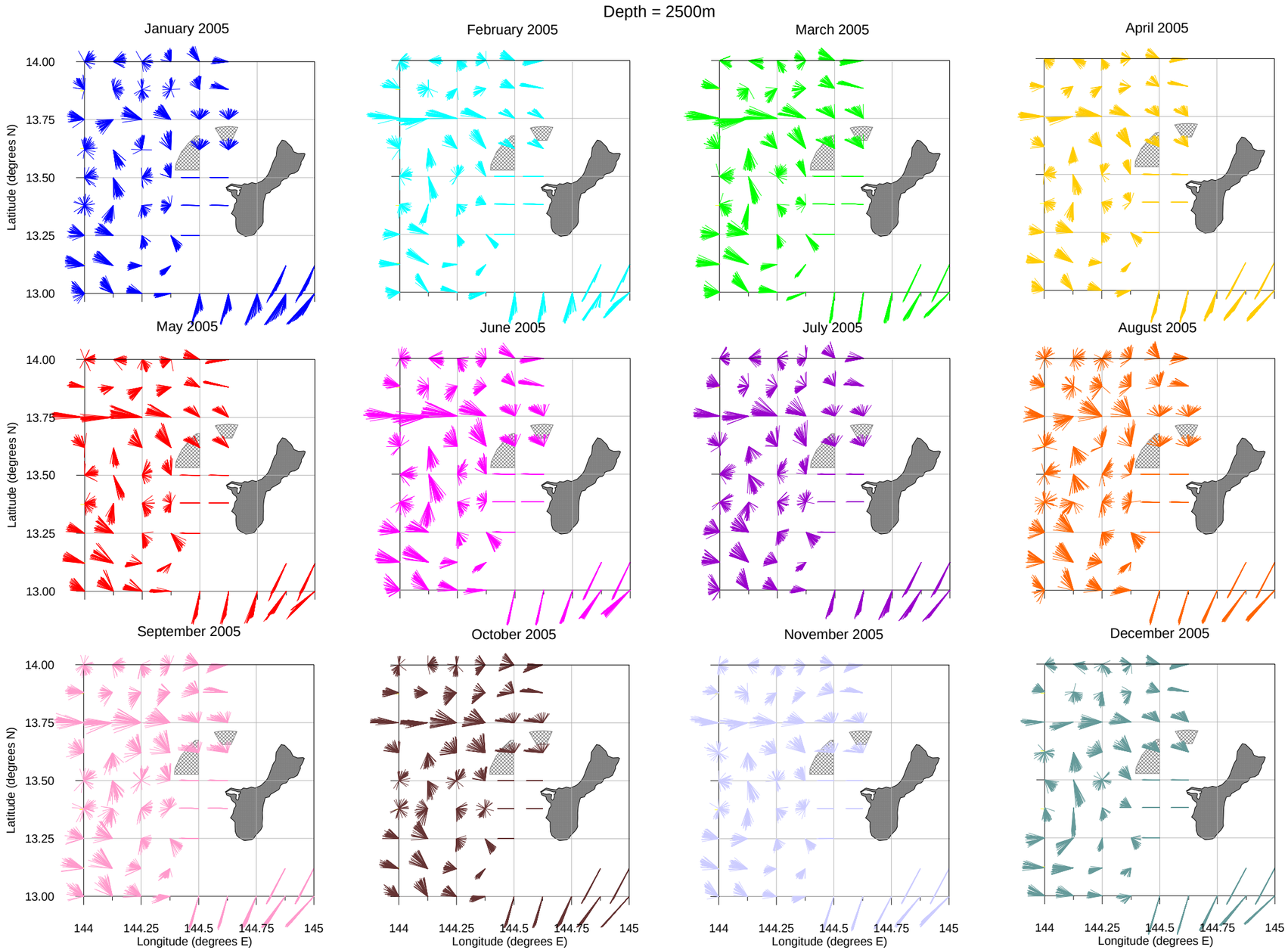

Figure 29. Vector Plots of Daily Averaged Current Velocities by Month for Each Location at 8,200 ft (2,500 m) Depth

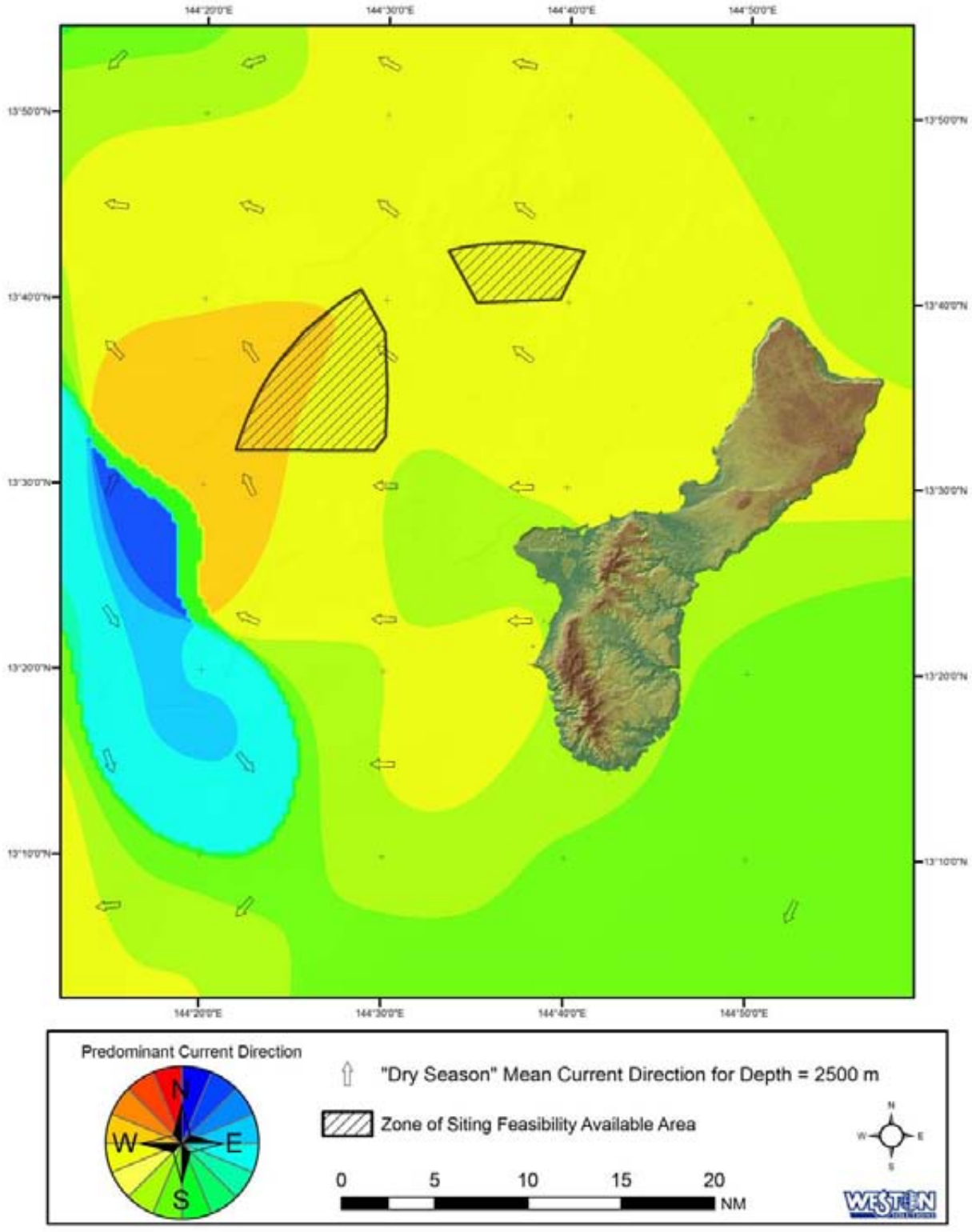

Figure 30. Interpolation of Mean Current Directions at 2500 Meters Depth for the Dry Season

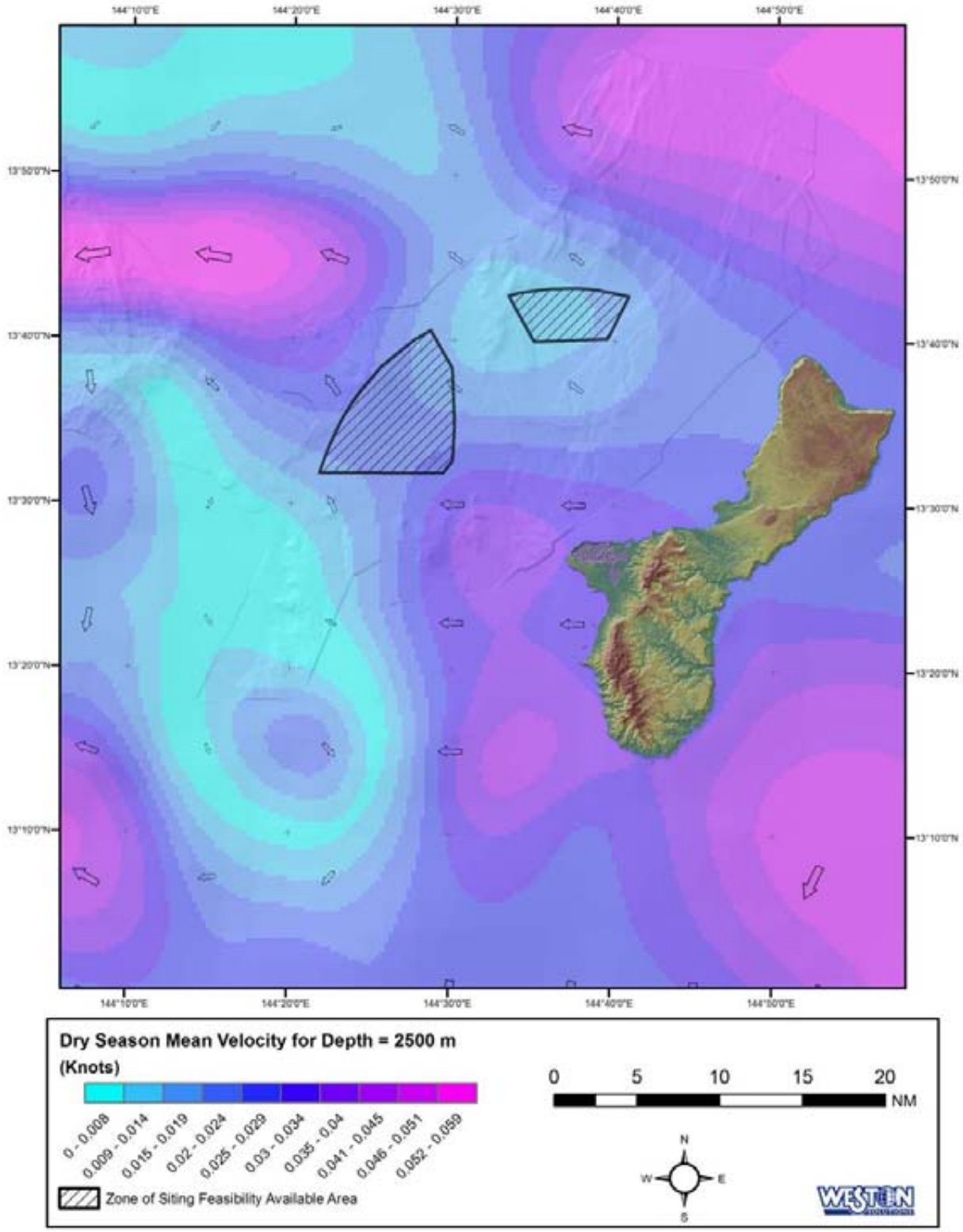

Figure 31. Interpolation of Mean Current Speeds at 2500 Meters Depth for the Dry Season

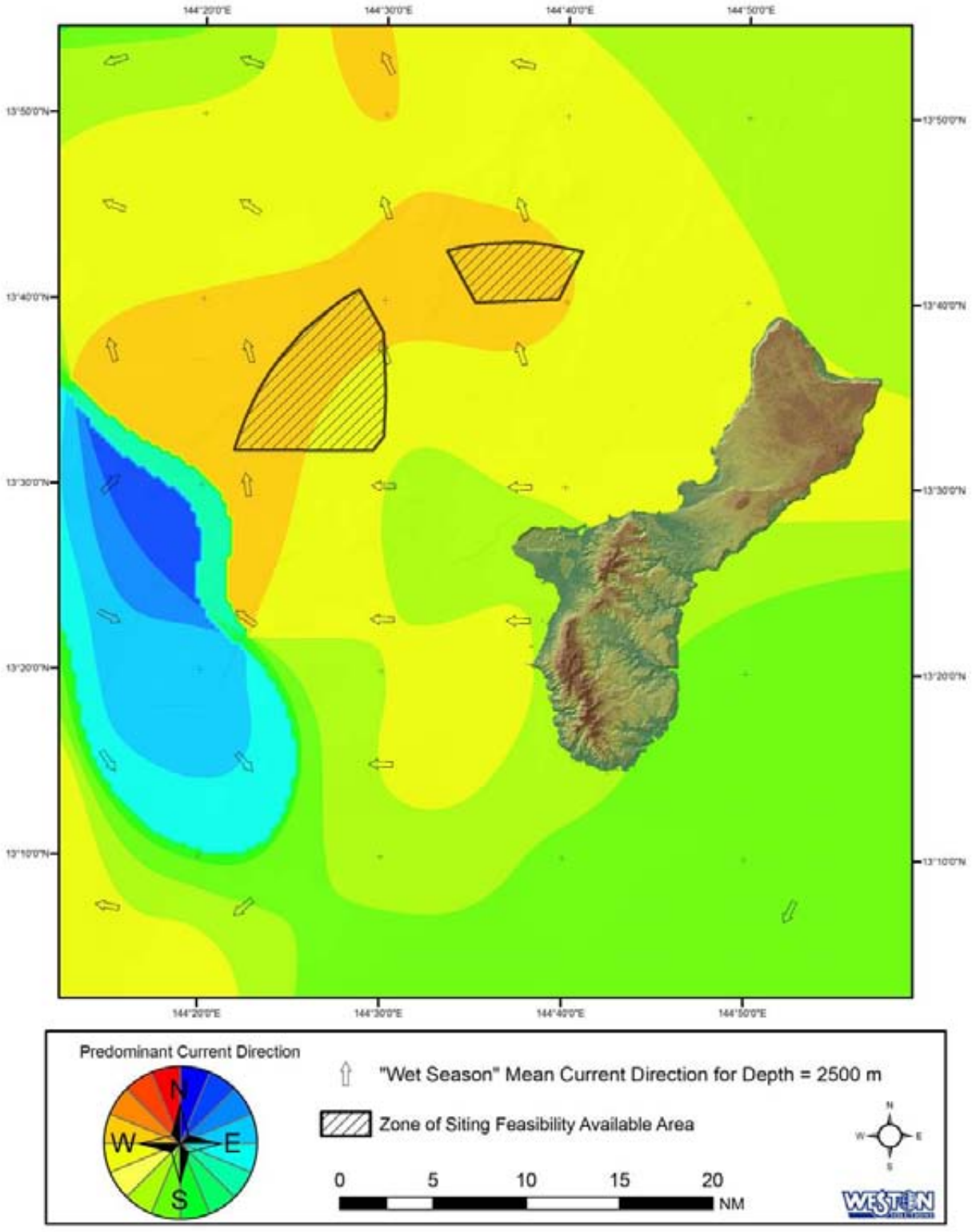

Figure 32. Interpolation of Mean Current Directions at 2500 Meters Depth for the Wet Season

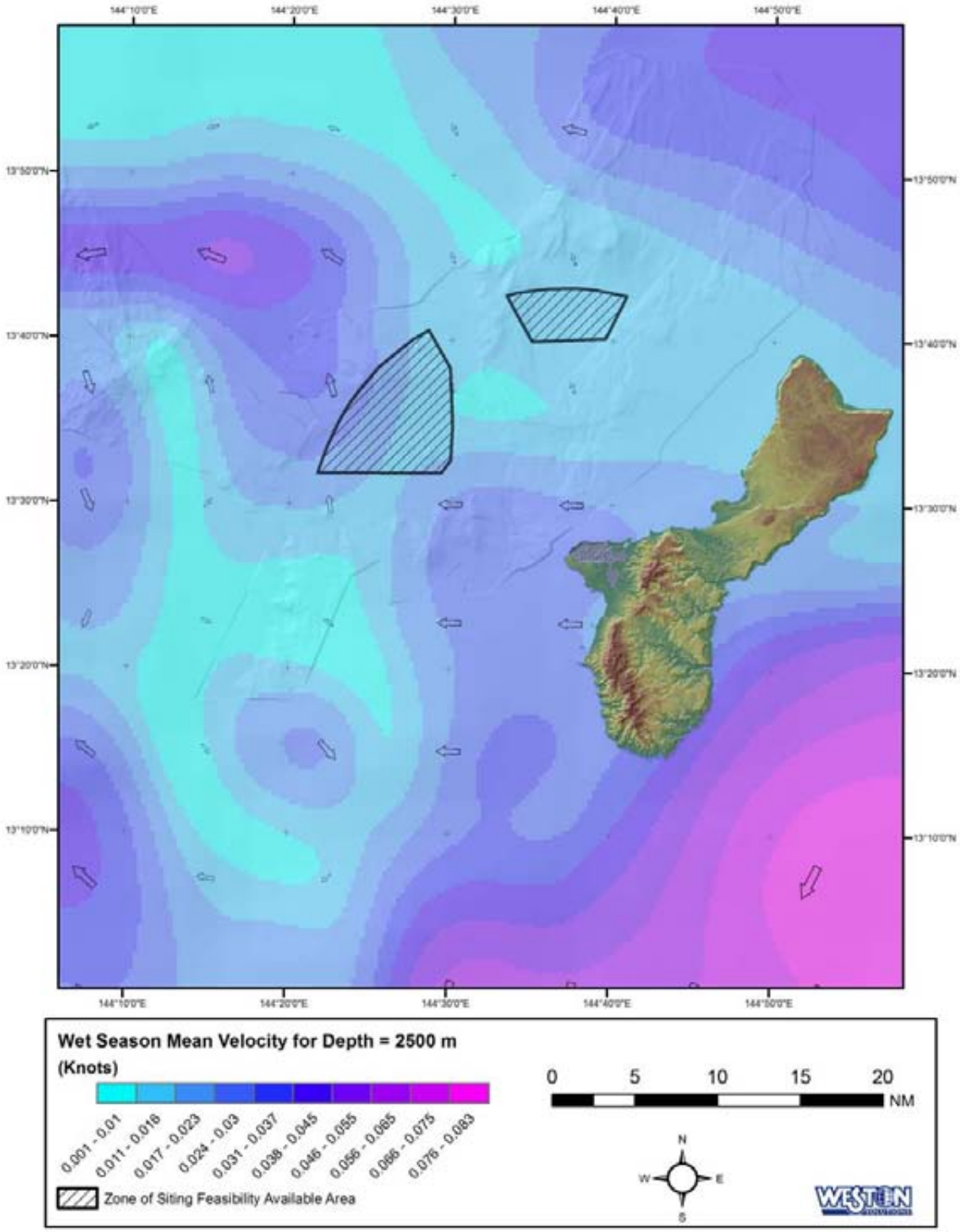

Figure 33. Interpolation of Mean Current Speeds at 2500 Meters Depth for the Wet Season

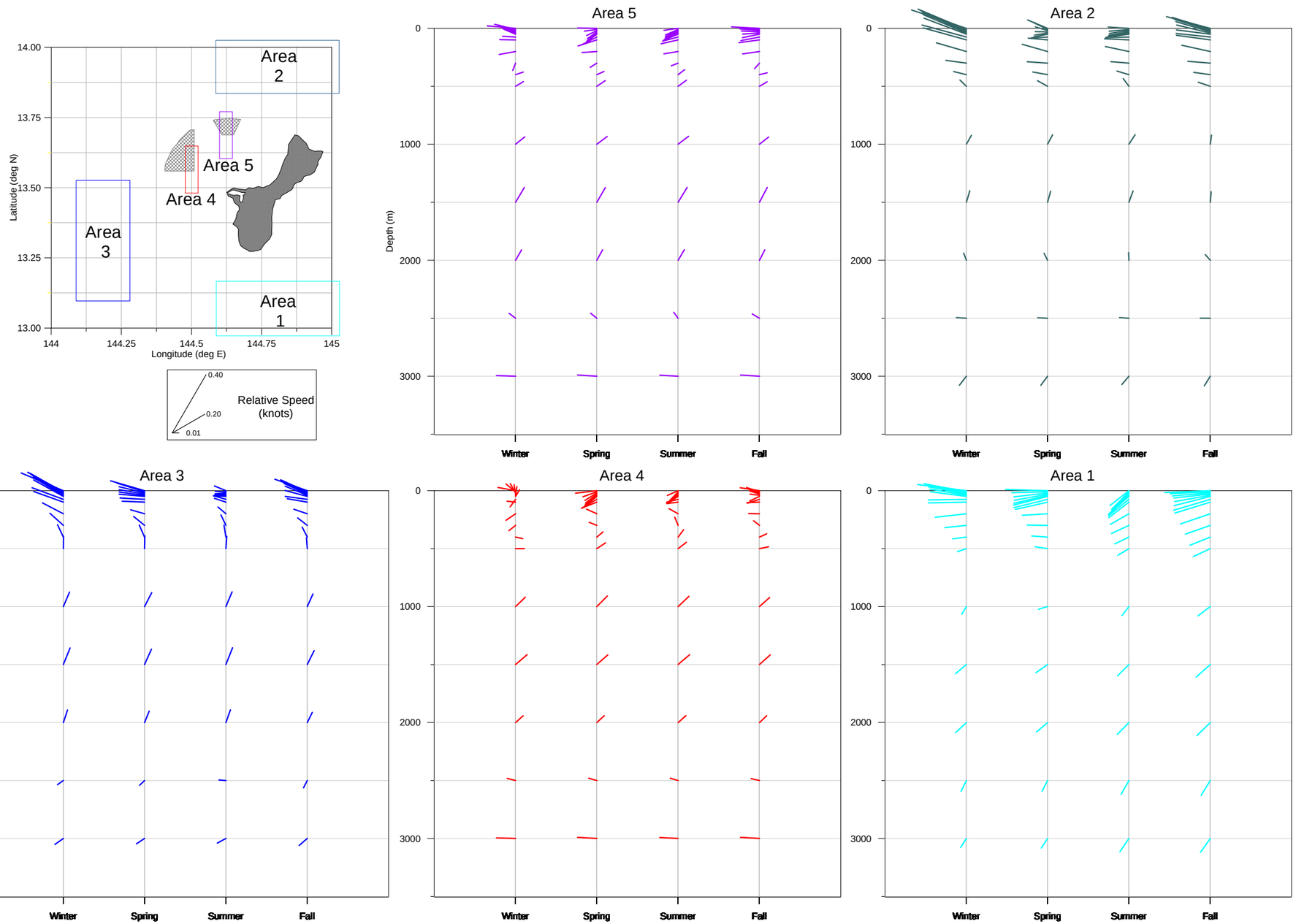

Figure 34. Vector Plots of Seasonal Average Currents by Depth for Specific Areas within the Regional Study Area

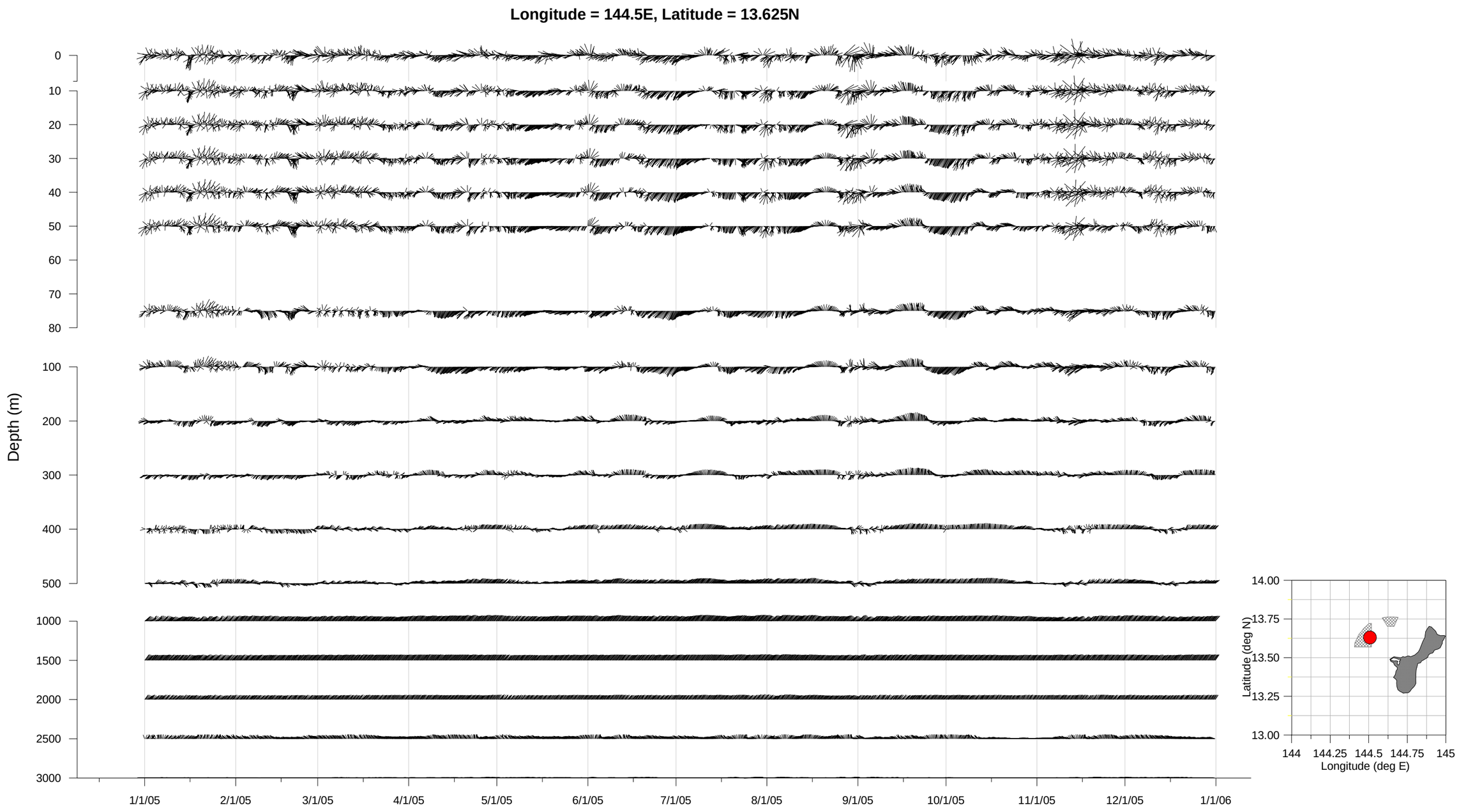

Figure 35. Vector Plots of Current Velocity by Depth for a Location Near the Northwest ODMDS Alternative Area.

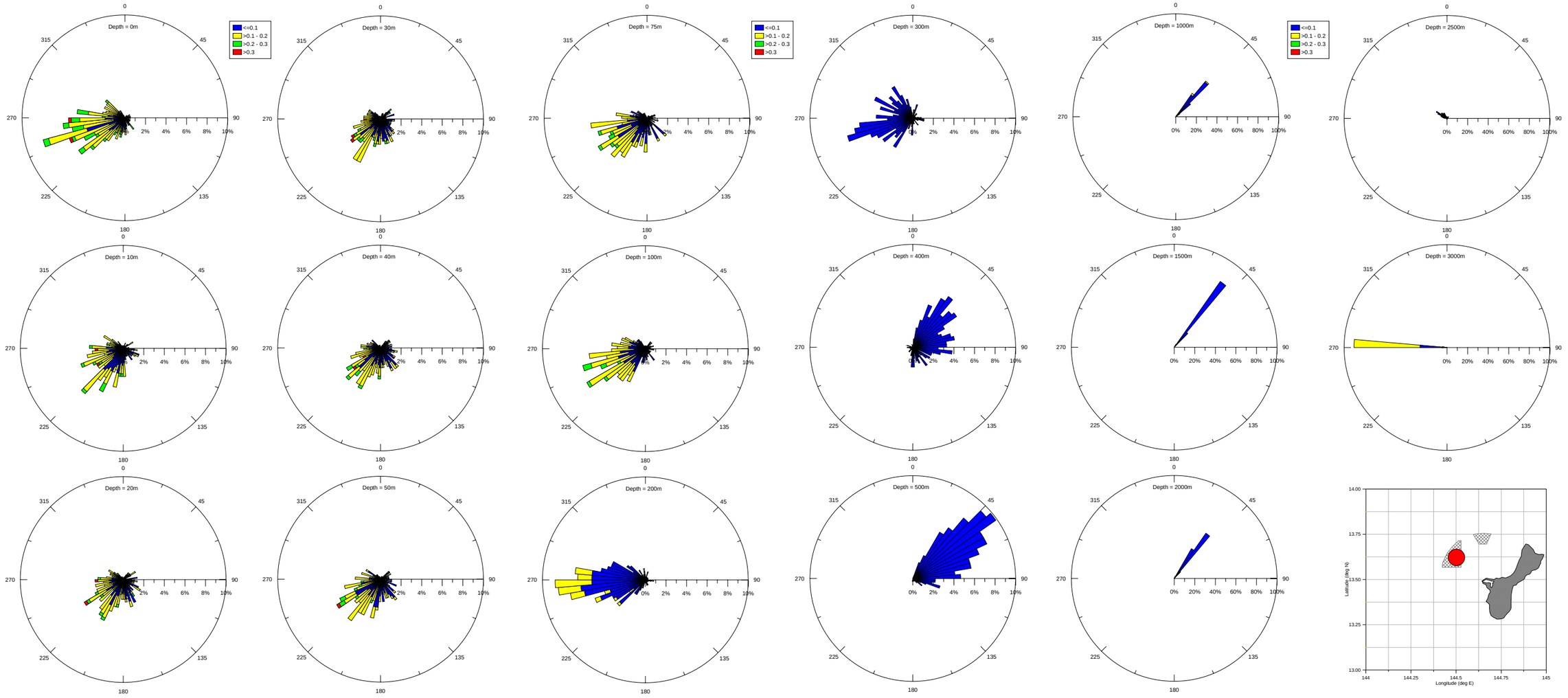

Figure 36. Rose Diagram of Current Velocities by Depth for a Location Near the Northwest ODMDS Alternative Areaa

4.2.1.2 North Alternative

Surface currents are shown in the vector plots in Figure 37 and Figure 38 and the corresponding rose diagrams in Figure 39 and Figure 40. Surface currents at the north alternative exhibit a more consistent pattern than those at the northwest alternative, having a stronger and more westerly component. This is likely a result of its closer proximity to the uniform westward flows around the north side of the island. However, two to three week periods consisting of irregular, poorly developed currents occurred at this site. The southern portion of this site experiences greater variability than the northern portion.

4.2.2 Intermediate Layer Currents

Consistent with the pattern observed at the regional scale, intermediate layer currents (1,300 ft [400 m] to 6,550 ft [2,000 m]) at the northwest and north alternative have similar patterns with a few exceptions. Currents in this layer tend towards the northeast with decreasing variability with increasing depth (Figure 37 through Figure 40). Current speeds are about 0.10-0.16 ft/s (3–5 cm/s) in the intermediate layer.

4.2.3 Bottom Currents

On a regional scale, the bottom currents were highly variable; however, in the area of the potential ODMDS alternatives, the bottom currents below 8,200 ft (2,500 m) are more consistent, trending in a north-northwesterly direction at a speed of approximately 0.07 ft/s (2 cm/s; Figure 37 through Figure 40).

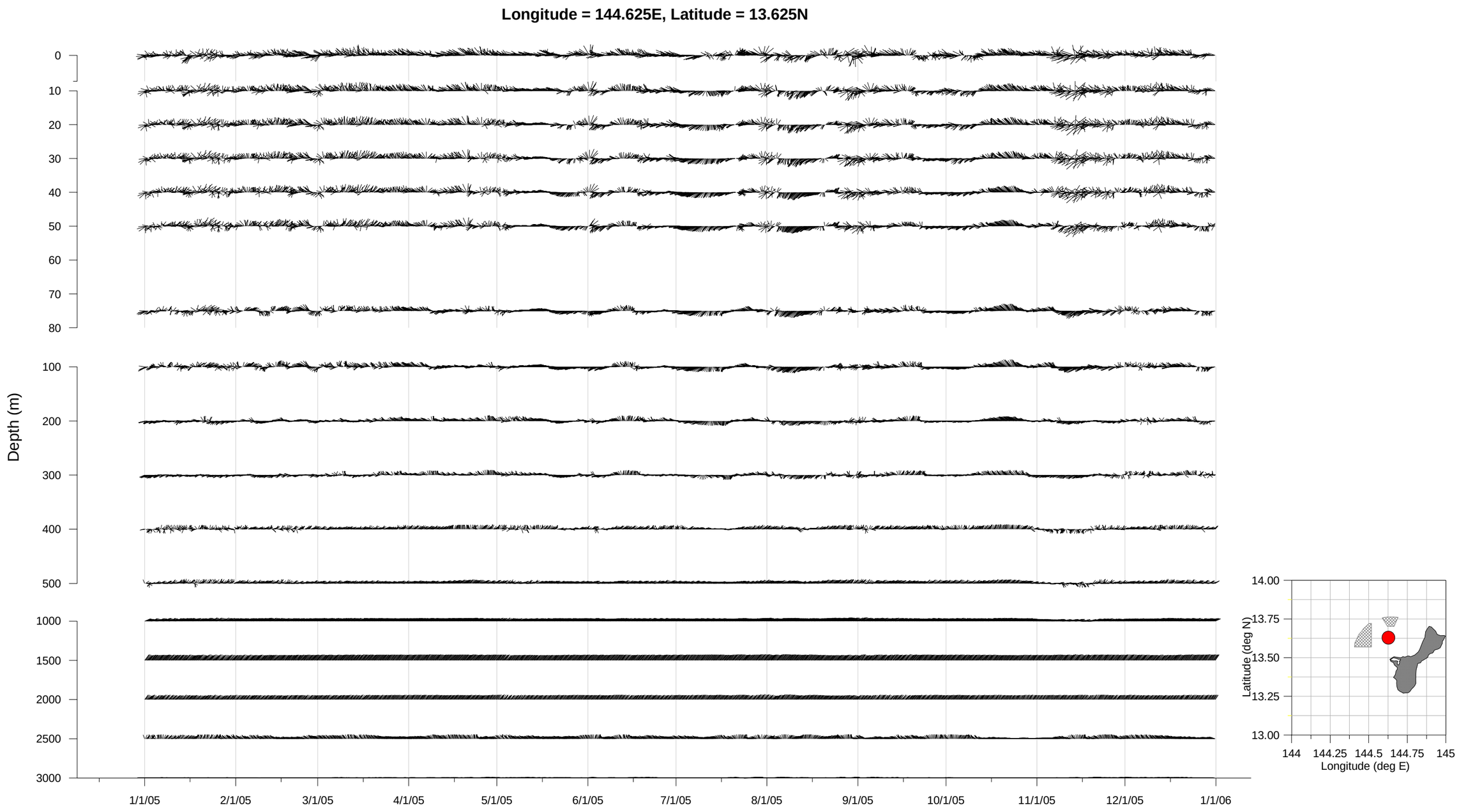

Figure 37. Vector Plots of Current Velocity by Depth for a Location Near the North ODMDS Alternative Area.

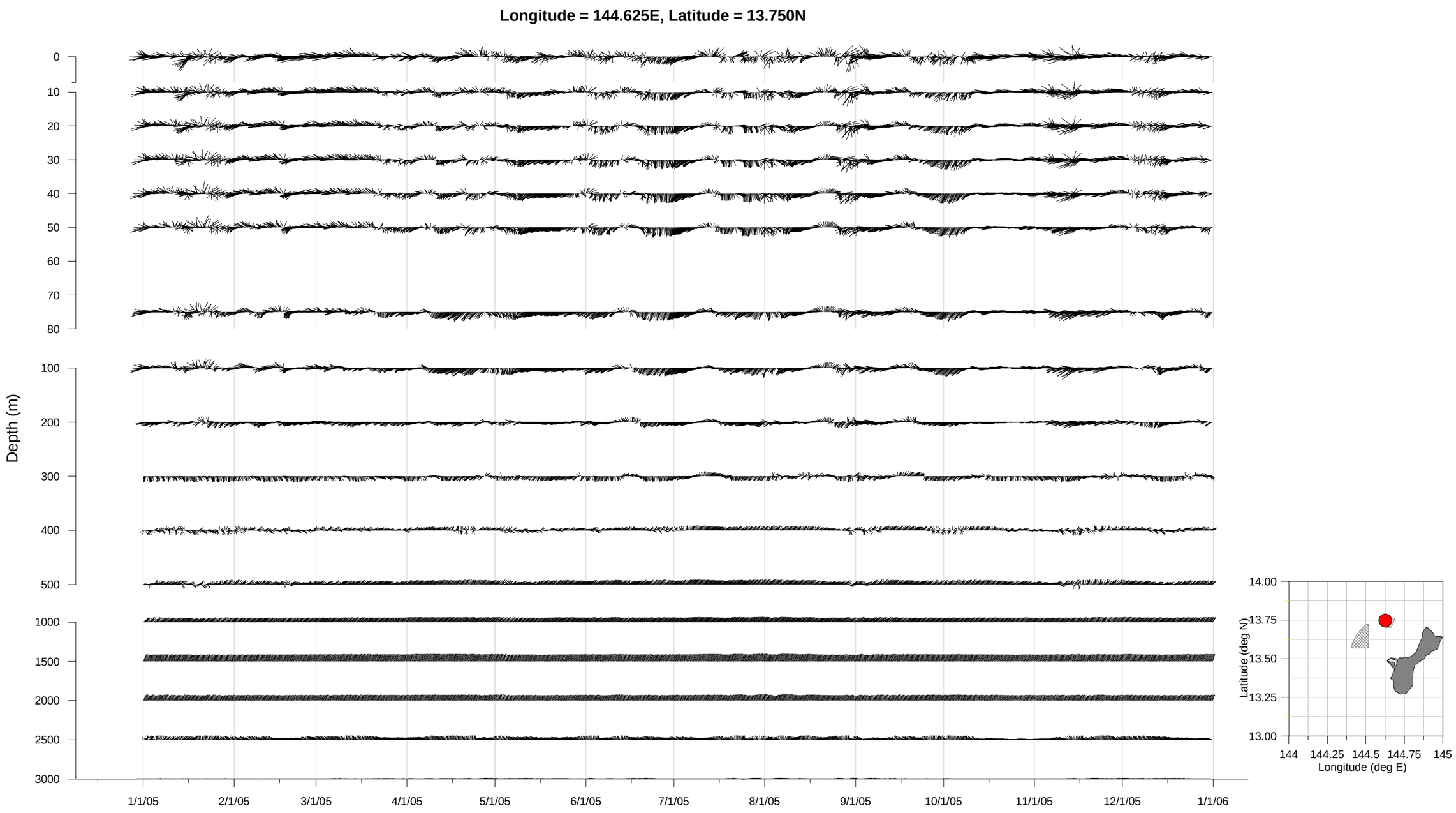

Figure 38. Vector Plots of Current Velocity by Depth for a Location Near the North ODMDS Alternative Area

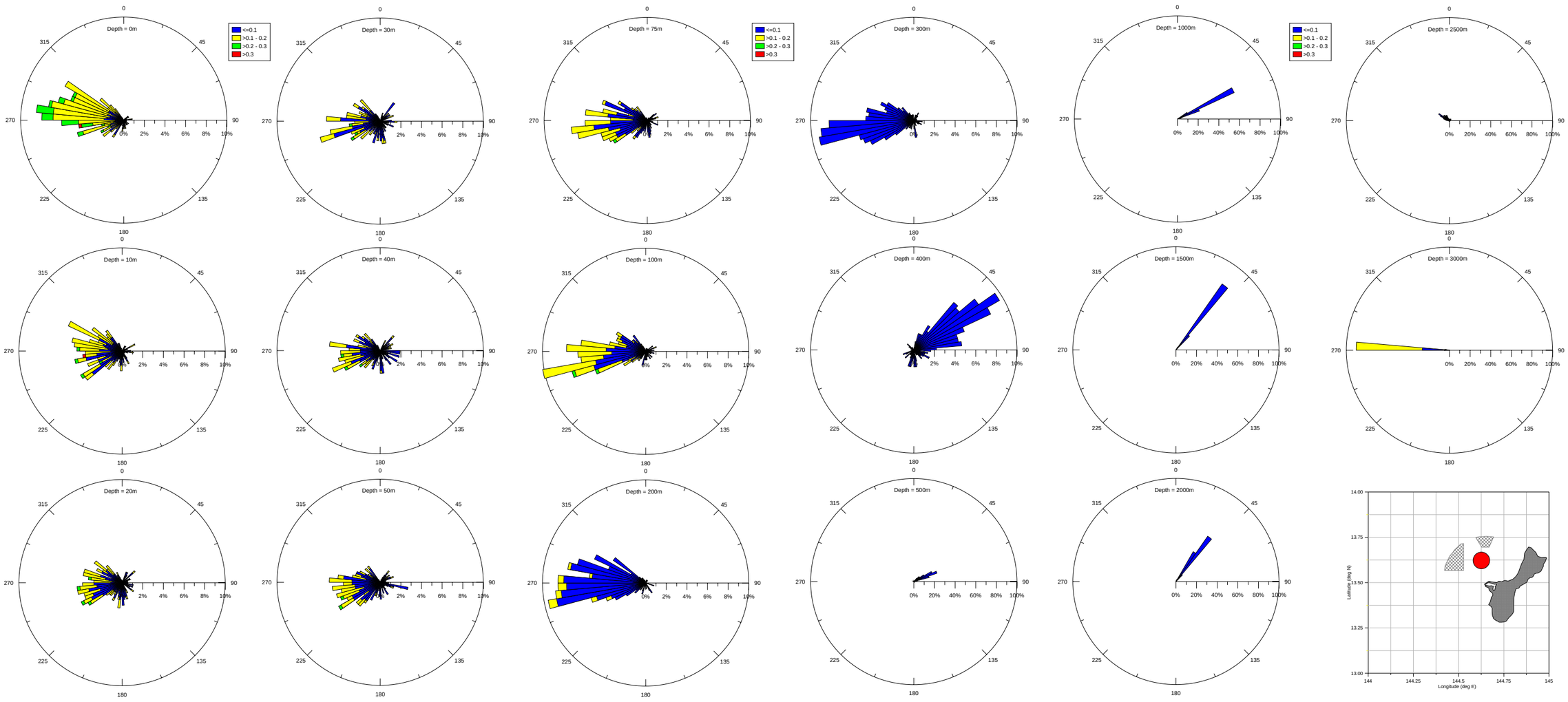

Figure 39. Rose Diagram of Current Velocities by Depth for a Location Near the North ODMDS Alternative Area

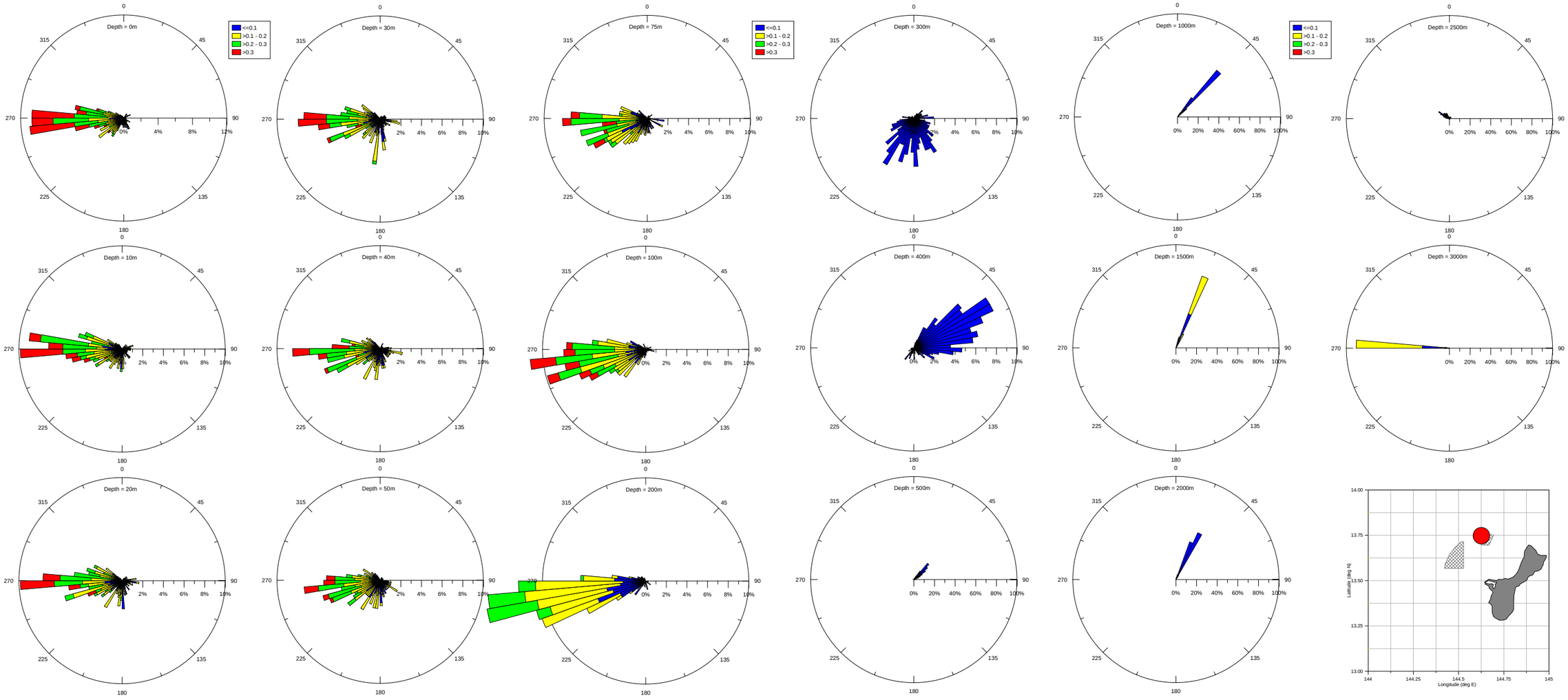

Figure 40. Rose Diagram of Current Velocities by Depth for a Location Near the North ODMDS Alternative Area

4.3 Suitability of Modeled Current Data

The current patterns identified in the previous section as developed from NCOM data were compared to observations of regional current patterns as published in physical oceanographic texts and journals. Also, the Pacific El Niño/Southern Oscillation (ENSO) phenomenon was considered. These qualitative comparisons, conducted to develop an idea of the suitability of the modeled current data, provide evidence that the NCOM data reflect oceanographic current patterns previously described in the literature.

At the surface, currents approaching Guam are characterized by the NPEC. The NPEC flows westward at an average speed of 0.33 to 0.66 ft/s (10 to 20 cm/s; Uda 1970 in Geo-Marine 2005) and reaching approximately 0.98 ft/s (30 cm/s; Wolanski et al. 2003) in response to the trade winds typically between 10° N and 15° N (Reid 1997). The NCOM data reflect this observation, with currents approaching Guam, on the eastern side of the study area, trending towards the west.

Wolanski et al. (2003) predicted the development of coastal eddies in the lee of the island as a result of the NPEC flowing past Guam. The strength and location of these coastal eddies were dependent on the angle at which the NPEC approaches Guam. During the period of study, Wolanski identified a cyclonic eddy likely associated with a tropical storm. Each of these eddies were capable of producing return flow towards the island. The NCOM data reflect this observation, with highly variable currents in the lee of the island, suggesting eddies capable of producing eastward flow in the surface layers. During the wet season, when tropical storms are most prevalent, vector plots from the NCOM data show greater variability in the current data.

Heron et al. (2006) examined surface currents in the vicinity of Palau, using both *in situ* data and model output. Seasonal differences were identified with currents during the dry season (winter months) more uniform than currents during the wet season (summer months). During the wet season, Heron et al. (2006) indicated a disordered current pattern of slower moving current speeds. This increased directional variability was hypothesized to be the result of large-scale eddies forming, that also appear to influence the angle at which the NPEC approaches Guam. The NCOM data reflect this observation, with increased variability in the surface current structure during the dry season, and a greater uniformity in the surface current structure during the wet season.

Siedler et al. (2004) examined deep water current patterns in the Mariana and Caroline Basins. Two predominant deep water masses in this region are the North Pacific Deep Water (NPDW) and the Lower Circumpolar Water (LCPW). The NPDW flows westward from the northeastern Pacific and the LCPW, after flowing northwestward across the equator east of Guam, branches into two limbs, a northward flow into the Pacific Basin and a westward flow towards the West Mariana Basin. Siedler et al. (2004) indicated that these deep waters flow from the East Mariana Basin into the West Mariana Basin through the Yap Mariana Junction, southwest of Guam. This suggests that on the eastern side of the Mariana Ridge, deep water would flow along isobaths, trending southwest, towards this junction. The NCOM data reflect these observations, with consistent west-southwestward flow on the eastern side of the Mariana Ridge, southeast of Guam. Published observations of oceanographic current patterns in the West Mariana Basin,

west of Guam, did not distinguish characteristics of the deep water in this region; therefore, no comparisons could be made.

Current data from NCOM were also determined to be representative of near normal conditions based on observations and forecasts provided by the Pacific ENSO Applications Center (PEAC) and a comparison to the Multivariate ENSO Index (MEI) developed by the National Oceanographic and Atmospheric Administration's (NOAA) Earth System Research Laboratory. In 2005, 25 tropical cyclones developed in the western North Pacific compared to an average of 31 tropical cyclones during a normal calendar year. None of these tropical cyclones made direct landfall in Micronesia in 2005 (PEAC 2006). With regards to the ENSO phenomenon, the January through April, 2005 were classified as weak El Niño events (NOAA 2007). May through October were classified as near normal conditions and November through December conditions were classified as weak La Niña events. Classification was determined by first ranking the MEI for each bimonthly period using the terciles (grouping the ranks into thirds). If the MEI was in the upper third, it was considered an El Niño event and if the MEI was in the lower third, it was considered a La Niña event. MEI scores in the middle third were indicative of near normal conditions. Next, the strength (strong or weak) of the El Niño and La Niña events were determined by ranking the data using the upper and lower quintiles (grouping the ranks into fifths). MEI scores falling within the upper or lower fifth classified the El Niño or La Niña event as strong. None of the MEI scores for 2005 ranked in the upper or lower fifths, therefore the events were not strong.

Based on the results of this comparison, it was determined the NCOM data appropriately reflected what is known about the regional current patterns around Guam and were representative of near normal conditions with respect to ENSO.

5.0 MODELED DISPOSAL EVENTS

5.1 STFATE Model

The STFATE model was evaluated for its efficacy in modeling dredged material disposal events at a deep sea ODMDS, similar to the environment offshore of Guam. STFATE predicts the transport of disposed dredged material through the water column and ultimately the area and thickness of material deposition. STFATE is a module of the Automated Dredging and Disposal Alternatives Management System (ADDAMS) and was developed by the USACE. A detailed discussion of the model's capabilities and assumptions can be found in the Inland Testing Manual (ITM; USEPA and USACE 1995).

Briefly, STFATE models the transport of dredged material based on three phases of movement: convective descent, dynamic collapse and passive transport-dispersion. During convective descent, the dredged material falls vertically through the water column under the influence of gravity. Once the dredged material reaches a point of neutral buoyancy (dynamic collapse), vertical transport is replaced with horizontal spreading. Passive transport-dispersion occurs when ambient currents and turbulence dominates the movement of dredged material until the material is deposited (in a normal distribution) on the seafloor. The model assumes deposited material remains in place and is not transported due to erosion or bedload transport.

Model input and output is provided for a gridded area, scaled to represent the area of expected transport and deposition. The grid has cells of a user-specified size. Current velocity in the x, y direction for each of two vertical layers is applied to each cell. The model cannot account for site-specific bathymetry, and instead uses either a single disposal depth for each cell over the entire gridded area or a uniform slope.

Input parameters to the model include ambient environmental parameters such as time-invariant current velocity, density stratification and water depths, operational parameters such as barge position, speed, dimensions, draft and volume of dredged material to be disposed. Values representing entrainment, settling, drag, dissipation, apparent mass and density gradient differences can also be defined.

The primary limitation in using STFATE for this project is its inability to model multiple current patterns in both the horizontal as well as vertical directions. The model is restricted to only two discrete current patterns in the vertical direction. This constrains the model from accurate predictions in a deep sea environment which typically has a surface current attenuating with depth and multiple intermediate layer and bottom layer currents. Further, the model can only evaluate a maximum of 12 time-steps and is restricted in the lengths of each time-step. Due to the extreme depths of the disposal site and slow settling velocities of fine-grained material, the model would not run to completion (i.e., predict the deposition of all silts and clays).

5.1.1 Model Use

Although limitations to the STFATE model were identified, an approach was developed in order to use STFATE within its constraints to provide an initial assessment of the extended impact zone. This approach used depth-weighted average currents as input parameters to the model.

5.1.1.1 Design

The depth-weighted, average currents approach was used to model one disposal event, but the complexity of the currents through the water column is diminished. First, a constant settling velocity throughout the water column was assumed. Then a depth-weighted average current was calculated by proportionately weighting the length of time (distance) a particle would be subjected to a specific current. For example, if the water body was 3,300 ft (1,000 m) deep and had two predominant current regimes, a surface current extending to a depth of 650 ft (200 m), or occurring over 20% of the water column, and a bottom current extending from 650 ft (200 m) to 3,300 ft (1,000 m), or occurring over 80% of the water column, then the surface current was given a weight of 20% and the bottom current was given a weight of 80%.

Two separate depth-weighted average currents were calculated, one for an upper water body occurring from the surface to a depth of 1,000 ft (≈300 m) and one for a lower water body occurring from a depth of 1,300 ft (≈400 m) to the seafloor. This depth regime was indicated by the typical change in current direction between 1,000 ft (300 m) and 1,300 ft (400 m) in the model results. Further delineation included calculating depth averaged currents for a typical dry season (February and March) and a typical wet season (August and September).

5.1.1.2 Input Parameters

Model Characteristics

The model grid consisted of 45 cells in the north-south direction and 45 cells in the east-west direction. The dimensions of each cell were 2,000 ft x 2,000 ft (609.6 m x 609.6 m). Therefore, the model grid had dimensions of 90,000 ft x 90,000 ft (27,432 m x 27,432 m), representing and area of approximately 219 sq. nm (751.1 km^2).

As specified above, STFATE is limited in the number and duration of time-steps to evaluate the transport and deposition of dredged material. The most suitable and practical input parameters were determined to be 12 time-steps, each 16 hours in duration for the duration of the model run (192 hours).

Disposal Operations

A single discharge event was modeled assuming the disposal of 3,000 cy (2,294 m^3) of dredged material from a split-hull barge. For the purposes of this report, the target disposal area for each suitable region (northwest and north alternative) was selected to represent the shortest transit (i.e., closest point) from the entrance to Outer Apra Harbor (Figure 41).

Section 5.1.2 (STFATE Model – Results) extrapolates the model results from a single discharge event to numerous discharge events, occurring over a 1-year period for the disposal of both 300,000 cy (229,367 m^3; assumed to be a yearly average as specified in the ZSF) and 1,000,000 cy (764,555 m^3; assumed to be a worst-case scenario).

Dredged Material Characteristics

Two scenarios were run each with different dredged material characteristics, separated into four distinct particle size classes (gravel, sand, silt and clay). First, a disposal event of predominantly coarse-grained material was evaluated and second, a disposal event of predominantly fine-grained material was evaluated. The coarse-grained scenario assumed dredged material characteristics similar to those measured for a proposed construction dredge project at Kilo Wharf (Table 2). The fine-grained scenario assumed dredged material characteristics similar to those measured for a proposed construction dredge project in Inner Apra Harbor (Table 2). Sediment characteristics were taken from core samples collected in 2006 from the proposed construction dredge footprints (Weston Solutions and Belt Collins 2007). These two scenarios bound the range of dredged material expected to be generated from Apra Harbor.

Table 2. Physical Characteristics of Coarse and Fine-Grained Dredged Material Suitable for Disposal at a Potential ODMDS

Physical Characteristics	Coarse-grained Scenario	Fine-grained Scenario
Particle Size Class		
Gravel	20.97 %	3.25 %
Sand	74.11 %	13.08 %
Silt	2.56 %	23.83 %
Clay	2.36 %	59.84 %
Total Solids	69.1 %	42.9 %

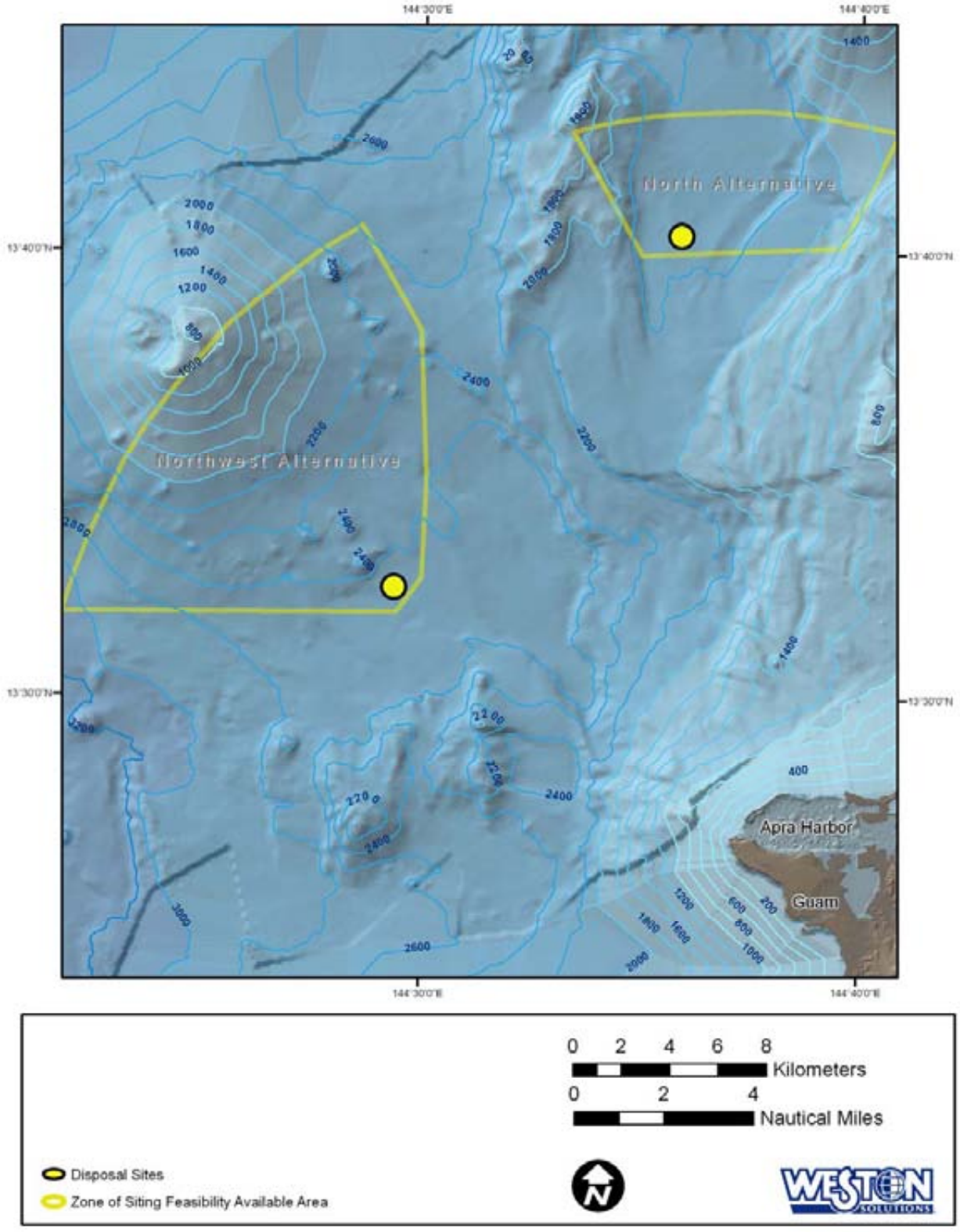

Figure 41. Assumed Surface Target Location for Each Ocean Dredged Material Disposal Site

Regional Topography

Due to the limitations of STFATE, as described above, the model did not use detailed regional bathymetry data. Instead, the disposal depth and bottom slope was modeled using a flat bottom at a depth of 6,550 ft (≈2,000 m).

Water Column Structure

A homogeneous density profile (1.025 g/cc) was assumed throughout the entire water column.

ODMDS Alternative Site Specific Currents

As specified in Section 5.1.1.1 (STFATE Model – Model Use – Design), two separate current patterns were evaluated, representing the dry and wet seasons. As described above, the dry season currents tended to be more uniform and the wet season currents tended to be more variable. Although modeled currents at each 1/8° point in the lee of the island, and consequently within the potential ODMDS alternative areas, were more variable than currents at points north, south and east of the island, the currents at points in the lee of the island were similar to each other. Therefore, the seasonal and depth averaged currents used for the STFATE model were derived from a single station, located at 13.625° N, 144.5° E.

An average current representing each season (February and March for the dry season and August and September for the wet season) was calculated for two different depth intervals (surface to 1,000 ft [≈300 m] and 1,300 ft to 6,550 ft [≈400 m to 2,000 m]). Between the two layers, currents were interpolated. In the upper layer, the dry season, depth averaged current flowed at 0.08 ft/s (2.4 cm/s) in a west-southwesterly direction (253° from N) and in the wet season the current flowed at 0.05 ft/s (1.4 cm/s) in a westerly direction (270° from N). In the lower layer, the dry season, depth average current flowed at 0.06 ft/s (1.9 cm/s) in a northeasterly direction (37° from N) and in the wet season the current flowed at 0.05 ft/s (1.4 cm/s) in a north-northeasterly direction (28° from N). Table 3 shows the individual vectors used in the modeling for each season.

Table 3. Current Vectors Used for Dry and Wet Season Scenarios in STFATE Model Runs

Season	Layer	X (ft/s) (+east, -west)	Y (ft/s) (+north, - south)	Resultant (ft/s)	Resultant (cm/s)	Direction (° from N)
		STFATE Coordinates				
		Z (ft/s) (+east, - west)	X (ft/s) (+north, - south)			
Dry	Upper	-0.075	-0.023	0.078	2.39	253
	Lower	+0.037	+0.049	0.061	1.87	37
Wet	Upper	-0.045	+0.0002	0.045	1.37	270
	Lower	+0.021	+0.039	0.044	1.35	28

Section 5.1.2 (STFATE Model – Results) extrapolates the model results from a single discharge event for each current pattern to the disposal of dredged material over an entire year. Deposition of dredged material on the seafloor was extrapolated using the dry season results for a period of six months and wet season results for a period of six months.

5.1.2 Results

STFATE model output provides results for a single disposal event of the total volume and associated deposit thickness for each particle size, as well as cumulative results for all disposed material, in each model grid cell. In addition, it provides results predicting the physical characteristics of the sediment cloud remaining in suspension at model termination. Model results for a single disposal event (3,000 cy [2,294 m^3]) were extrapolated to represent 100 disposal events over the course of a year (300,000 cy [229,367 m^3]) and the 333 disposal events over the course of year (1 mcy [764,555 m^3]). Based on findings in the ZSF study, 300,000 cy (229,367 m^3) represents the likely dredged volume for a typical average year. One million cubic yards was chosen to represent a maximum dredged volume for a given year associated with any specific construction dredge project.

To extrapolate the deposit thickness for each of dredge volume scenarios (300,000 cy [229,367 m^3] and 1 mcy [764,555 m^3]), the deposit thickness from a single disposal event was multiplied by the total number of trips expected during each season (dry and wet), assuming a consistent, regular pattern of disposal throughout the year. For example, to dispose 300,000 cy [229,367 m^3] of dredged material using a scow having a capacity of 3,000 cy [2,294 m^3], would require 100 trips, 50 trips during each season. As specified in Section 5.1.1.2 (Input Parameters), two separate current structures were evaluated: dry season and wet season. For the purposes of the extrapolation, it was assumed that dredged material disposed at the potential ODMDS alternative sites would be exposed to dry season currents 50% of the time (50 trips) and wet season currents the remaining 50% of the time (50 trips). These calculations were input into a GIS and isopachs were developed for deposit thicknesses greater than 0.04 in (1 mm), 0.4 in (10 mm), 2 in (50 mm), 4 in (100 mm), 8 in (200 mm) and 20 in (500 mm), as appropriate.

In some respects, this additive method is conservative as it does not account for compaction of material over time or redistribution of sediment deposits due to physical processes such as bedload transport or biological processes such as bioturbation; therefore this method provides the greatest potential deposit thickness. It may be considered that this additive method is not conservative as it assumes that each disposal event occurs at the same location within the target surface disposal area, rather than at multiple locations distributed throughout the target surface disposal area; therefore, the overall footprint on the seafloor is reduced. However, since the model grid cell size is only slightly smaller than the target surface disposal area and assuming a normal distribution of disposal events about the center of the target surface disposal area, variations in the predicted footprints are not anticipated to be significant.

In all four scenarios (coarse vs. fine-grained material and dry vs. wet season currents), as expected, coarser-grained material deposited more quickly than finer-grained material and the coarser-grained material did not disperse as far relative to finer-grained material. For example, gravel material settled within 16 hours of the disposal event and was not transported beyond the boundaries of the model grid cell in which the disposal event occurred (an area of approximately 0.11 sq. nm [0.37 km^2]). In contrast, only a small percentage of the silts and clays settled to the seafloor within the time limits of the model (192 hours) and these materials were transported over a much greater area with nearly all model grid cells within the bounds of the model limits

(an area of approximately 219 sq. nm [752 km^2]) predicting some deposition, however minute, of these materials.

Table 4 lists the area of deposits for deposits greater than 0.04 in (1 mm), 0.4 in (10 mm), 2 in (50 mm), 4 in (100 mm), 8 in (200 mm) and 20 in (500 mm) for each of the four scenarios. Figure 42 through Figure 46 illustrate these results. Figure 42 and Figure 43 show the predicted footprints at each of the potential ODMDS alternative sites for the disposal of 300,000 cy (229,367 m^3) of either coarse or fine-grained material, respectively. Figure 28 and 29 show the predicted footprints following the disposal of 1 mcy (764,555 m^3) of either coarse or fine-grained material. The largest footprint is associated with the disposal of 1 mcy (764,555 m^3) of predominantly fine-grained material. Figure 46 presents the same results as Figure 45, but at a larger scale to better illustrate the spatial distribution with regards to the island of Guam.

As the current data would suggest, the footprint of material deposited on the seafloor is elongated towards the northeast. This is most evident in the disposal of fine-grained material which would tend to stay in suspension the longest (Figure 46). At the northwest alternative site, the footprint of deposits thicker than 0.04 in (1 mm) is contained within a bathymetric depression, in depths of approximately 8,530 ft (2,600 m) at the disposal site and shoaling at the northwestern, northeastern and southeastern edges of the footprint to about 7,220 ft (2,200 m). At the north alternative site, the footprint of deposits thicker than 1 mm is also centered within a bathymetric depression, but the extent of the footprint covers a much more dynamic area. The center of the north alternative disposal site occurred in approximately 7,220 ft (2,200 m) with the edges of the footprint occurring in shallower areas comprised of seamounts to the northwest and northeast and on the island slope to the southeast to depths of about 5,900 ft (1,800 m).

Also, in all four scenarios, the total thickness of new material deposited on the seafloor was much greater in the model grid cell directly below the disposal site than in all adjacent model grid cells. After a single disposal event, new material in the grid cell directly below the disposal site was approximately 0.03 in (0.8 mm) for the disposal of predominantly fine-grained material and was approximately 0.08 in (2.0 mm) for the disposal of predominantly coarse-grained material (approximately 0.91 ft [0.27 m] and 2.19 ft [0.67 m], respectively, after the placement of 1 mcy [764,555 m^3]). The maximum deposit thickness in any of the immediately adjacent cells after a single disposal event was <0.01 in (0.2 mm) for the disposal of fine-grained material and 0.01 in (0.3 mm) for the disposal of coarse-grained material (approximately 0.22 ft (0.07 m) and 0.33 ft (0.1 m), respectively, after the placement of 1 mcy [764,555 m^3]). These predictions represent a 4 to 6 fold decrease in the amount of material within approximately 3,000 ft (914 m) of the disposal site.

Table 4. Modeled Thickness and Area of Deposits for Disposal of 300,000 cy or 1 mcy of Fine or Coarse-Grained Dredged Material

Scenario	Deposit Thickness mm (m)	Diameter (km)	Area of Deposits (km^2)
Fine-grained Material 300,000 cy	>1 (>0.001)	4.4	15.8
	>10 (>0.01)	1.9	2.6
	>50 (>0.05)	-	-
	>100 (>0.1)	-	-
	>200 (>0.2)	-	-
	>500 (>0.5)	-	-
Coarse-grained Material 300,000 cy	>1 (>0.001)	5.9	27.4
	>10 (>0.01)	3.0	6.9
	>50 (>0.05)	0.7	0.3
	>100 (>0.1)	0.4	0.1
	>200 (>0.2)	-	-
	>500 (>0.5)	-	-
Fine-grained Material 1,000,000 cy	>1 (>0.001)	12.0 x 15.0 (oval)	141.8
	>10 (>0.01)	3.1 x 3.3 (oval)	8.2
	>50 (>0.05)	1.5	1.7
	>100 (>0.1)	0.6	0.3
	>200 (>0.2)	-	-
	>500 (>0.5)	-	-
Coarse-grained Material 1,000,000 cy	>1 (>0.001)	9.3	66.5
	>10 (>0.01)	5.0	19.6
	>50 (>0.05)	2.5	4.8
	>100 (>0.1)	1.9	2.6
	>200 (>0.2)	0.7	0.3
	>500 (>0.5)	>0.2	>0.03

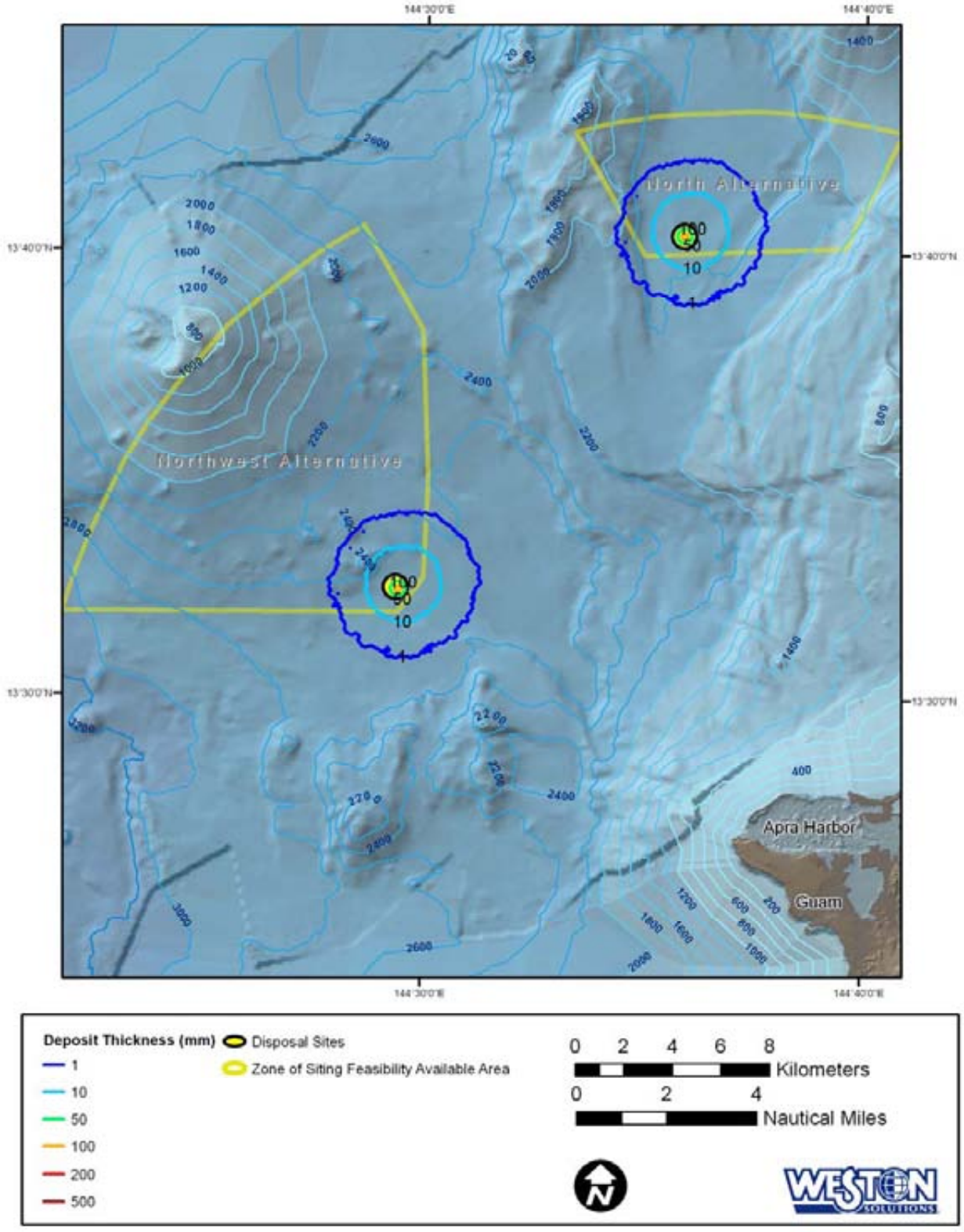

Figure 42. Isopachs Showing Increasing Deposit Thickness for the Disposal of 300,000 cy of Predominantly Coarse-Grained Material

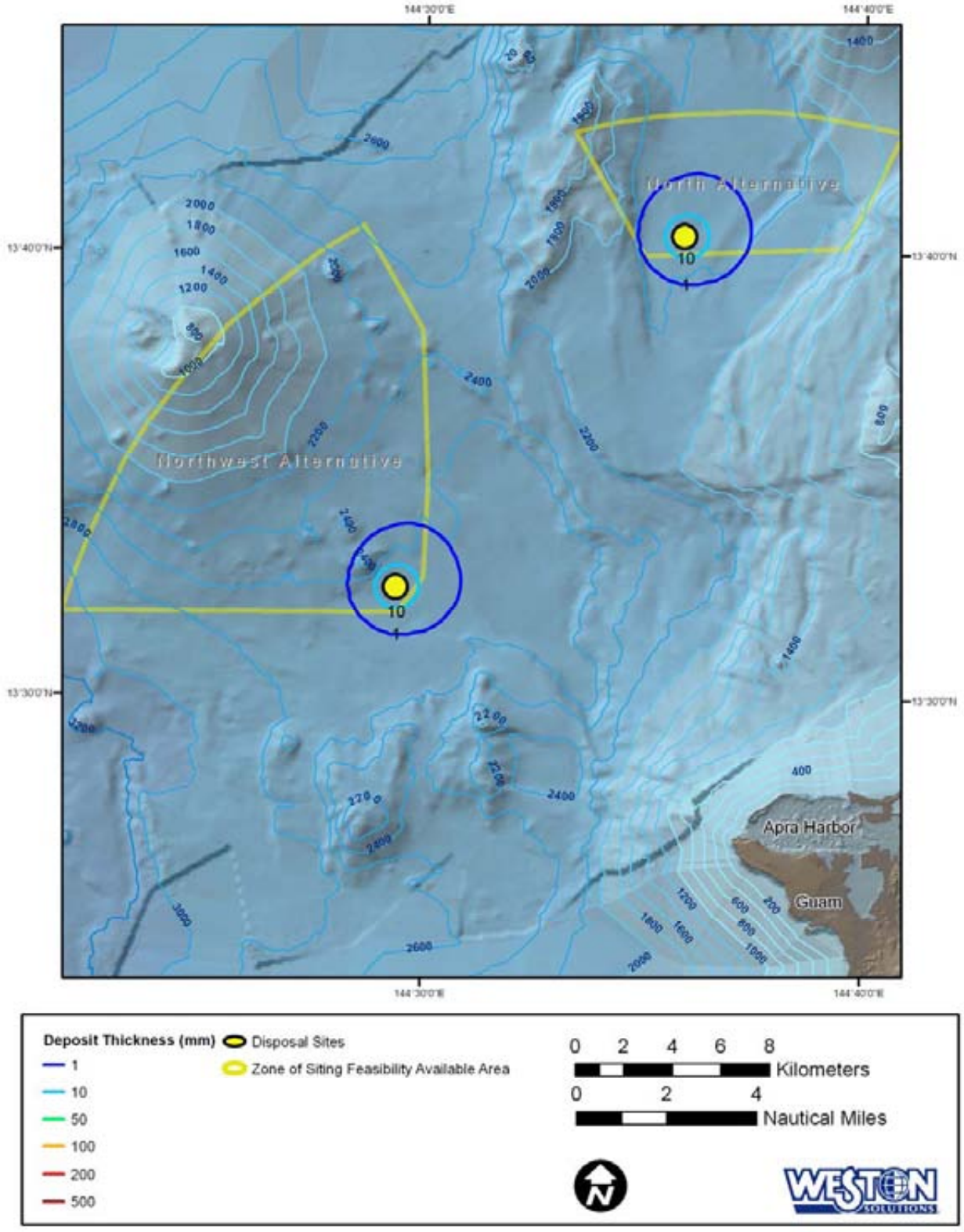

Figure 43. Isopachs Showing Increasing Deposit Thickness for the Disposal of 300,000 cy of Predominantly Fine-Grained Material

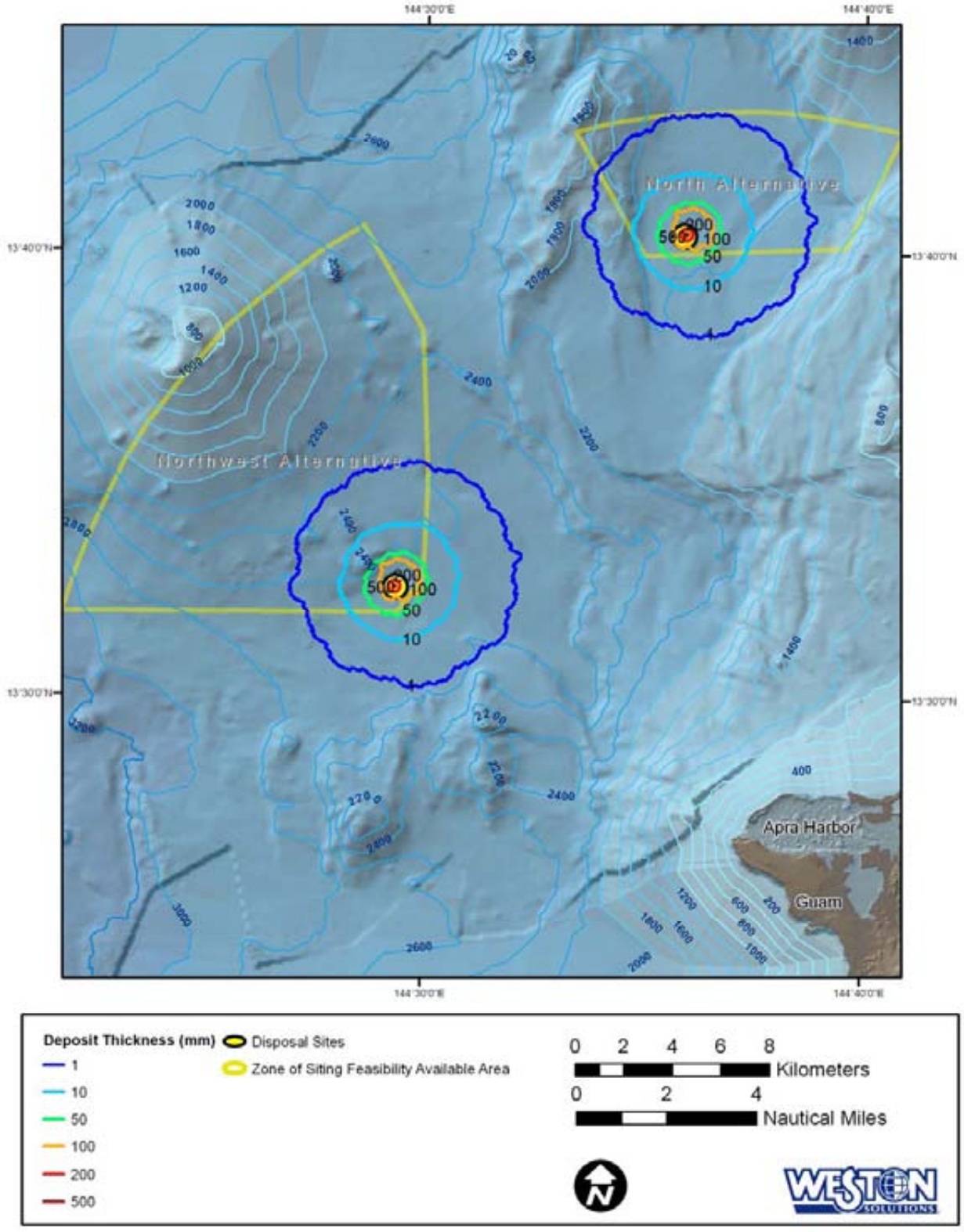

Figure 44. Isopachs Showing Increasing Deposit Thickness for the Disposal of 1 mcy of Predominantly Coarse-Grained Material

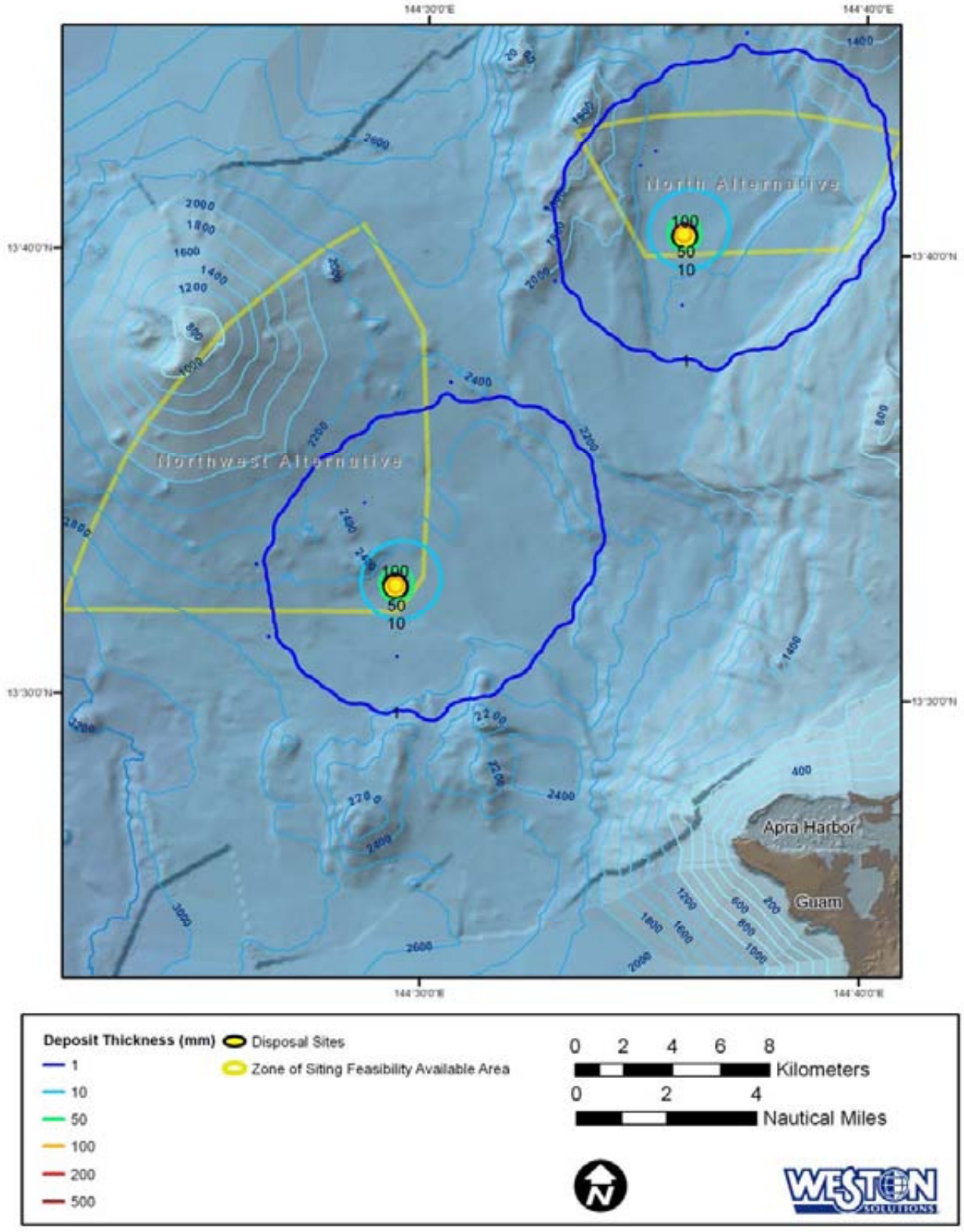

Figure 45. Isopachs Showing Increasing Deposit Thickness for the Disposal of 1 mcy of Predominantly Fine-Grained Material

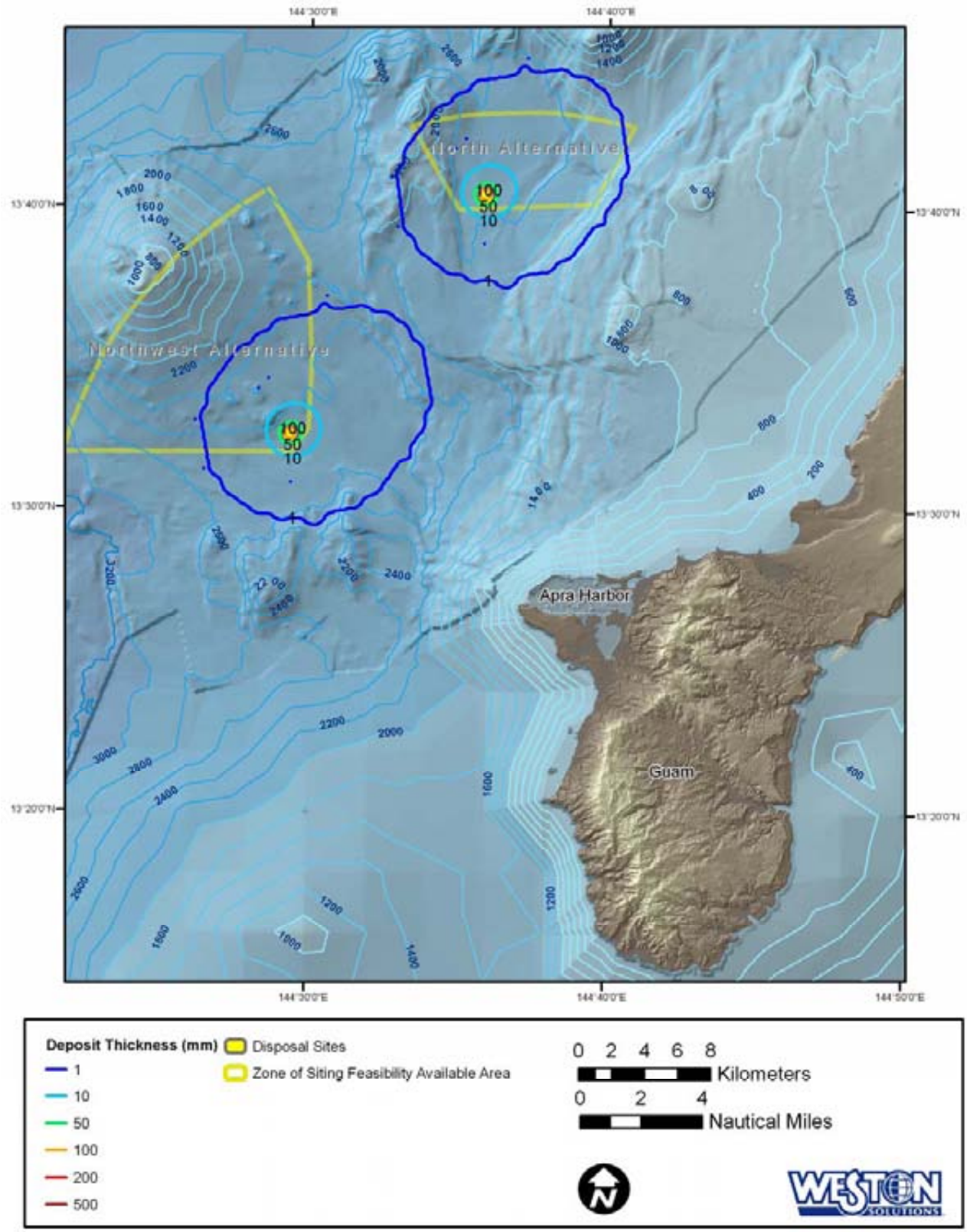

Figure 46. Expanded View of Isopachs Showing Increasing Deposit Thickness for the Disposal of 1 mcy of Predominantly Fine-Grained Material

5.2 Hamilton Model

At the request of the USEPA, Weston evaluated the Hamilton model as an alternate method for predicting the transport and deposition of dredged material through the water column and onto the seafloor. The Hamilton model was developed by SAIC for the USEPA in 1992 as part of the designation studies for the San Francisco Deep Ocean Disposal Site (SFDODS). Unlike the STFATE model, the Hamilton model is capable of using multiple, time-varying and depth dependent current velocity data and non-uniform bottom slopes to predict deposition from multiple disposal events over specified time periods. It was designed to model the transport and deposition of dredged material subjected to the complex oceanographic conditions typical of a deep water environment.

Unfortunately, after substantial effort and input from Peter Hamilton (2007), the creator of the Hamilton model, Weston determined the Hamilton model could not be adapted to forecast the transport and deposition of dredged material offshore of Guam. The Hamilton model was developed specifically for the SFDODS with the current velocity and bathymetric data for that site hardwired into the program code. Consequently, the Hamilton model was not used to predict the fate of disposal events offshore of Guam.

As a point of comparison, in the *Environmental Impact Statement (EIS) for Designation of a Deep Water Ocean Dredged Material Disposal Site off San Francisco, California* (USEPA and SAIC 1993), the Hamilton model predicted the size of the alternative site, or extended impact zone, to be an oval shape with dimensions of approximately 3.7 nm (6.9 km) long and 2.2 nm (4.1 km) wide and an area of 6.4 sq. nm (22 km^2). This represented the area having deposits greater than 0.4 in (10 mm) thick after a one-year dredged material disposal period of nearly 6 mcy (4,587,330 m^3).

The predicted area of at least 0.4 in (10 mm) thick deposits in the SFDODS study (6.4 sq. nm [22 km^2]) is an order of magnitude greater than the area this study predicts would have similar deposit thickness for the deposition of 300,000 cy (229,367 m^3) of predominantly fine-grained material (0.76 sq. nm [2.6 km^2]) and is similar in size to the area this study predicts would have similar deposit thicknesses for the deposition of 1 mcy (764,555 m^3) of predominantly coarse-grained material (5.7 sq. nm [19.6 km^2]). It should be noted that the SFDODS study assumed the disposal of 6 mcy (4,587,330 m^3), an order of magnitude greater than this study's average volume scenario of 300,000 cy (229,367 m^3).

6.0 CONCLUSIONS

NCOM derived current data were evaluated and were determined to be representative of oceanographic conditions near Guam. The ENSO index was near normal conditions for the year NCOM data were provided.

Depth-averaged current velocities representing two distinct seasons (dry and wet weather) were calculated from the NCOM data and used in a USACE developed model (STFATE) to predict

the transport of dredged material through the water column and subsequent deposition on the seafloor. STFATE was used despite its restrictions to model a deep water environment primarily because the SAIC model developed for the SFDODS designation could not be manipulated for use in Guam (i.e., the bathymetric and current data offshore of San Francisco were hardwired into the model and could not be altered).

Despite the constraints of using the STFATE model to predict the transport and deposition of dredged material in a deep ocean environment as found offshore of Guam, a suitable estimate of the sediment deposits was obtained. The modeling of a single disposal event predicted coarse-grained material to settle to the seafloor within 32 hours of the disposal event, with gravel material settling directly beneath the disposal site and sand material being deposited within 4.1 nm (7.6 km), nearly radially, of the disposal site. Only a small percentage of the fine-grained material settled within the time limits of the model, with silt and clay deposits predicted over the entire area (219 sq. nm [752 km^2]).

The area representing deposits greater than 0.4 in (10 mm) ranged from 0.76 sq. nm (2.6 km^2) for the disposal of approximately 300,000 cy of predominantly fine-grained material to 5.7 sq. nm (19.6 km^2) for the disposal of approximately 1 mcy of predominantly coarse-grained material. The latter area is roughly equivalent to the area predicted by the Hamilton model during the designation of the SFDODS for the disposal of approximately 6 mcy of material.

7.0 REFERENCES

Barron. C.N., A.B. Kara, R.C. Rhodes, C. Rowley, L.F. Smedstad, 2007. Validation Test Report for the 1/8 Global Navy Coastal Ocean Model Nowcast/Forecast System. Naval Research Laboratory. Report No. NRL/MR/7320-07-9019.

GEPA/Guam Environmental Protection Agency, 2000. Management of Contaminated Harbor Sediments in Guam. Guam Harbors Sediment Project, Phase III, Final Report. September.

Golden Software, 2005. Grapher Version 6. Golden Software, Incorporated. Golden, Colorado.

Hamilton, P. 2007. Personal Communication. SAIC.

Heron, S.F., E. J. Metzger and W.J. Skirving. 2006. Seasonal Variations of the Ocean Surface Circulation in the Vicinity of Palau. Journal of Oceanography. Volume 62. 413-426.

MEC-Weston, 2005. Phase I Dredged Material Management Plan, COMNAVMARIANAS, Guam. Prepared for Department of the Navy, Pacific Division, Naval Facilities Engineering Command. March.

NOAA 2007. National Oceanic and Atmospheric Administration. Multivariate ENSO Index (MEI). Earth System Research Laboratory, Physical Sciences Division. Updated March 7.

PEAC 2006. Pacific ENSO Applications Center. Pacific ENSO Update, 1st Quarter, 2006. Volume 12, Number 1. February 3.

Reid, J. L. 1997. On the Total Geostrophic Circulation of the Pacific Ocean: Flow Patterns, Tracers, and Transports. Progress in Oceanography. Volume 39. 263-352.

SAS® 2005. SAS Version 9.1. SAS Institute, Incorporated. Cary, North Carolina.

Sato, 2005. Personal Communication with Weston Solutions, Inc. Naval Facilities Engineering Command, Pacific. February 22.

Siedler, G., J. Holfort, W. Zenk, T.J. Muller and T. Csernok. 2004. Deep-Water Flow in the Mariana and Caroline Basins. Journal of Physical Oceanography. Volume 34. 566-581.

USEPA and SAIC. 1993. Environmental Impact Statement (EIS) for Designation of a Deep Water Ocean Dredged Material Disposal Site off San Francisco, California. August.

Weston Solutions and Belt Collins. 2006. Final Report: Zone of Siting Feasibility Study, Ocean Dredged Material Disposal Site, Apra Harbor, Guam. September.

Weston Solutions and Belt Collins. 2007. Final Report: Dredged Material Sampling and Tier III Analysis Evaluation for Apra Harbor Projects (P-436, P-502, P-518), Guam. April.

Wolanski, E., R.H. Richmond, G. Davis, E. Deleersnijder and R.R. Leben. 2003. Eddies Around Guam, an Island in the Marianas Islands Group. Continental Shelf Research. Volume 23. 991-1003.

Appendix A

The following figures illustrate the currents patterns on a regional scale for 17 separate depth intervals. Each figure contains 12 separate vector plots, one for each month of the year, and represents a single depth. In each monthly plot, daily averaged currents for each of the 81 stations are presented. Depths for which current data were provided and that are represented in each figure are listed in the following table.

Depth Intervals of NCOM Derived Current Data

Depth Intervals of NCOM Data	
(meters)	(≈feet)
0	0
10	33
20	66
30	100
40	130
50	165
75	250
100	330
200	650
300	1000
400	1,300
500	1,650
1,000	3,300
1,500	4,900
2,000	6,550
2,500	8,200
3,000	9,850

Depth = 0m

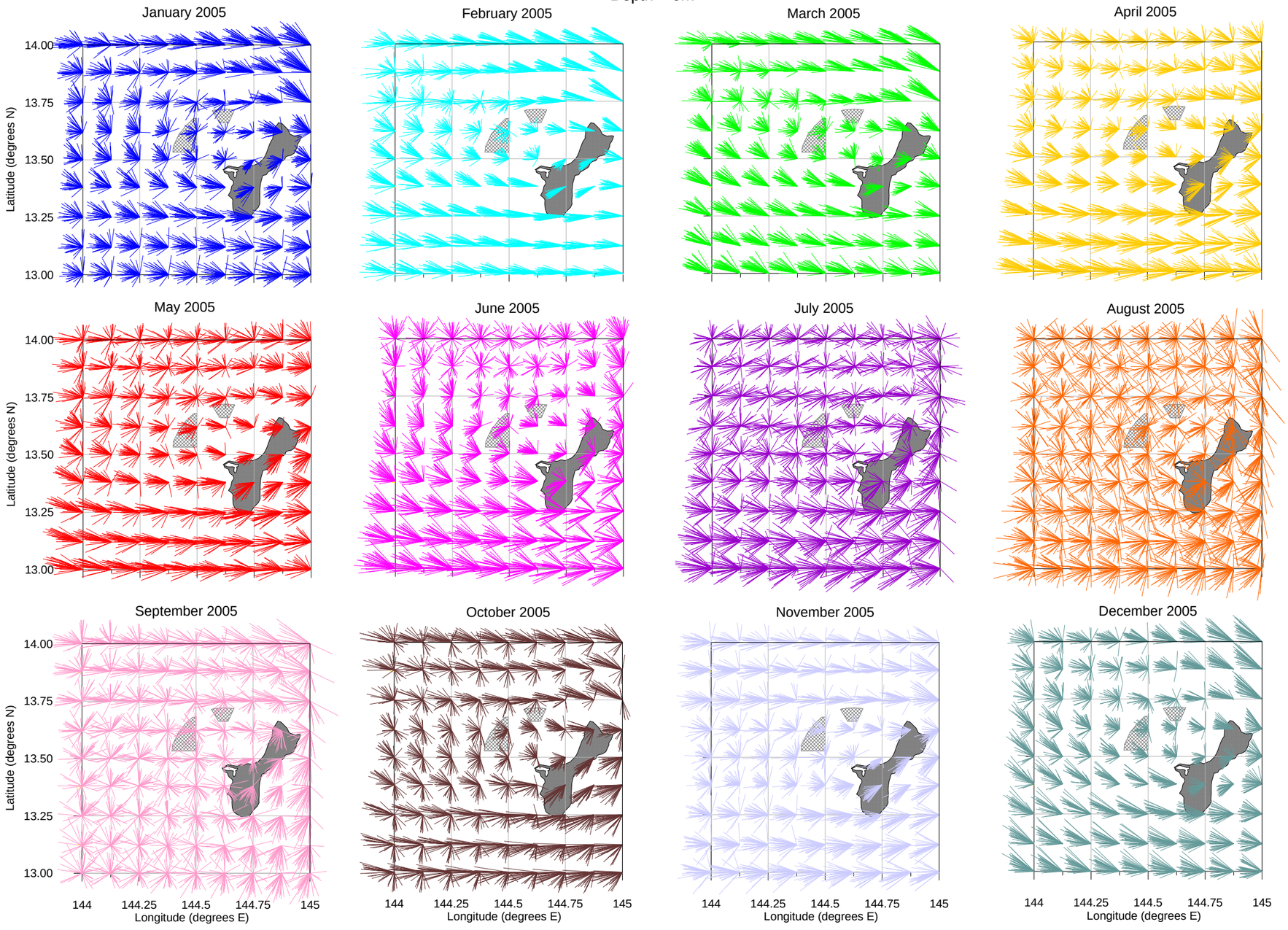
January 2005
February 2005
March 2005
April 2005
May 2005
June 2005
July 2005
August 2005
September 2005
October 2005
November 2005
December 2005
Latitude (degrees N)
14.00
13.75
13.50
13.25
13.00
144
144.25
144.5
144.75
145
Longitude (degrees E)

Depth = 10m

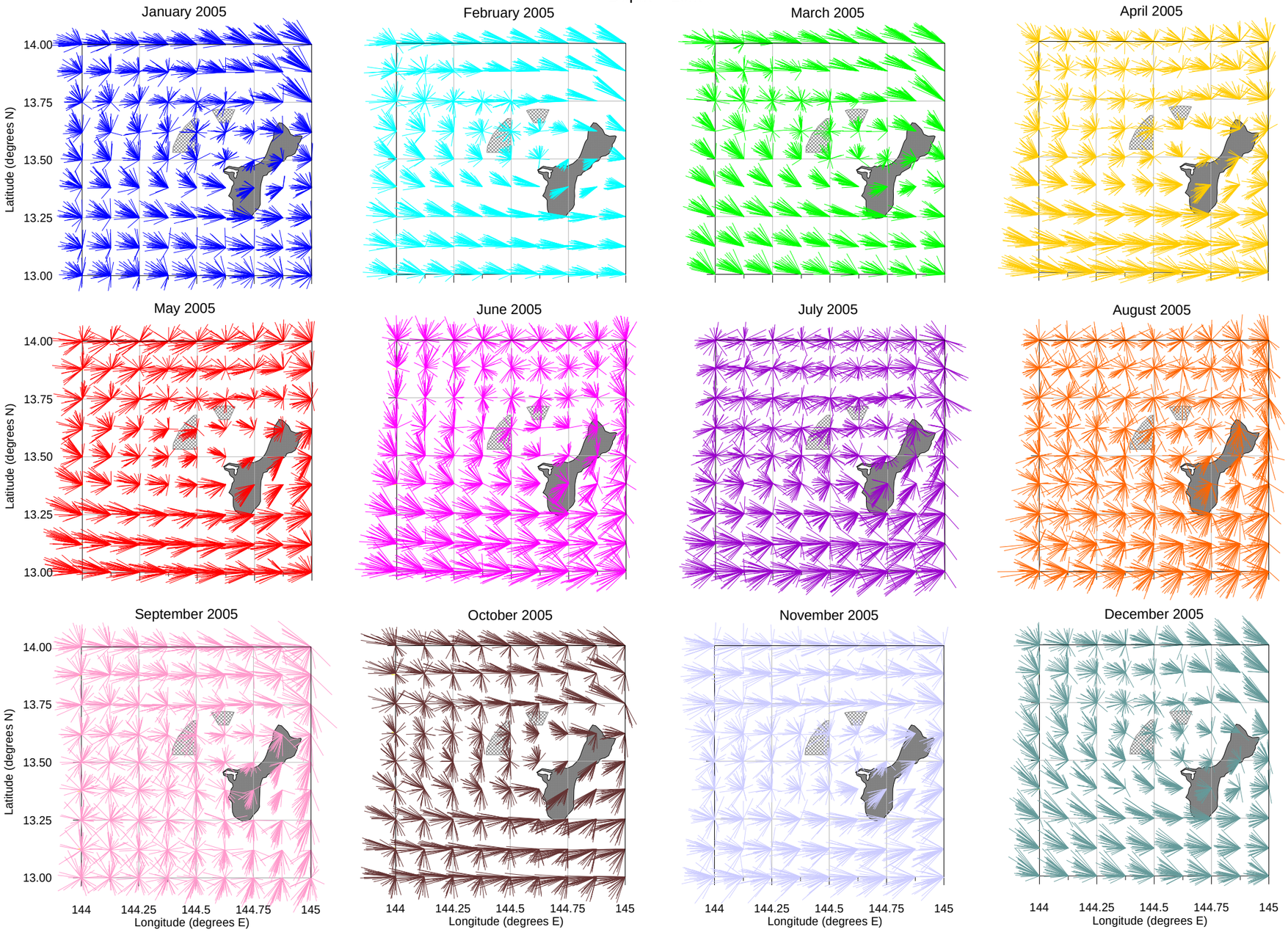
January 2005
February 2005
March 2005
April 2005
May 2005
June 2005
July 2005
August 2005
September 2005
October 2005
November 2005
December 2005
Latitude (degrees N)
14.00
13.75
13.50
13.25
13.00
144
144.25
144.5
144.75
145
Longitude (degrees E)

Depth = 20m

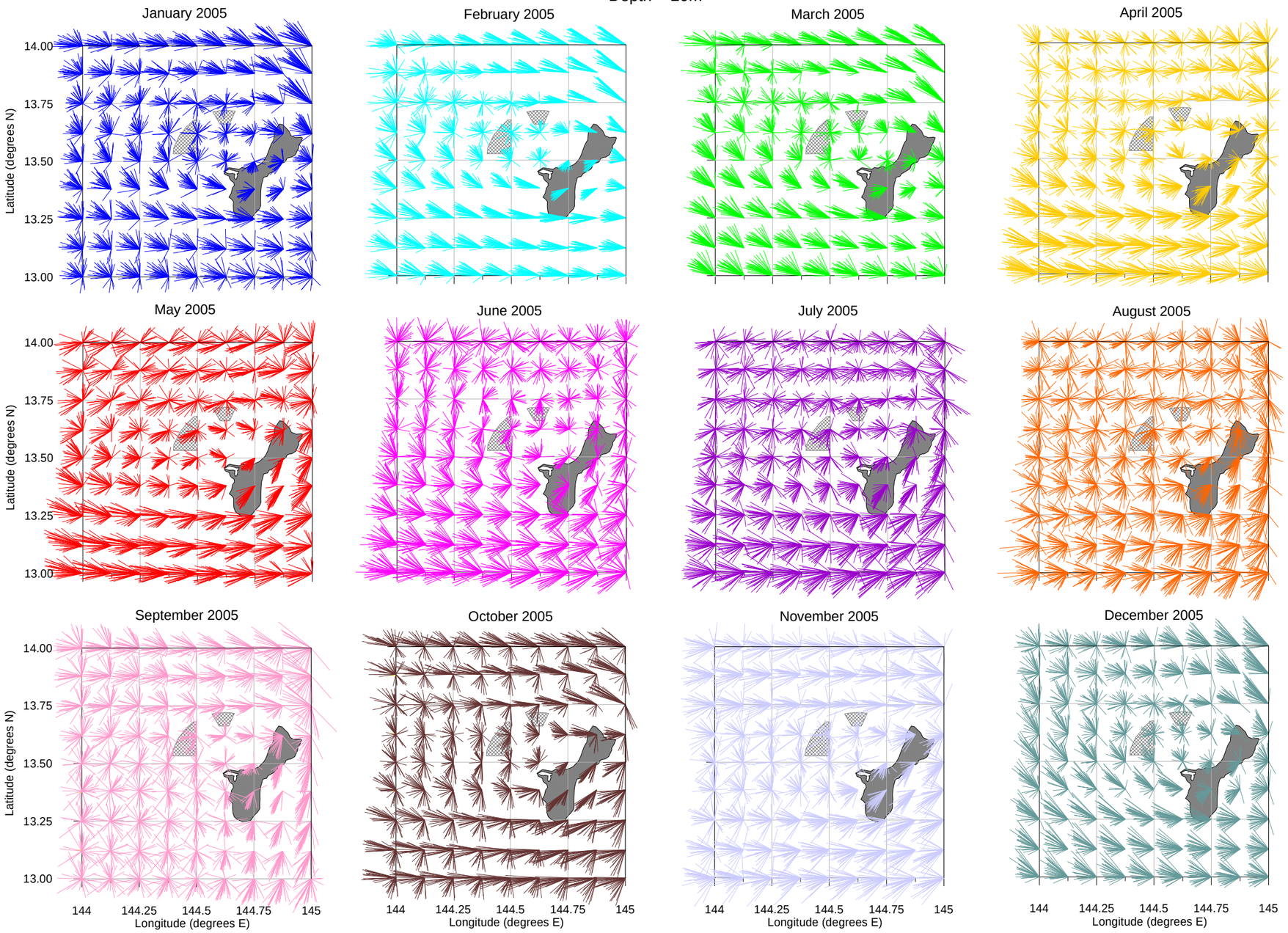
January 2005
February 2005
March 2005
April 2005
May 2005
June 2005
July 2005
August 2005
September 2005
October 2005
November 2005
December 2005
Latitude (degrees N)
14.00
13.75
13.50
13.25
13.00
144
144.25
144.5
144.75
145
Longitude (degrees E)

Depth = 30m

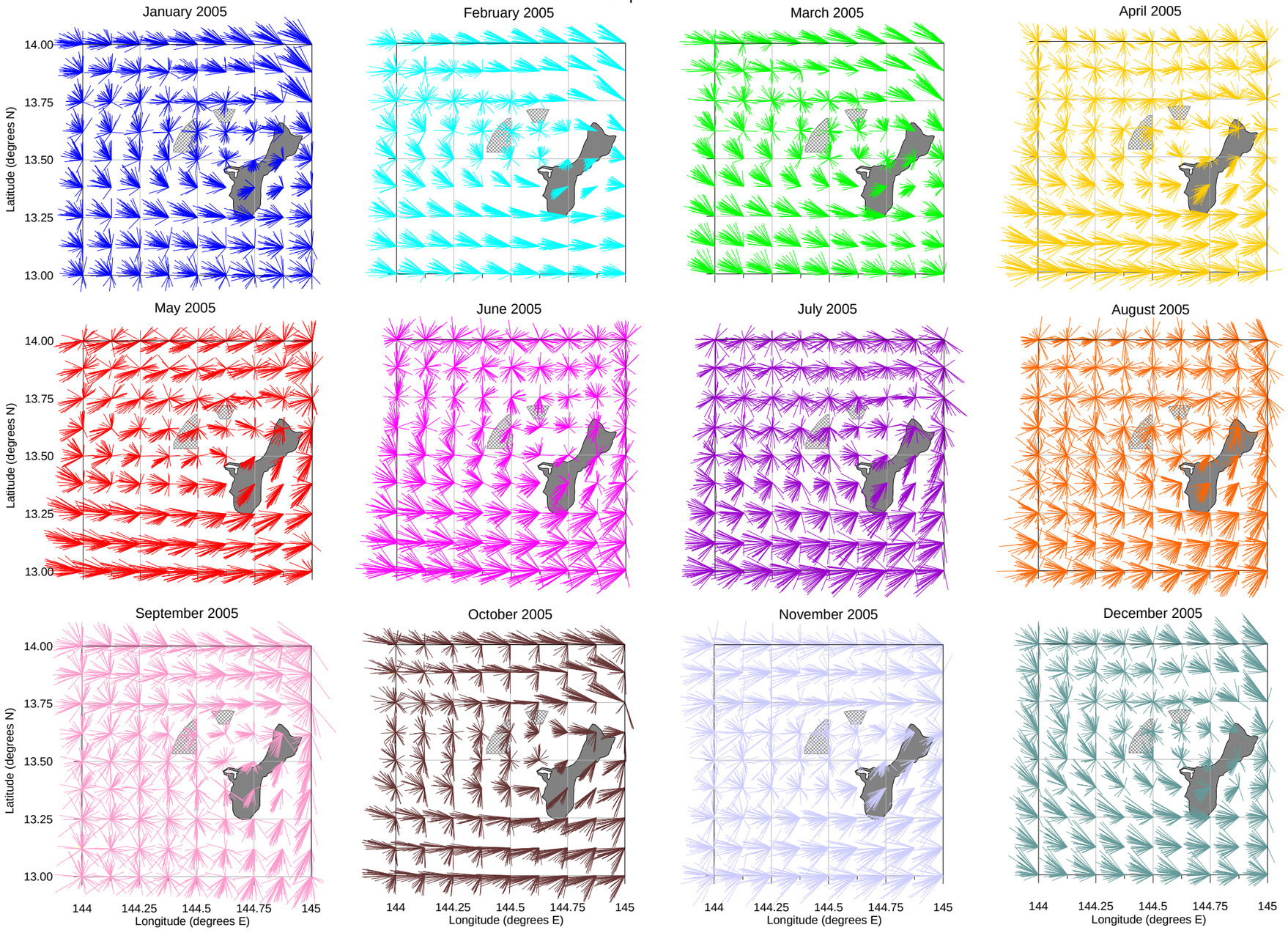
January 2005
February 2005
March 2005
April 2005
May 2005
June 2005
July 2005
August 2005
September 2005
October 2005
November 2005
December 2005
Latitude (degrees N)
14.00
13.75
13.50
13.25
13.00
144
144.25
144.5
144.75
145
Longitude (degrees E)

Depth = 40m

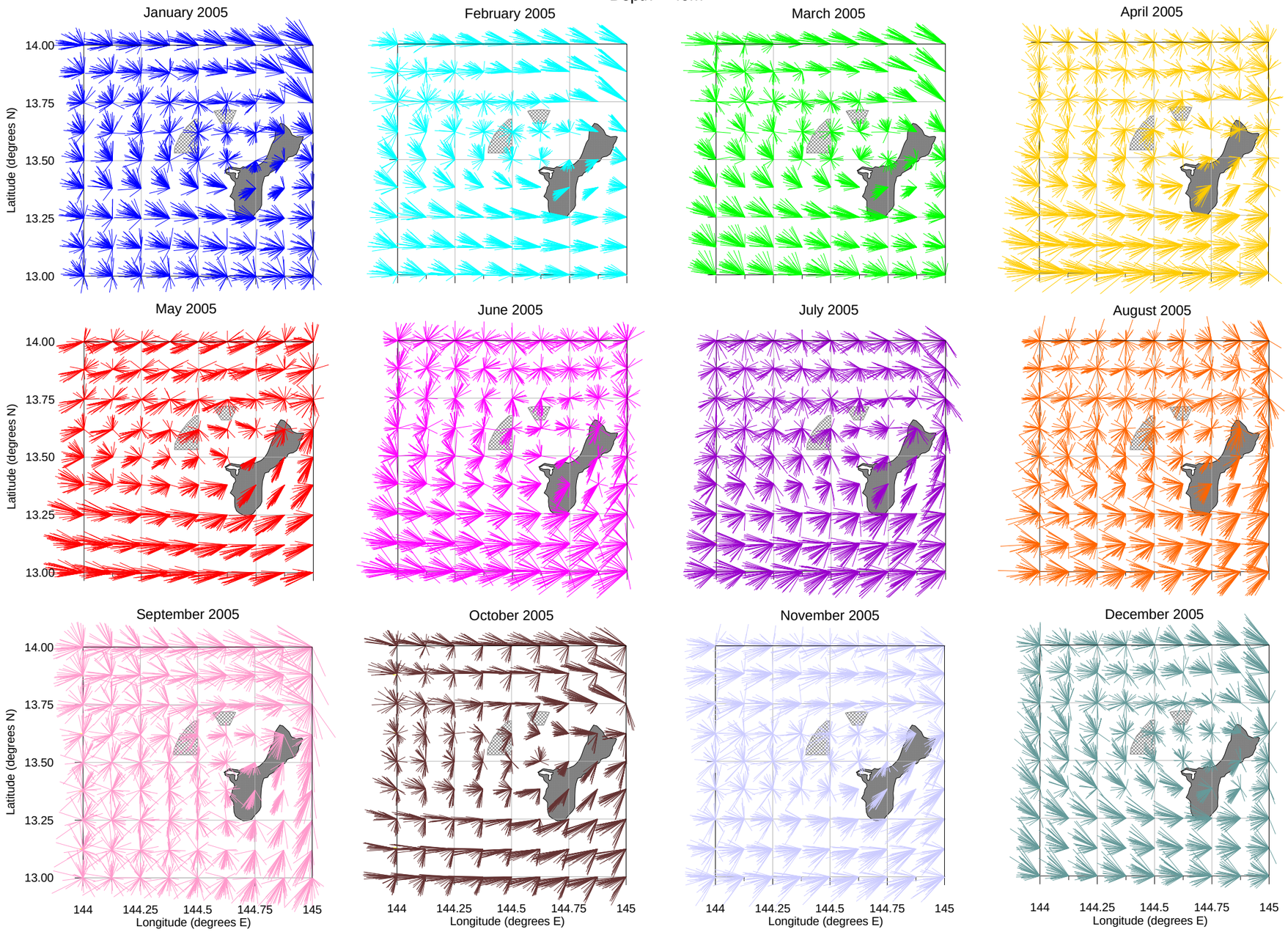
January 2005
February 2005
March 2005
April 2005
May 2005
June 2005
July 2005
August 2005
September 2005
October 2005
November 2005
December 2005
Latitude (degrees N)
14.00
13.75
13.50
13.25
13.00
144
144.25
144.5
144.75
145
Longitude (degrees E)

Depth = 50m

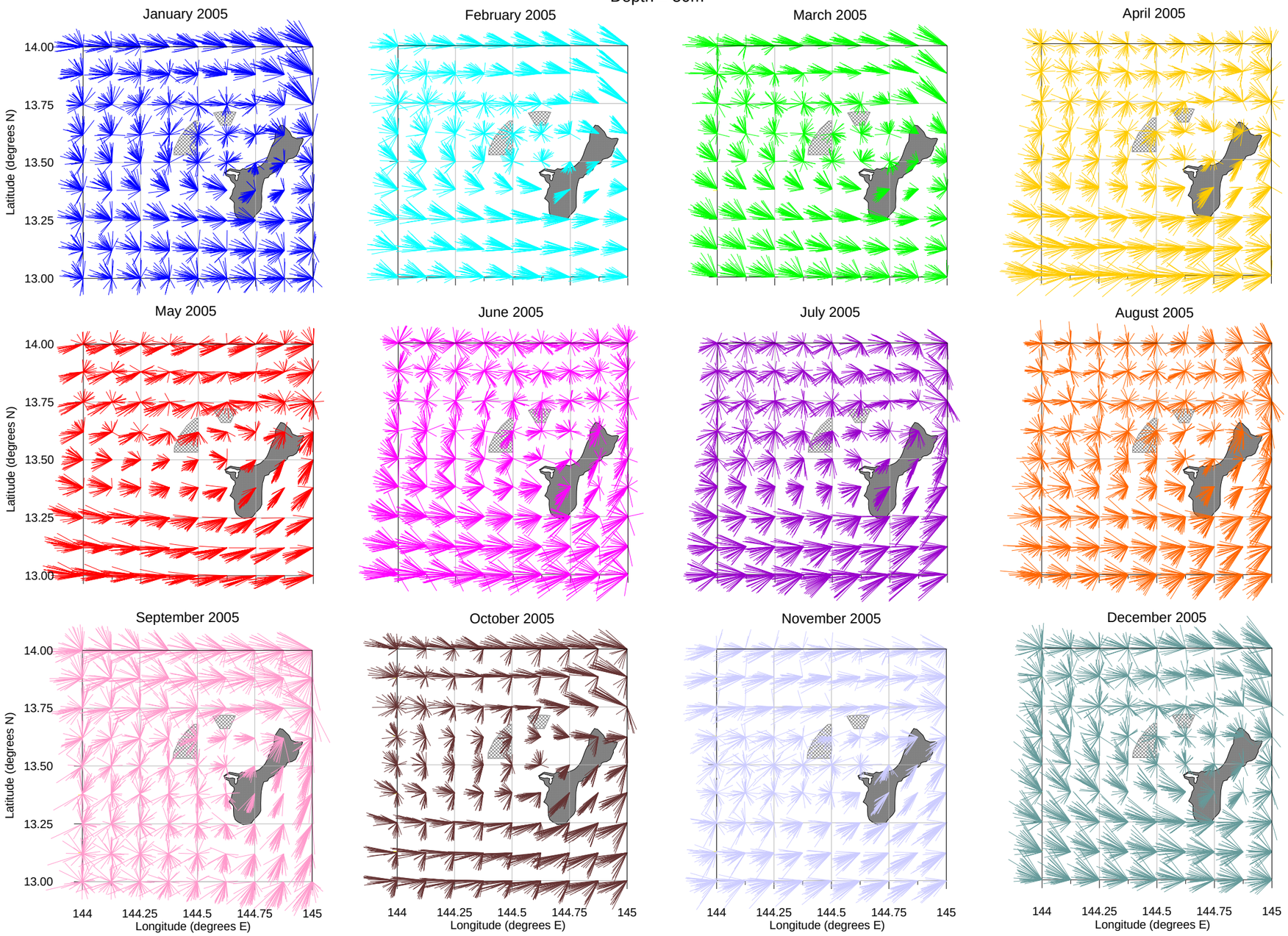
January 2005
February 2005
March 2005
April 2005
May 2005
June 2005
July 2005
August 2005
September 2005
October 2005
November 2005
December 2005
Latitude (degrees N)
14.00
13.75
13.50
13.25
13.00
144
144.25
144.5
144.75
145
Longitude (degrees E)

Depth = 75m

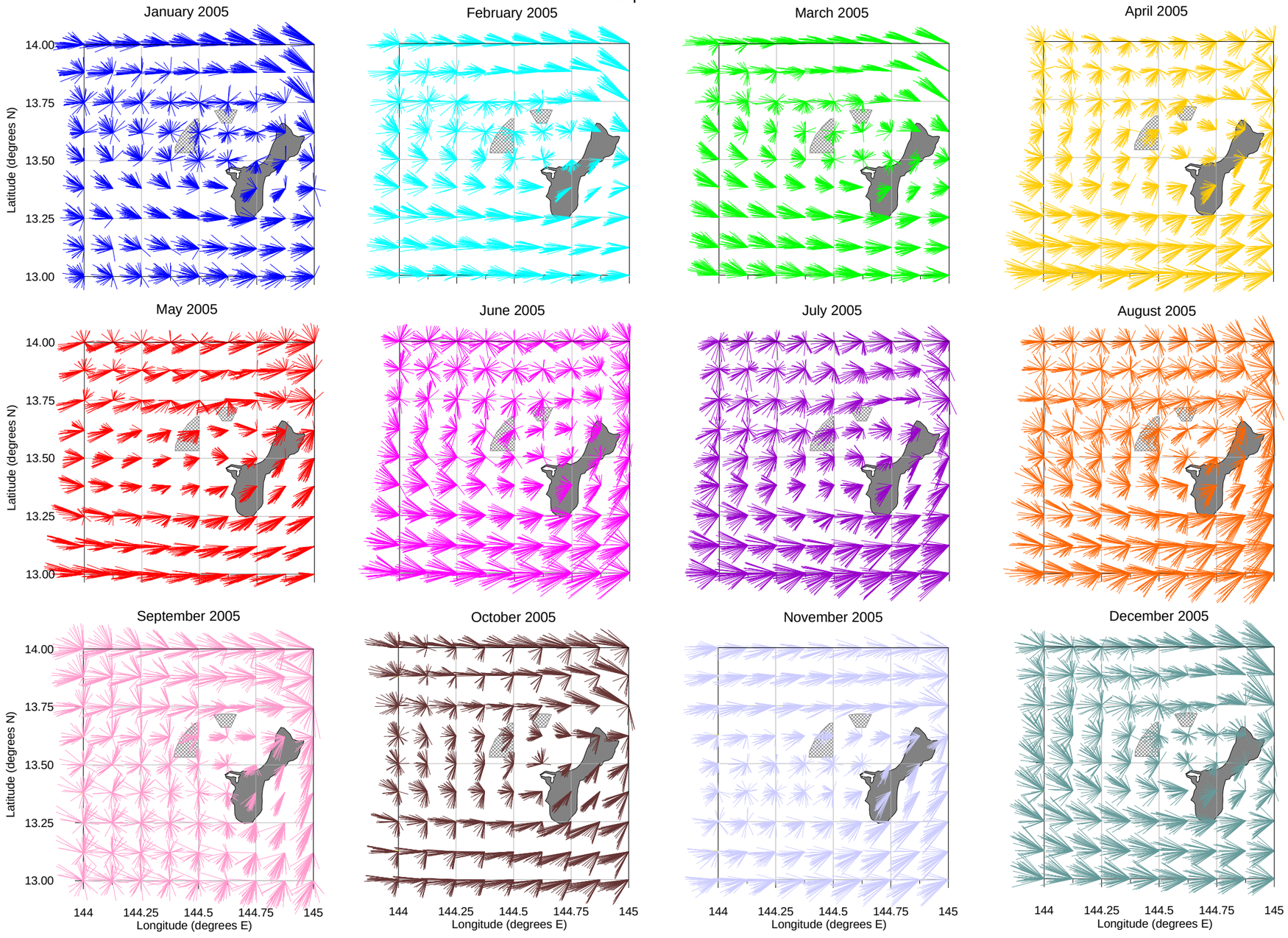
January 2005
February 2005
March 2005
April 2005
May 2005
June 2005
July 2005
August 2005
September 2005
October 2005
November 2005
December 2005
Latitude (degrees N)
14.00
13.75
13.50
13.25
13.00
144
144.25
144.5
144.75
145
Longitude (degrees E)

Depth = 100m

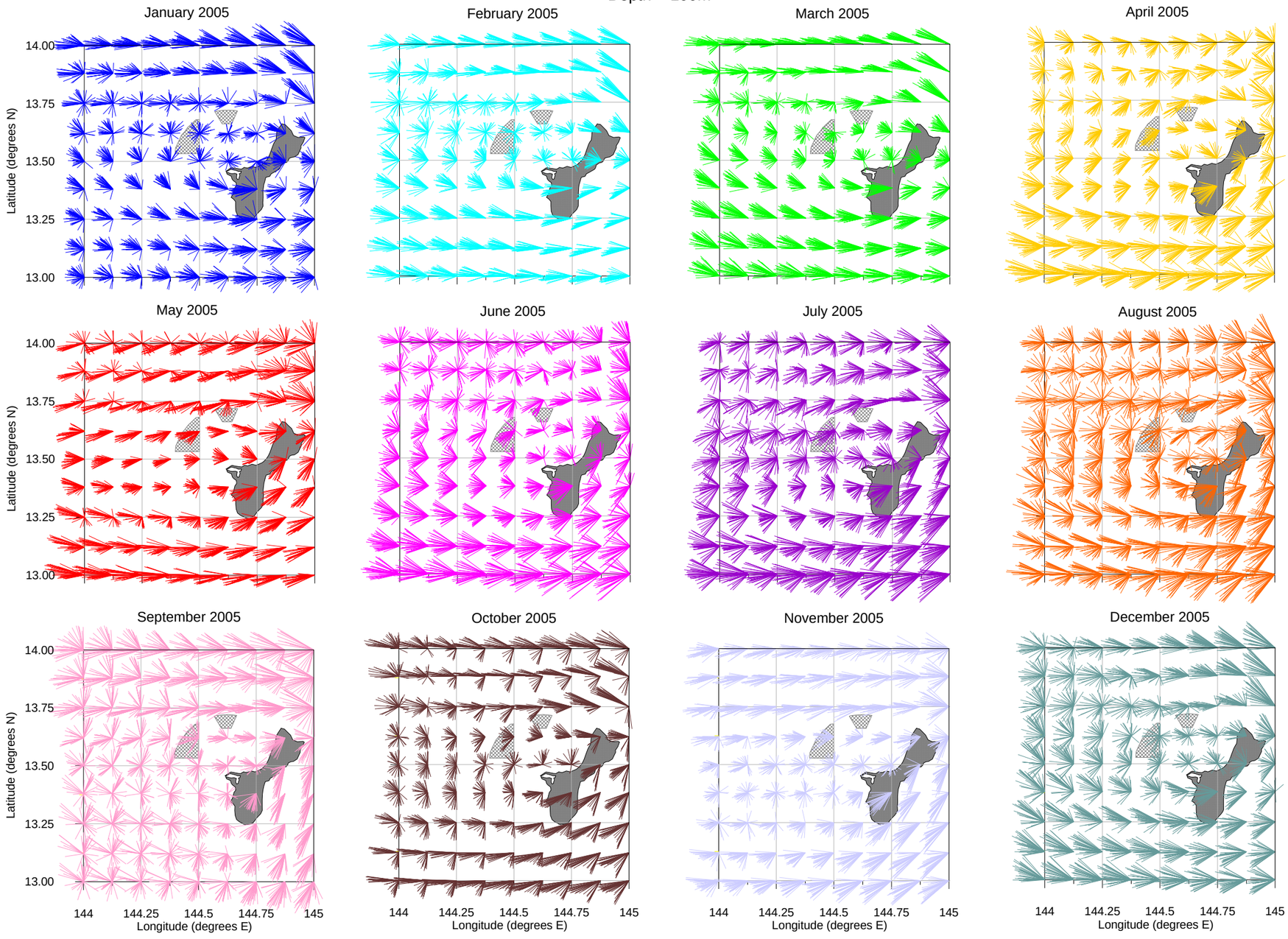
January 2005
February 2005
March 2005
April 2005
May 2005
June 2005
July 2005
August 2005
September 2005
October 2005
November 2005
December 2005
Latitude (degrees N)
14.00
13.75
13.50
13.25
13.00
144
144.25
144.5
144.75
145
Longitude (degrees E)

Depth = 200m

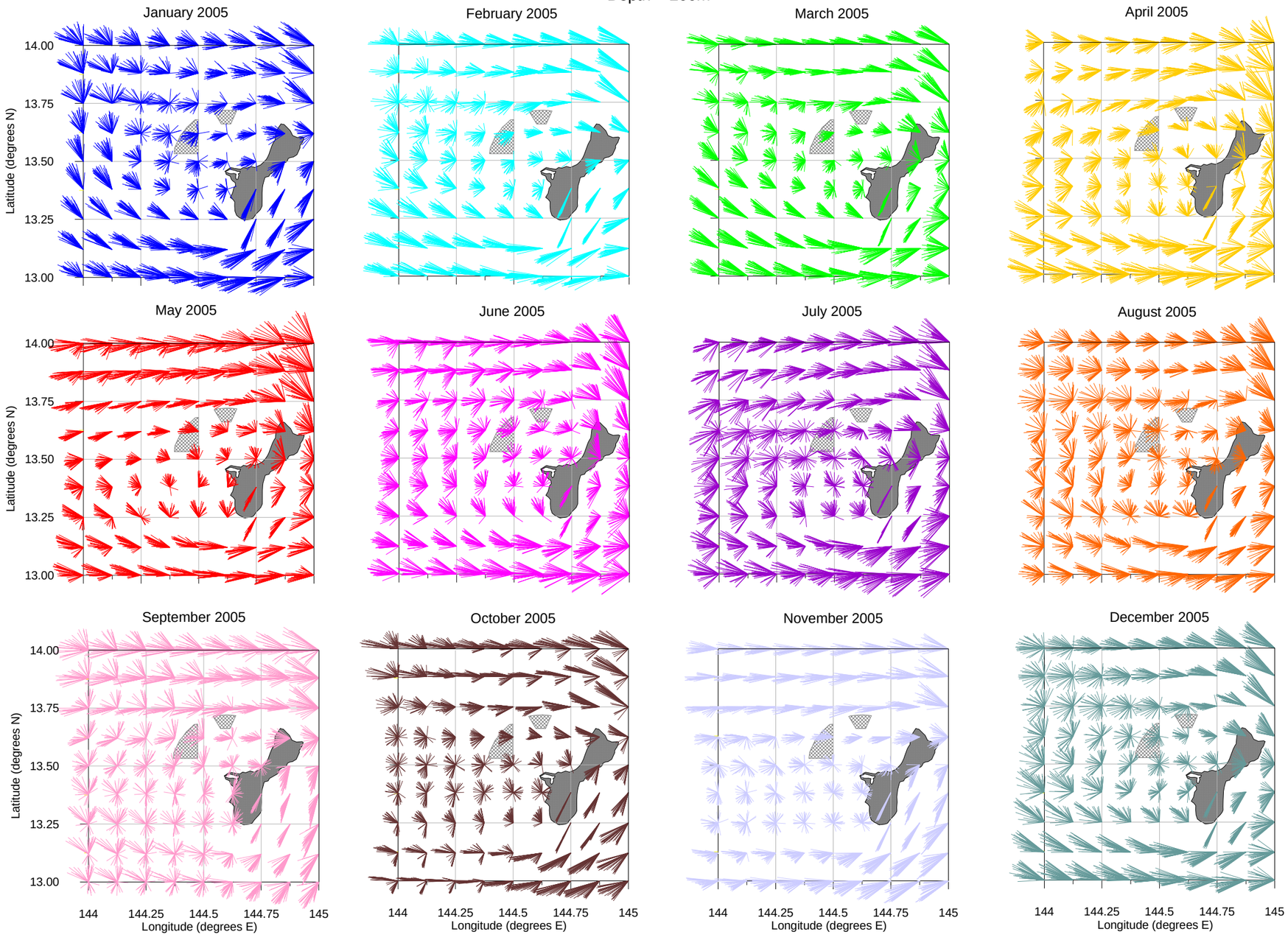
January 2005
February 2005
March 2005
April 2005
May 2005
June 2005
July 2005
August 2005
September 2005
October 2005
November 2005
December 2005
Latitude (degrees N)
14.00
13.75
13.50
13.25
13.00
144
144.25
144.5
144.75
145
Longitude (degrees E)

Depth = 300m

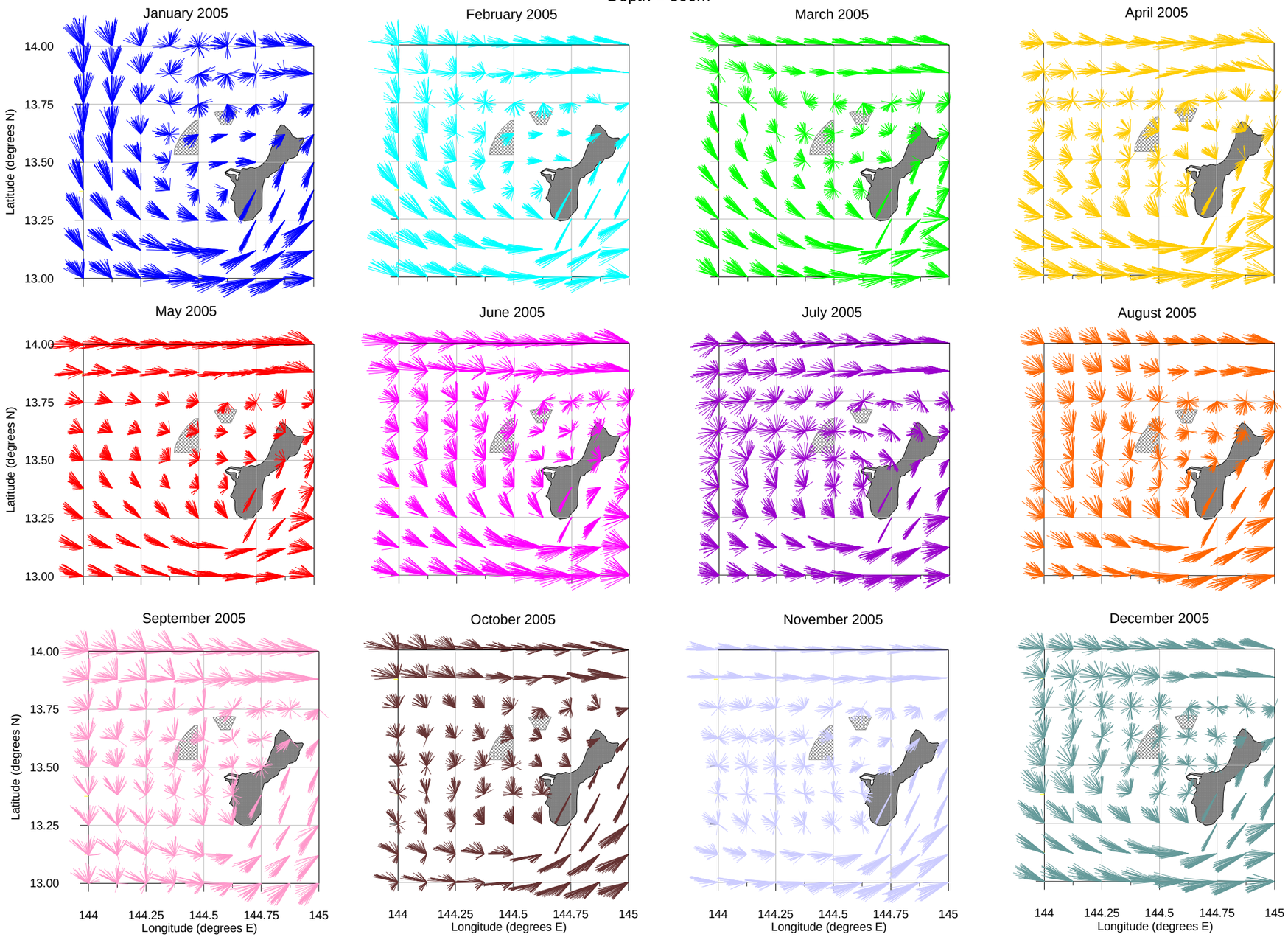
January 2005
February 2005
March 2005
April 2005
May 2005
June 2005
July 2005
August 2005
September 2005
October 2005
November 2005
December 2005
Latitude (degrees N)
14.00
13.75
13.50
13.25
13.00
144
144.25
144.5
144.75
145
Longitude (degrees E)

Depth = 400m

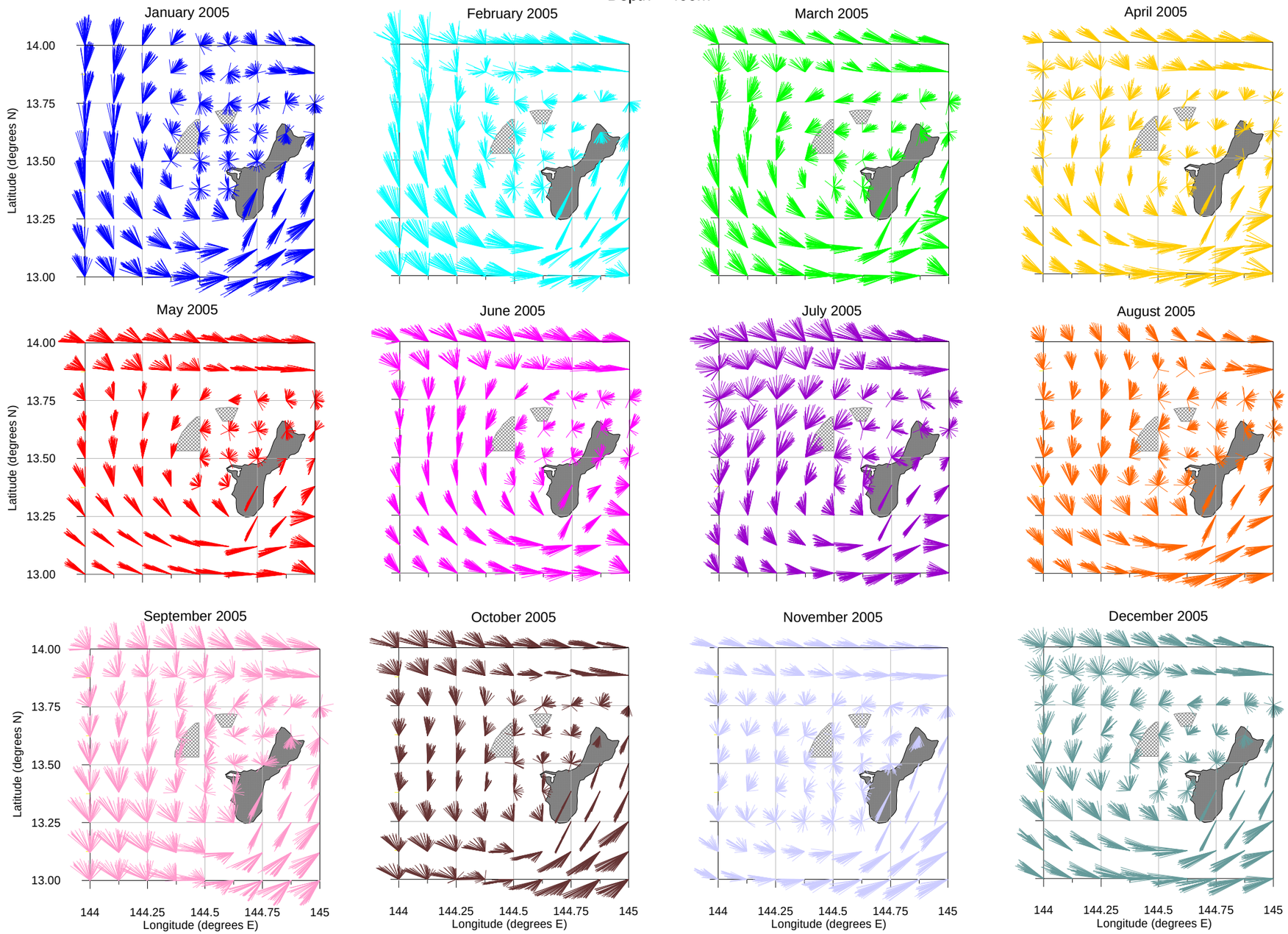
January 2005
February 2005
March 2005
April 2005
May 2005
June 2005
July 2005
August 2005
September 2005
October 2005
November 2005
December 2005
Latitude (degrees N)
14.00
13.75
13.50
13.25
13.00
144
144.25
144.5
144.75
145
Longitude (degrees E)

Depth = 500m

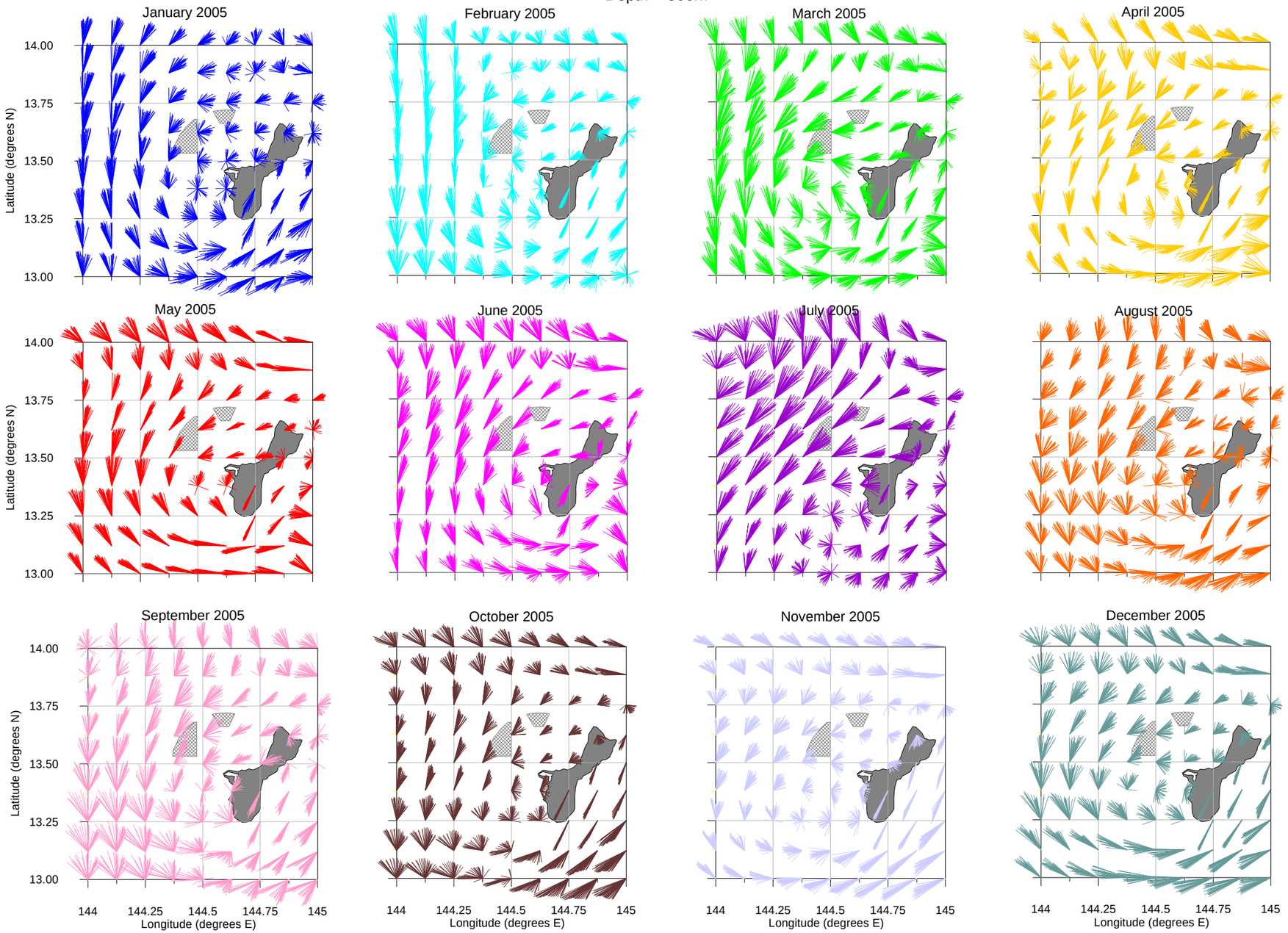
January 2005
February 2005
March 2005
April 2005
May 2005
June 2005
July 2005
August 2005
September 2005
October 2005
November 2005
December 2005
Latitude (degrees N)
14.00
13.75
13.50
13.25
13.00
144
144.25
144.5
144.75
145
Longitude (degrees E)

Depth = 1000m

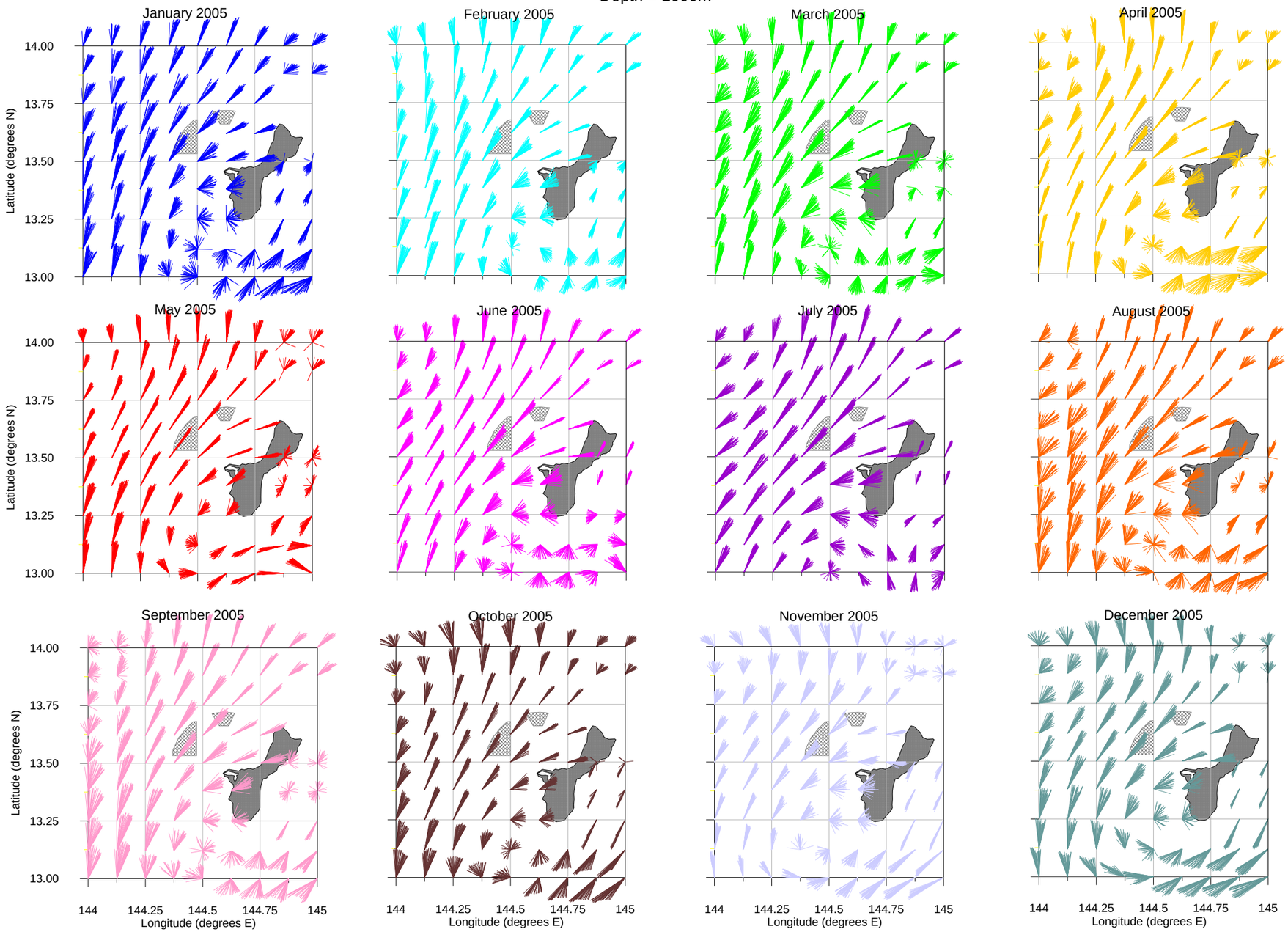
January 2005
February 2005
March 2005
April 2005
May 2005
June 2005
July 2005
August 2005
September 2005
October 2005
November 2005
December 2005
Latitude (degrees N)
14.00
13.75
13.50
13.25
13.00
144
144.25
144.5
144.75
145
Longitude (degrees E)

Depth = 1500m

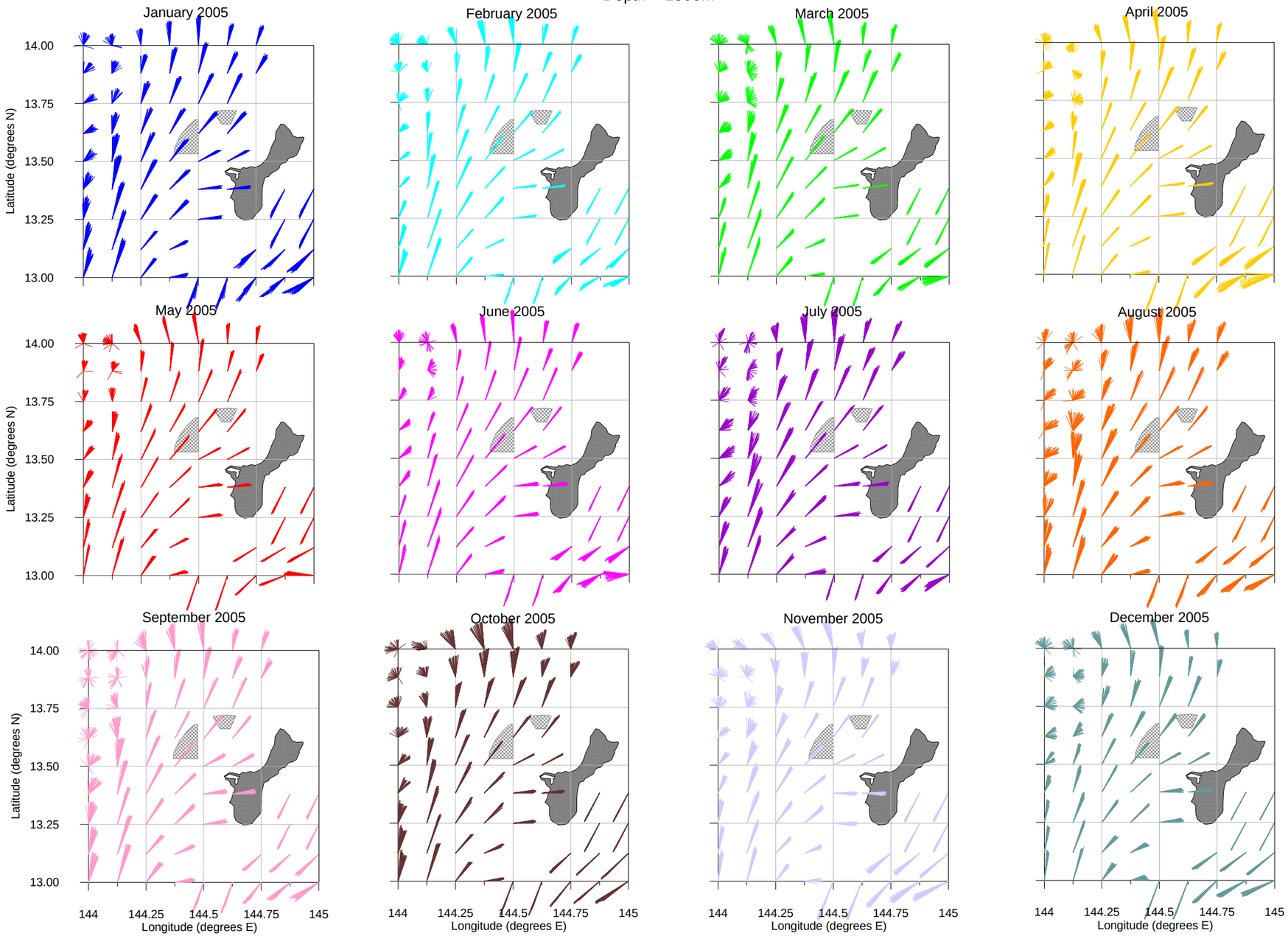
January 2005
February 2005
March 2005
April 2005
May 2005
June 2005
July 2005
August 2005
September 2005
October 2005
November 2005
December 2005
Latitude (degrees N)
14.00
13.75
13.50
13.25
13.00
144
144.25
144.5
144.75
145
Longitude (degrees E)

Depth = 2000m

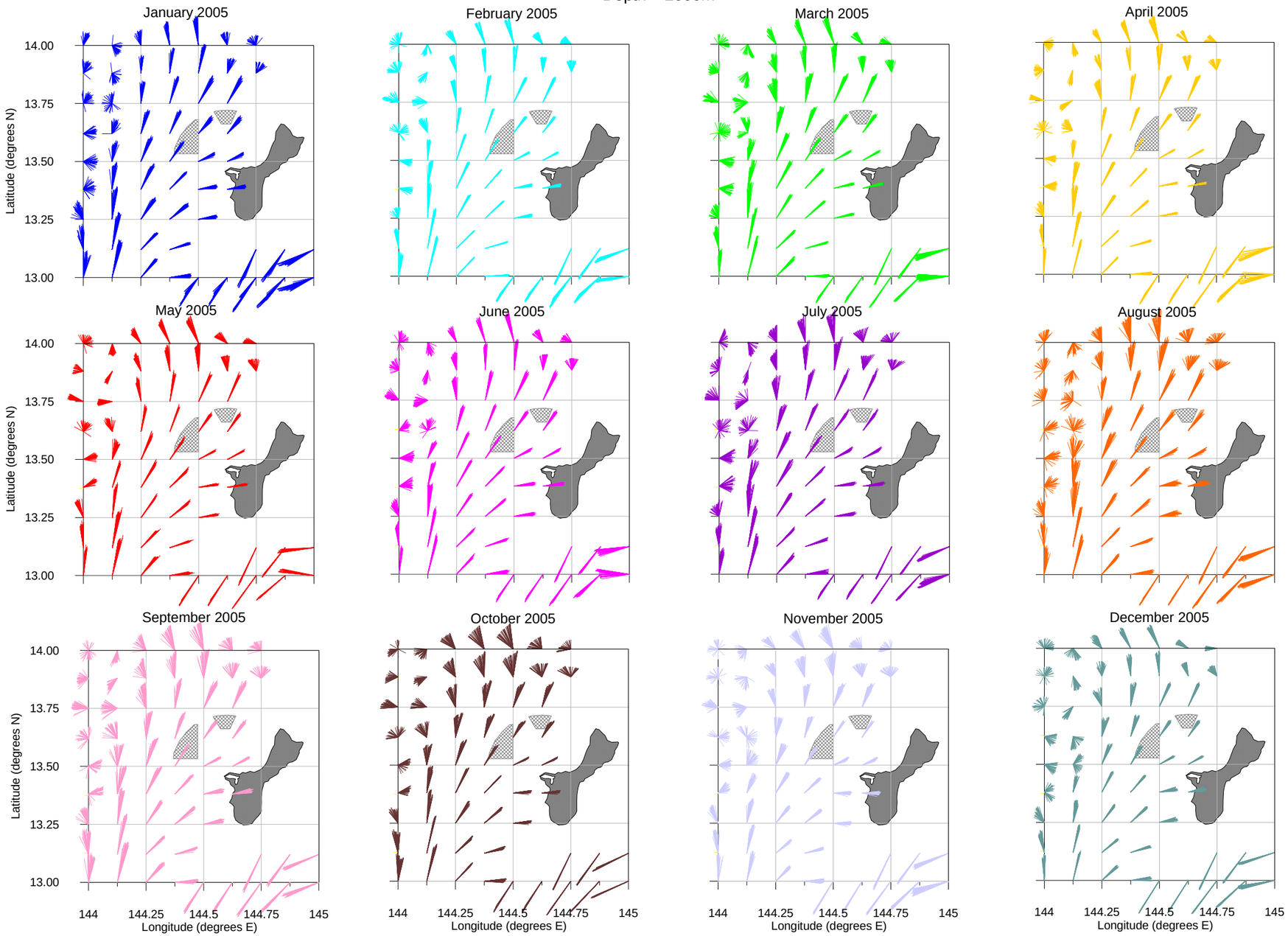
January 2005
February 2005
March 2005
April 2005
May 2005
June 2005
July 2005
August 2005
September 2005
October 2005
November 2005
December 2005
Latitude (degrees N)
14.00
13.75
13.50
13.25
13.00
144
144.25
144.5
144.75
145
Longitude (degrees E)

Depth = 2500m

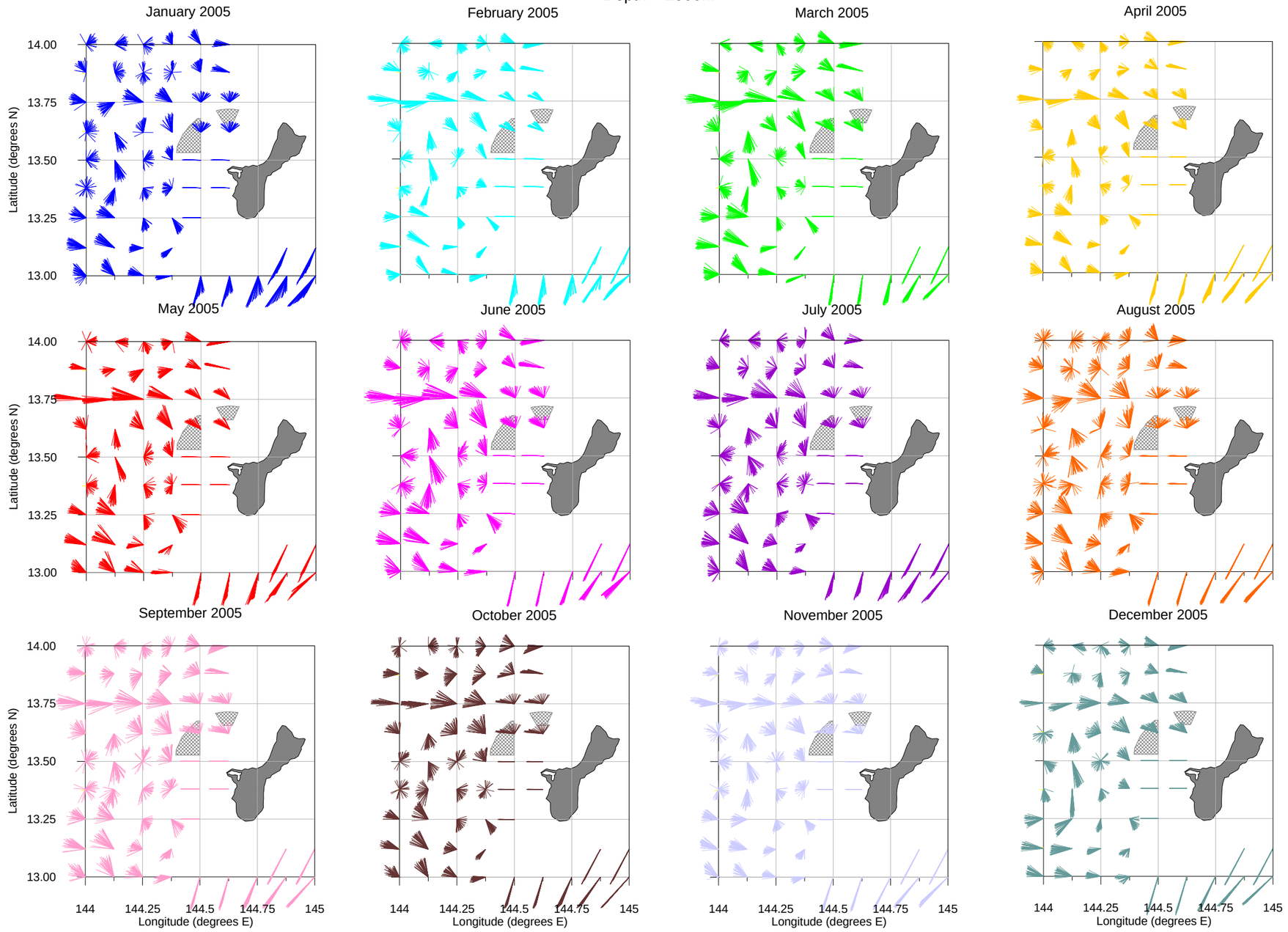
January 2005
February 2005
March 2005
April 2005
May 2005
June 2005
July 2005
August 2005
September 2005
October 2005
November 2005
December 2005
Latitude (degrees N)
14.00
13.75
13.50
13.25
13.00
144
144.25
144.5
144.75
145
Longitude (degrees E)

Depth = 3000m

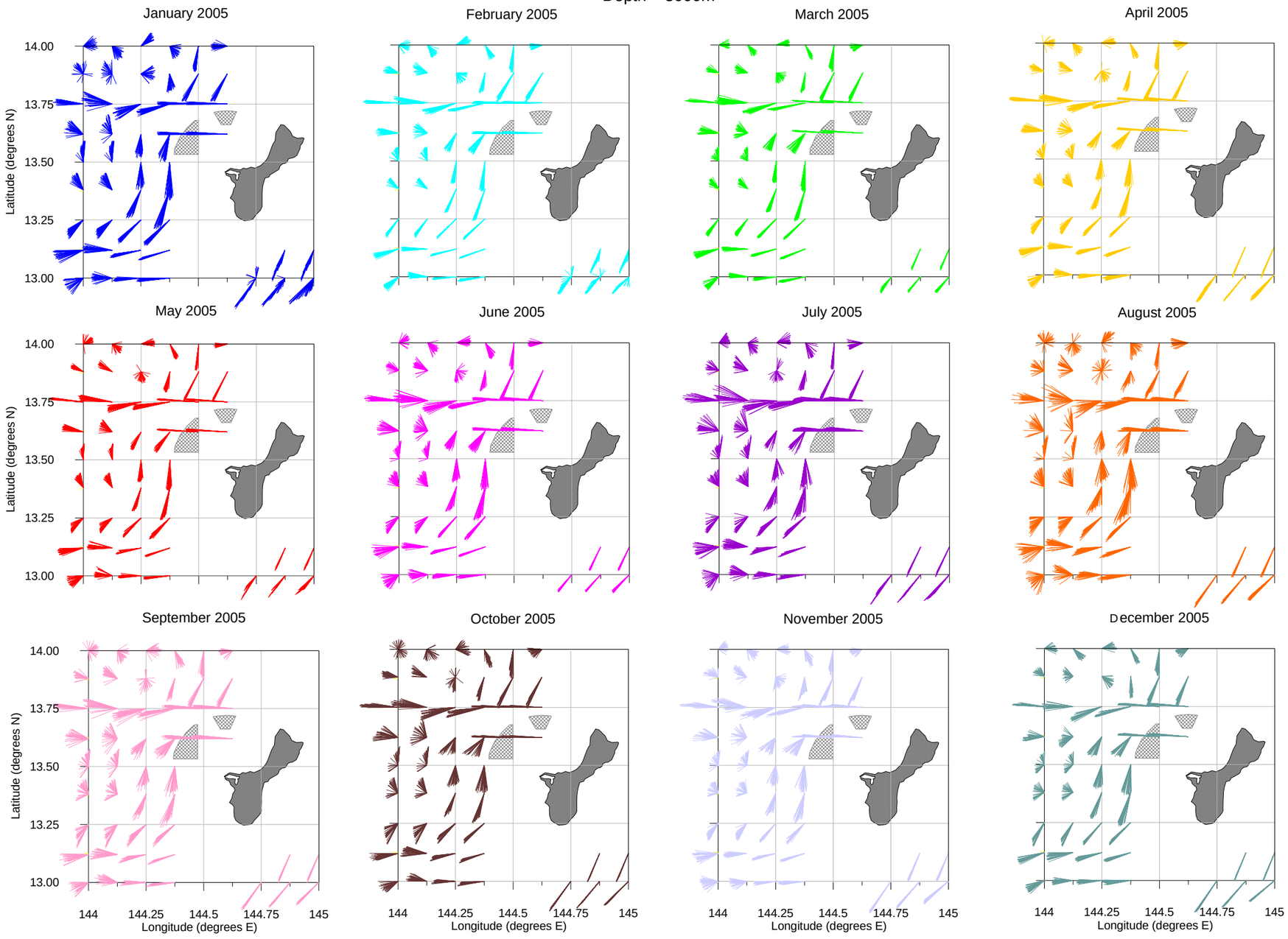
January 2005
February 2005
March 2005
April 2005
May 2005
June 2005
July 2005
August 2005
September 2005
October 2005
November 2005
December 2005
Latitude (degrees N)
14.00
13.75
13.50
13.25
13.00
144
144.25
144.5
144.75
145
Longitude (degrees E)